(3) The Database

Of database for 1992~1996 available to the Study Team, the 1994 data set is opted for calibration of the biogeochemical sub-model, since the year was an anomaly in view of the extent of algal bloom. In 1994, the bloom spread to the entire lake basin and the maximum Chla reached 210 mg/m3 in the Keszthely basin. In addition, the Zala River load in the year is more representative of the current load condition than that in the earlier years prior to the completion of Kis-Balaton II. The data set of the following year, 1995, is also utilized to test the multi-year reproducibility of the calibrated model. The year 1995 was noted for low productivity in the lake despite the steady trend in nutrients load condition.

The water-quality and -quantity of Zala River in the both the years are shown in *Figure C.41* (KDT-KÖFE). The input data include the daily loads from Zala River; direct runoff; and atmospheric deposition; hourly wind; water-temperature measured once a day at 7:00 am; daily total solar radiation; and daily water level. The data except the solar radiation are linearly interpolated at every time step. The daily total solar radiation is distributed assuming a sinusoidal function each day from sunrise to sunset. The daily solar radiation recorded at the Keszthely weather station and the water-temperature measured by KDT-VISIG at the center of Keszthely Bay are shown in *Figures C.42* and *C.43* Wind magnitudes and directions recorded at the same weather station for 1994 and 1995 are shown in *Figures C.44* and *C.45*.

(4) Calibration of Biogeochemical Sub-Model

The equations of the four dependent variables shown in *Table C.2* were solved using 4th-order *Runge-Kutta* method with a time step of 0.005 *hour*. The short time step was required to obtain stable solutions at very low PO_4-P levels. Start-time of the calculation was chosen just after the spring diatom-bloom when measured records are available. The initial conditions were taken as average values of *Chla* and *TP* measured at the center and two locations near the west coast of *Keszthely Bay*. The calculation was terminated when the summer algal-bloom ceased.

Simulated results were compared with measurements taken by *KDT-KÖFE* at three locations in *Keszthely Bay* as shown in *Figure C.46*. The calibration process was focused on matching the measured and calculated *Chla* for the following reasons: 1) The standard water and wastewater technique used for PO_4-P analysis by *KDT-KÖFE* is unsuitable and unreliable for low levels of PO_4-P concentrations encountered in the lake (a comment to the study team by Dr. Sandor Herodek, 1997; see also Herodek, 1986). Concentrations of PO_4-P of the lake water analyzed in 1994 by *KDT-KÖFE* ranged 0 to 108 $mg\text{-}P/m^3$ with an average of 20 $mg\text{-}P/m^3$, while those analyzed by Présing, Herodek, Vörös, and Kóbor (1996) were within 0 to 4 $mg\text{-}P/m^3$; and 2) Major fraction of *SS* is

formed by $CaCO_3$ and *TP* (Tóth *et al.*, 1975), and large fluctuations of *TP* concentration in the lake water have been observed. However, no data are available for the phosphorous release from *SS* other than in the form of PO_4-*P*. The study team, therefore, has opted to exclude *TP* from the calibration process.

As already discussed, the model parameters used in the present study have been supported by existing data taken from field and laboratory studies for *Lake Balaton*. Since there still remain some uncertainties in those studies as well as in the model itself, sensitivity analyses were conducted by changing the parameters only within realistic ranges. Standard values of the parameters are listed in *Table C.6* with references, and cases of the sensitivity study undertaken are shown in *Table C.7*.

1) Chlorophyll-a Hindcasts in 1994 and 1995

Figure C.48 shows calculated *Chla* in 1994 using the standard parameter values as listed in *Table C.6*. In the figure, the measured *Chla* values were taken from the database at *KDT-KÖFE* except those at the center of *Keszthely Bay* in 1994 which were taken from Présing *et al.* (1996), whose data conform to the measurements taken by *KDT-KÖFE* except the peak value. The calculated *Chla* transition in 1994 reproduces the timing the maximum peak as well as the overall trend very favorably. The PO_4-*P* level during the bloom stays at less than 1 $mg\text{-}P/m^3$, in agreement with the measurements by Présing *et al.* (1986). A hindcast of *Chla* in 1995 was also performed using the same parameter values. The result is shown in *Figure C.49*. It is seen in the figure that the hindcast prominently replicates the much lower levels of *Chla*, 50 mg/m^3 at the maximum, as compared to 1994. The lower water temperature is the most probable reason of the much lower productivity in 1995 as suggested by Tóth and Padisák (1986) as well as by Padisák and Istvánovics (1996). When the water temperature of 1995 is replaced by that of 1994, the maximum *Chla* approaches close to the 1994 level as shown in *Figure C.49*, underlining the critical role of water temperature in the explosive algal bloom in 1994.

2) Sensitivity Study

For *Case I* (*Figures C.50 to C.54*) according to *Table C.7*, the influence of the minimum cell quota (ψ_{min}) was examined by adjusting ψ_{min} and the maximum growth rate (μ_{max}) to match the calculated maximum *Chla* to the measured values, while keeping other parameters fixed at the standard values. While shifting ψ_{min} between 0.0015 and 0.003 *mg-P/mg-d.w.*, μ_{max} was increased from 1.7 to 2.3 day^{-1}. As seen in the table, the calculated *Chla* and *P*-forms for the five cases are very similar, ψ_{min} in this range presents the same effect as μ_{max} on the model response.

In *Case II* (*Figures C.55 to C.59*), the effect of the maximum cell quota (ψ_{max}) was examined by fixing all other parameters at the standard values. The effect of ψ_{max} is conspicuous in PO_4-P response during the low-growth period in which PO_4-P concentration increases as ψ_{max} is decreased. When the ψ_{max} value is kept low at 0.01 to 0.015, PO_4-P shoots up to high levels at 20 to 40 *mg-P/m*^{3}. On the other hand, when ψ_{max} is close to the standard value at 0.018 as seen in *Sub-Case II-3*, PO_4-P level responds reasonably within a range of 0 to 5 *mg-P/m*^{3}.

In *Case III* (*Figures C.60 to C.63*), the maximum phosphorus uptake rate and the half saturation constant were adjusted to reproduce the maximum *Chla* level. In all the test cases, using parameters within reasonable ranges, *Chla* is not very susceptible to these parameters. The response modes of all the phosphorus-forms are similar.

In *Case IV*, parameters related to the sediment-water interaction were varied. The rate of phosphorus desorption, ΔC, per unit dry weight of *SS*, was varied from 0.004 to 0.1 *mg-P/g-DM* in *Sub-Cases IV-1 to 4* while other parameters were fixed. *Chla* and the various forms of *P* respond rather sluggishly among the test cases, even at an extreme value of ΔC=0.1. The equilibrium concentration of the sediment-water exchange, P_{eq}, was also varied between 10 and 100 *mg-P/m*^{3} in *Sub-Cases IV-5 to 8* in which the maximum growth rate, μ_{max}, was adjusted to reproduce the measured maximum *Chla* between 2.5 and 1.5 *day*$^{-1}$. At a low P_{eq}, a very high μ_{max} is required to match the maximum *Chla*, while all the *P* forms including algal-*P* stay at very low levels. In response to increased P_{eq}, concentrations of all the *P* forms also increase. When P_{eq} is greater than 50 *mg/m*^{3}, PO_4-P and *TP* turn to unreasonably high levels. The same responses are found when the exchange rate, C_{ex}, is varied as seen in *Sub-Cases IV-9* to *12*. The effect of the reduction is more pronounced when either of the parameters is decreased, resulting in severer nutrient limitation on algal growth. The implication in *Case IV* is that the bulk *P*-diffusion from the bottom sediment plays a major role in the phosphorous cycle and the algal growth. By comparison, the effect of phosphorus desorption from *SS* is minor.

In *Case V*, the maximum PO_4-P uptake rate, k_u, the half saturation constant, P_{1k}, and the fraction of organic-*P* of dead phytoplankton, f_{op}, were varied. Net phosphorus uptake rate excluding the cell quota contribution can be roughly estimated since the external (ambient) PO_4-P concentration, P_{ext}, is less than *1 mg-P/m*^{3} during the bloom. The response of the net uptake rate, k_{net}, is within ranges $0.06P_{ext}$ to $0.17P_{ext}$ for k_u = 0.5, and $0.02P_{ext}$ to $0.08P_{ext}$ for k_u = 1.5 in which the unit is *mg-P/mg-d.w./day*. The effect of variation in k_{net} in these ranges is insignificant on the algal growth, and the PO_4-P level during the lag

phase of the growth responds to the change of f_{op}. The effect of the parameters variation is similar in all the cases, responding by about 17 % reduction in *Chla* or biomass.

In *Case VI* (*Figures C.64 to C.69*), the optimum and the minimum growth temperatures, T_{opt} and T_{min} were varied. The effect of varying T_{opt} is most conspicuous during the exponential growth phase in which a lower T_{opt} promotes the growth. Lowering T_{min} has a similar effect on *Chla* to the lowered T_{opt}, whereas the PO_4-P level during the lag phase of the bloom is also influenced by T_{opt} significantly.

Although the previous water-quality studies for *Keszthely Bay* invariably assumed a constant water depth, the fluctuation of depth and volume of the bay could also affect the water quality. In *Case VII*, to examine the effect of the water level, the standard values found in literature: *depth*=2.2 *m* and *volume*=82x10^6 m^3, were varied $\pm 10\%$ with all the other parameters fixed. As seen in *Figures C.70* and *C.71*, and as expected from the simple mass balance concept, increased depth and volume result in perceivable inverse responses of both *TP* and *Chla* levels. Since the annual fluctuation of the mean water depth in *Keszthely Bay* exceeds 10% of the annual average as seen *Figure C.47*, it is preferable to apply variable water depth and volume in model calculations.

4.2 Two Dimensional Water Quality Model: 2-D WQSM

A two-dimensional mass transport model as the base unit for the two-dimensional water quality model (*2-D WQSM*) has been developed. The biogeochemical component (*0-D WQSM*), as described previously, has been incorporated into the mass transport model to assemble the two-dimensional water quality model. The mass transport equation for the two-dimensional water quality component is a simultaneous set of multiple vertically-integrated two-dimensional convective-dispersion equations, representing each of the modeling constituents in a water column including the reaction and source/sink terms as shown in *Table C.8*.

In the equation, R_i represents the combined biogeochemical reaction and internal source/sink terms arising from the *0-D WQSM* model described in the previous section. The convective terms are driven by the two-dimensional flow fields generated by the aforementioned hydrodynamics component (*2-D HDSM*). The dispersion terms are evaluated as local parameters using the Smagorinsky's *LES* concept.

4.3 Numerical Method of 2-D WQSM

The computational method for the water quality component also utilizes the finite element method that is compatible with the hydrodynamics component and

shares the same mesh. The time-integration method utilizes a special implicit scheme which also eliminates matrix operation as with the case for the hydrodynamics component. The approach allows a significantly larger time step for optimal computational efficiency than those restricted in the usual explicit schemes.

4.4 PARAMETER ADJUSTMENTS FOR 2-D WQSM

The property of the sediment differ between eastern and western basins. The sediment in *Keszthely Bay* has about 3 to 4 times greater settling velocity than in the *Szemes* and *Siófok* basins although it is finer (Somlyódy and Koncsos, 1991). The reason for the higher settling velocity is that during a storm coarser sediment fractions are more readily re-suspended in the shallower *Keszthely Bay*, which settle faster when the wind-speed diminishes. In the *2-D* computations, therefore, calibration of *SS*-related parameters in the eastern basins is also required as previously undertaken for *Keszthely Bay*. Measured *SS* data in the *Siófok* basin have been used for the calibration process in which the best-fit values for settling velocity and critical wave height are 0.018 *cm/s* and 14.3 *cm*. While those for *Keszthely Bay* are 0.022 *cm/s* and 0.0 *cm*, while the differences are distributed in proportion to the square root of the normalized distance from *Keszthely* along the major axis of the lake.

Phosphorus diffusion rate is lower in the *Siófok* basin than that in *Keszthely Bay*, reflecting a difference in the mobilizable phosphorus contents in the sediments in the two areas (Istvánovics, 1988). The maximum diffusion rates of 0.3 and 2.8 $mg\text{-}P/m^2/day$ were reported in the *Siófok* and the *Keszthely* basins in 1980 by Istvánovics (1988), while those measured during the present study in August 1997 are 0.9, 2.2, 2.9, and 2.1 $mg\text{-}P/m^2/day$ on the third day of incubation, respectively, in the *Siófok*, the *Szemes*, the *Szigliget*, and the *Keszthely* basins. Although the variance among the data is rather large, the equilibrium concentrations are varied from a basin to a basin in proportion to the measurement.

4.5 INPUT DATA FOR TWO DIMENSIONAL WATER QUALITY MODEL

The computation period and the time step for *2-D WQSM* are the same as those used in the *0-D WQSM* calculations. The initial values are determined by using measured values of *Chla*, PO_4-*P*, *TP* and *SS* in each of the four basins, and by distributing uniformly within a basin. The four stations of the measurement are indicated in *Figure C.46*. The input data include: daily loads from major rivers; distributed direct runoff from 19 sub-regions; loads by atmospheric deposition; hourly wind record at the *Keszthely* and the *Siófok* stations; daily water-temperature recorded at four stations in each basin; daily total solar radiation measured at the *Keszthely* station; and daily precipitation recorded at the *Akali* and the *Szemes* stations. Since the water temperature varies among the basins,

higher toward the West as shown in *Figure C.72*, measured T_Ws at the four stations are linearly interpolated along the major axis of the lake. The input data, except the solar radiation, are linearly interpolated in time at every time step as in the case of *0-D WQSM* calculations. The daily total solar radiation is distributed sinusoidally from sunrise to sunset in the manner as described in the previous section. The wind magnitudes and directions recorded at the *Siófok* weather station in 1994 and 1995 are shown in *Figures C.73* and *C.74*.

4.6 RESULTS OF 2-D WQSM

Figure C.75 shows computed *SS* distributions in the lake under two distinct wind events on July 4 and August 26 in 1994. In the former case, high concentrations of *SS* prevail in the southern region of *Keszthely Bay* corresponding to the northerly winds of about 5 *m/s* for 5 *hours* measured at the *Keszthely* station. In the latter case, the persistent easterly strong wind blow of 10~14 *m/s* for 12 *hours* at the *Siófok* station resulted in very high concentrations, about 180 $g\text{-}DM/m^3$, in the *Siófok* and the *Szemes* basins.

Figures C.76 and *C.77* show the computed *Chla* distributions in 1994 and 1995 when *Chla* levels reached the maximum during the respective year. As seen in both the figures, the maximum *Chla* concentrations occurred in *Keszthely Bay*, while the minimum spread over the *Siófok* basin. *Figures C.78* and *C.79* are comparisons of the computed and the measured time-series of *Chla* values for 1994 and 1995 at the locations (see *Figure C.46*) where the measurements were taken. The computed time-series of *Chla* for both 1994 and 1995 compare favorably with the measurements at all the locations, capturing the overall trends effectively in the respective year.

Nonetheless, in 1994, *Chla* levels at the *Szigliget* station are considerably lower than the measurements, and in 1995, the computed values somewhat overestimate the measurements in all the basins. Also, in 1994, there are significant phase lags between the computed and measured *Chla* except for the *Keszthely* basin. Whereas in the computed results the *Chla* peaks occur simultaneously in the four basins corresponding to the water temperature peak, the measured *Chla* trails behind the temperature trend, notably eastward to the *Siófok* basin.

Since *C. raciborskii* was the monodominant specie exceeding 90 % of the biomass in the entire lake in 1994 (Présing *et al.*, 1996), variability in algal species among the basins cannot be the reason for the phase lag. Disparities in wind conditions among the basins can also be excluded since the wind data at both the *Keszthely* and the *Siófok* stations were utilized in the simulation. Similarly, inaccuracies in the external load estimate in the eastern basins or variance in the solar radiation, if any, are unlikely to generate such phase lags.

On these rationales, it finally points to the possibility that the water temperature

data not being representative of the reality, as one of the most probable sources for the mismatch in phase. It is recalled that the measuring points are sparse and measurements are infrequent, only once a day in early morning, when the water temperature is expected to be near its daily minimum. In addition, it is well-known that diurnal temperature variance in shallow bodies of water can easily exceed few *Celsius* degrees in a summer climate. On September 3rd ,1997, *JICA Study Team* observed a diurnal variation of vertical water temperature profile at the center of the *Keszthely* basin. Although the day was not a typical summer day, the surface water temperature varied from 22.5 ^{o}C to 25.9 ^{o}C, a difference of 3.4 ^{o}C, while at the depth of 2.5 *m*, it stayed constant at 21.1 ^{o}C. Moreover, it must be that deeper the water, the slower is the water temperature response and, therefore, the daily maximum near-surface temperature is higher in shallower water than in deeper water under a similar external weather forcing. With a 1.5 *m* difference in water depth, on the average, between the *Keszthely* and the *Siófok* basins, it is most likely that the seasonal ascent in surface water temperature during the summer in the *Siófok* basin trails behind that in the *Keszthely* basin. It follows, therefore, that the sparse and infrequent water temperature records measured at an unspecified depth only once a day at 7:00 *am*, cannot represent the transition of daily maxima in the upper water both in terms of their extents and phase lags.

5. CONCLUDING REMARKS

Through detailed calibration studies, the two-dimensional hydrodynamics sub-model has been fully verified by reproducing near-perfectly the recorded water-level fluctuations during several storm events.

The biogeochemical sub-model, being a less exact science, has required an especially rigorous effort in calibration as well as in trial-and-error process for finalizing the model structure. By targeting reproducibility in annual *Chla* levels, and striving to utilize every available information found in the past *Lake Balaton* studies, the *Study Team* has managed to develop a model component that is robust, not excessively sensitive to particular parameters.

The two-dimensional water quality model, an aggregation of the hydrodynamics, and the biogeochemical sub-models as well as a newly-developed two-dimensional mass transport sub-model, has been confirmed to be able to hindcast *Chla* concentrations in the two consecutive years, 1994 and '95, the two contrasting years in terms of algal productivity. The final form of the model is, therefore, believed to be qualified for prediction of *Chla* response of *C. raciborskii* to a variety of weather and nutrient-load conditions.

6. LIST OF REFERENCES

Anderson, M. J., "Nitrogen and phosphorus budgets and the role of sediments in

six shallow Danish lakes," Arch. Hydrobiol. Vol. 74, pp. 528-550.

Baker, R. M., Comparison of Water Quality Models of Keszthely Bay, Lake Balaton, Hungary , M. S. Thesis, submitted in Partial Fulfillment of the Requirements of the Degree of Master of Science in Civil Engineering, at the Massachusetts Institute of Technology, 247 P., September, 1983.

BVK, Balaton Branch Office, H-8600 Siofok, Somogyi B. u. 6., Hungary, "Experimental Thin-Layer Dredging in the Keszthely Basin," 82P., 1992.

Boström B., Jannson M. and Forsberg C. "Phosphorus release from lake sediments. " Arch. Hydrobiol.Vol.18, pp. 5-59,1982

Bowie, G. L., Mills, W. B., Porcella, D.B., Campbell, C. L., Pagenkopf, J. R., Rupp, G. L., Johnson, K. K., Chan, P. W. H., Gherini, S. A., and Chamberlin, C. E. "Rates, Constants, and Kinetics Formulations in Surface Water Quality Modeling," EPA/600/3-85/040, 475 P., June 1985.

CERC, Shore Protection Manual, Vol. 1, U.S. Army Corps of Engineers, Coastal Engineering Research Center, Fort Velvoir, VA, 1977.

Cook, N. J., The designer's guide to wind loading of building structures, Part 1, Butterworth Pub., London, 371 P., 1985.

Di Toro, D. M., "Optics of Turbid Estuarine Waters: Approximations and Applications," Water Research, No.12, pp. 1059-1068, 1978.

Dobolyi E., "Study of the Sediment of Lake Balaton (in Hungarian)," KDT-KÖFE, 1995.

Dobolyi, E. and Ördög, V., "The Phosphorous Accumulation and the Bioavailability of the Phosphorous in Lake Balaton," In: Eutrophication Research, Proceedings at Wageningen, The Netherlands, pp. 63-70., August 1997.

Droop, M. R., "Nutrient Limitation in Osmotrophic Protista," Am. Zoologist, No. 13, pp. 209-214, 1973.

Gelencser, P., Szilágyi, F., Somlyódy, L., and Lijklema, L. "A study on the influence of sediment in the phosphorous cycle in Lake Balaton," Collaborative Paper, CP-82-4, Internat. Inst. Appl. Systems Analy. (IIASA), Laxemburg, Austria, 73 P., July 1982.

Herodek, S., Lacko, L., and Virag, A. Lake Balaton -research and management-, ILEC Pub., 110 P., 1988.

Herodek, S., "Phhytoplankton changes during eutrophication and P and N

metabolism," In: Somlyódy, L., and van Straten, G. (Editors); Modeling and Managing Shallow Lake Eutrophication, Springer Verlag, pp. 183-203, 1986.

Hirayama, A., Nakanishi, M., Miyajima, T., Nakano, S., and Kumagai, M., "Light environment and photosynthesis in the south basin of Lake Biwa: Calibration of water quality model parameters," Vehr. Internat. Verein. Limnol., 25., pp. 811-816, 1993.

IBP (International Biological Programme), Symbols, Units, and Conversion Factors in Studies of Fresh Water Productivity, Winberg, G. G. (Ed), IBP Central Office, London, 23P., 1971.

Istvánovics, V, "Seasonal Variation of Phosphorus Release from the Sediments of Shallow Lake Balaton (Hungary)," Water Res., Vol. 22, No. 12, pp. 1473-1481, 1988

Istvánovics, V, "Differential Response of Blue-Green Algal Groups to Phosphorus Load Reduction in a Large Shallow Lake: Balaton, Hungary," Verh. Internat. Verein. Limnol., Vol. 26, 1996.

Istvánovics, V, Herodek, S, and Szilágyi, F., "Phosphate Adsorption by Different Sediment Fractions on Lake Balaton and Its Protecting Reservoirs," Water Res., Vol. 23, No. 11, pp. 1357-1366, 1989.

Istvánovics, V, Herodek, S., "Estimation of net uptake and leakage rates of orthophosphate from ^{32}P-uptake kinetics by a linear force-flow," Limnol. Oceanogr. Vol. 40, No. 1, pp. 17-32, 1995.

JICA Study Team (SIGMA RELE KFt), "The Study on Environmental Improvement of Lake Balaton: Pollution Load Analysis," 72 P., October 1997.

KDT-KÖFE (Central-Transdanubian Environmental Protection Inspectorate), "Assessment of the Extraordinary Water Quality of Lake Balaton in 1994," Internal Report, Székesfehérvár, 93 P., November, 1994 (in Hungarian).

KDT- KÖVIZIG, "Report about the research in 1988: Revealing blue-green algae processes in Lake Balaton and some research (in Hungarian) ," 33 P., 1988.

KDT- VIZIG, "Research Report on the Effect of Surface Layer Dredging in Keszthely Bay (in Hungarian) ," 1994.

Kóbor, I., "Effects of meteorological and hydrological events on the trophic level of Lake Balaton (in Hungarian)," pp. 19-21, 1997.

Kovács, A., Koncz, E. and Vörös., L., "Changes of cyanobacteria populations in dependence on light intensity (in Hungarian)," pp. 14-16, 1987.

Kutas, T., and Herodeck, S., "Short description of Balaton Eutrophication Model : BEM," Working Paper MS/9, Computer and Automation Institute, Hungarian Academy of Sciences, Budapest , Hungary, 45 P., 1982.

Kutas, T., and Herodeck, S., "A complex model for simulating the Lake Balaton ecosystem," In: Somlyódy, L., and van Straten, G. (Editors); Modeling and managing Shallow Lake Eutrophication, Springer Verlag, pp. 309-322, 1986.

Lerman, J. T., Botkin, D. B., and Likens, G. E., "The assumptions and rationales of a computer model of phytoplankton population dynamics," Limnol. And Oceanogr., Vol. 20, No. 3, pp. 343-364, 1975.

Leonov, A. V., "Mathematical modeling of phosphorous transformation in the Lake Balaton ecosystem," Working Paper WP-80-149, International Institute for Applied Systems Analysis (IIASA), Laxemberg, Austria, 97 P., 1980.

Leonov, A. V., "Modeling and explaing the phophorus dynamics of Lake Balaton, 1976-1979," Working Paper RR-85-3, International Institute for Applied Systems Analysis (IIASA), Laxemberg, Austria, 1985.

Lijklema, L., Gelencsér, P., Szilágyi, P., "Sediments and sediment-water interaction," In: Somlyódy, L. (Editor); Eutrophication of Shallow Lakes: Modeling and Management, IIASA, Laxenburg, Austria, pp. 81-100, 1983.

Lijklema, L., Gelencsér, P., Szilágyi, P., and Somlyódy, L., "Sediment and its interaction with water," In: Somlyódy, L., and van Straten, G. (Editors); Modeling and managing Shallow Lake Eutrophication, Springer Verlag, pp. 157-181, 1986.

Luettich, R. A., and Harleman, D. R. F., "A Comparison of Water Quality Models and Load Reduction Predictions," In: Somlyódy, L., and van Straten, G. (Editors); Modeling and managing Shallow Lake Eutrophication, Springer Verlag, pp. 323-340, 1986.

Luettich, R., Harleman, D. R. F., and Somlyody, L., "Dynamic behavior of suspended sediment concentrations in a shallow lake perturbed by episodic wind events," Limnol. Oceanogr., 35(5), pp. 1050-1067, 1990.

Matsuoka, Y., "An eutrophication model of Lake Kasumigaura (in Japanese)," Res. Rep. Natl. Inst. Environ. Stud. Jpn., R-54-'84, pp. 53-242, 1984.

Muszkálay, L., "La Mesure des Denivellations Longitudinales et Transversales de la Nappe D'Eau du Lac Balaton," ("Measurement of Longitudinal and Transverse Water Surface Denivellations in Lake Balaton" – in French), Hydrology of Lakes and Reservoirs, Symposium of Garda, Vol. 1, IAHS-AISH Pub. No. 70, 100 P., October, 1966.

Padisák, J. and Istvánovics, V., "Differential response of blue-green algal groups to phosphorous load reduction in a large shallow lake: Balaton, Hungary,'' Verh. Internat. Verein. Limnol. 26: (in press), 1996.

Présing, M., Herodek, S., Vörös, V., and Kóbor, I., "Nitrogen fixation, ammonia and nitrate uptake during a bloom of *Cylindrospermopsis raciborskii* in Lake Balaton," Arch. Hydrobiol., Vol. 136, No. 4, pp. 553-562, 1996.

Riley, G. A., "Transparency-chlorophyll relations," Limnol. Oceanograph., Vol. 20, pp. 150-152, 1975.

Ryding, S.-O. and Forsberg, C., "Sediments as a nutrient source in shallow polluted lakes. In: Golterman H.L., (Editor); Interactions Between Sediments and Fresh Water, Junk, The Hague. 1977.

Segerlind, J. L., Applied Finite Element Analysis, Second Edition, John Wiley and Sons, Inc., New York, 427 P., 1984.

Shafik, H. M., Vörös, L., Présing, M., Kobács, A., "Growth of *Cylindrospermopsis raciborskii* in batch and continuous cultures (in Hungarian)," pp. 17-18, 1987.

Shanahan, P., and Harleman, D. R. F., "Linked Hydrodynamic and Biogeochemical Models of Water Quality in Shallow Lakes," Report No. 268, Ralph M. Parsons Laboratory, Dept. Civil Engineering, Massachusetts Institute of Technology, 280 P., March, 1982.

Shapiro, J., "Current beliefs regarding dominance by blue-greens: The case for the importance of CO_2 and pH," Verh. Int. Verein. Limnol., Vol. 24, pp38-54, 1990.

Smagorinsky, J., "General circulation experiments with the primitive equations : 1. The basic experiment," Monthly Weather Review, Vol. 91, No. 3, pp. 99-164, 1963.

Somlyódy, L. and Koncsos, L., "Influence of sediment resuspension on the light conditions and algal growth in Lake Balaton," Ecological Modeling, 57, pp. 173-192, 1991.

Sommer, U., "Sedimentation of principal phytoplankton species in Lake Constance," J. Plankton Res., Vol. 6, pp. 1-14, 1984.

Tezuka., Y., "The C:N:P ratio of *Microcystis* and *Anabaena* (blue-green algae) and its importance for nutrient regeneration by aerobic decomposition," Jpn. J. Limnol., Vol. 50, No. 2, pp. 149-155, 1989.

Tóth, L., Oláh, J. and Tóth, E. O., "Phosphorus metabolism of Lake Balaton,"

Report for the Committee of Lake Balaton Management (in Hungarian), 1975

Tóth, L. G. and Padisák, J., "Meteorological factors affecting the bloom of *Anabaenopsis raciborskii* Wolosz. (Cyanophyta: Hormogonales) in the shallow Lake Balaton," J. Plankton Research, Vol. 8, No. 2, pp. 353-363, 1986.

van Straten, G., "Analysis of model and parameter uncertainty in simple phytoplankton models for Lake Balaton," In: Dubois, D. M. (Editor); Progress in Ecological Engineering and Management by Mathematical Modeling, Editions, Cebedoc, Liege, Belgium, pp. 107-134, 1980.

van Straten, G., and Somlyódy, L., "Lake Balaton Eutrophication Study: Present Status and Future Program," Working Paper, WP-80-187, Internat. Institute for Applied Systems Analysis (IIASA), Laxenburg, Austria, 73 P., December 1980.

van Straten, G. "Lake Eutrophication Models," In: Somlyódy, L., Herodek S., and Fischer, J. (Editors); Eutrophication of Shallow Lakes: Modeling and Management, Proc. Workshop, Internat. Inst. Applied System Analysis (IIASA), Laxemburg, Austria, pp. 175-206, 1983.

Wu, J., "Prediction of Near-Surface Drift Current from Wind Velocity, " J. Hydrauric Div., ASCE 99, 1973.

Table C.1 Two Dimensional Hydrodynamics Equations

$$\frac{\partial H}{\partial t}+\frac{\partial q_x}{\partial x}+\frac{\partial q_y}{\partial y}=0 \quad \cdots\cdots (1)$$

$$\frac{\partial q_x}{\partial t}+\frac{\partial}{\partial x}\left(\frac{q_x^2}{H}\right)+\frac{\partial}{\partial y}\left(\frac{q_x q_y}{H}\right)$$
$$= -\frac{\partial N_p}{\partial x}+\frac{1}{\rho}\left(\frac{\partial N_{xx}}{\partial x}+\frac{\partial N_{yx}}{\partial y}\right)+fq_y+\frac{1}{\rho}\left(\tau_{sx}-\tau_{bx}\right)+g\eta\frac{\partial h}{\partial x} \quad \cdots\cdots (2)$$

$$\frac{\partial q_y}{\partial t}+\frac{\partial}{\partial x}\left(\frac{q_x q_y}{H}\right)+\frac{\partial}{\partial y}\left(\frac{q_y^2}{H}\right)$$
$$= -\frac{\partial N_p}{\partial y}+\frac{1}{\rho}\left(\frac{\partial N_{yy}}{\partial y}+\frac{\partial N_{xy}}{\partial x}\right)-fq_x+\frac{1}{\rho}\left(\tau_{sy}-\tau_{by}\right)+g\eta\frac{\partial h}{\partial y} \quad \cdots\cdots (3)$$

$$N_{ij}=\left\langle \tau_{ij}+\rho u_i' u_j' \right\rangle \equiv \int_{-h}^{\eta}\left(\tau_{ij}+\rho u_i' u_j'\right)dz \cong \rho\varepsilon_{ij}\left(\frac{\partial q_i}{\partial x_j}+\frac{\partial q_j}{\partial x_i}\right) \quad ;(i,j=x,y) \quad \cdots\cdots (4)$$

$$N_p=g\eta h+\frac{1}{2}g\eta^2 \quad \cdots\cdots (5)$$

$$\tau_{sx}=\rho_{air}C_D U^2 cos\theta_w \quad \cdots\cdots (6) \qquad \tau_{sy}=\rho_{air}C_D U^2 sin\theta_w \quad \cdots\cdots (7)$$

$$\tau_{bx}=\frac{C_f \rho q_x\sqrt{q_x^2+q_y^2}}{H^2} \quad \cdots\cdots (8) \qquad \tau_{by}=\frac{C_f \rho q_y\sqrt{q_x^2+q_y^2}}{H^2} \quad \cdots\cdots (9)$$

where q_i =mass flux per unit width; h =depth; η =surface elevation; $H=h+\eta$; f =Corioli's parameter; g =gravitational acceleration; ε =eddy viscosity; ρ_{air} =air density; τ_s =wind stress; τ_b =bottom shear stress; U =wind speed at 10 m above the water surface; C_D =drag coefficient (Wu, 1973); θ_w =angle between the wind direction and the x axis; friction coefficient $C_f=n^2gH^{-1/3}$; n =Manning's roughness coefficient.

Table C.2 0-D WQSM Equations

Dissolved inorganic phosphorus: P_1 [mg-P/m^3]

$$\frac{dP_1}{dt} = -k_f P_1 - k_u \frac{P_1 B}{P_{1k} + P_1} \frac{\psi_{max} - \psi}{\psi_{max} - \psi_{min}} + k_m \theta_m^{T_w - 20} P_3 + (1 - f_{op}) d_p \theta_p^{T_w - 20} P_2 + Sop(SS) + c_{ex}(P_{eq} \theta_m^{T_w - 20} - P_1) + L_1$$

Algal phosphorus: P_2 [mg-P/m^3]

$$\frac{dP_2}{dt} = -k_f P_2 + k_u \frac{P_1 B}{P_{1k} + P_1} \frac{\psi_{max} - \psi}{\psi_{max} - \psi_{min}} - d_p \theta_p^{T_w - 20} P_2 - \frac{v_{s4}}{h} P_2 + L_2$$

Algal biomass: B [mg dry-wt/m^3]

$$\frac{dB}{dt} = -k_f B + \mu_{max} f(\psi) f(I) f(T) B - d_p \theta_p^{T_w - 20} B - \frac{v_{s4}}{h} B + L_B$$

Detrital phosphorus: P_3 [mg-P/m^3]

$$\frac{dP_3}{dt} = -k_f P_3 + f_{op} d_p \theta_p^{T_w - 20} P_2 - k_m \theta_m^{T_w - 20} P_3 - \frac{v_{s3}}{h}(1 - r) P_3 + L_3$$

Chla [mg/m^3]

$$Chla = B / \left(\frac{\alpha I_{opt}}{\mu_{max} e} c_{b/c}\right)$$

where

k_f: flushing rate
k_u: maximum uptake rate
P_{1k}: half-saturation constant for uptake
ψ: cell quota, $\psi = P_2/B$
ψ_{max}, ψ_{min}: maximum and minimum cell qotas
d_p: mortality rate
θ_p: temperature factor for mortality
v_{s3}: settling rate of detritus
v_{s4}: settling rate of algae
h: depth
L_i: external loads
μ_{max}: maximum specific growth rate
$f(\psi)$: cell quota growth limiting factor,
α: initial slope of P-I curve
I_{opt}: optimum light intensity

$$f(T) = \exp[-2.3 \left(\frac{T - T_{opt}}{T_x - T_{opt}}\right)^2]$$

$$T_x = T_{min} \quad for \quad T \le T_{opt}$$
$$= T_{max} \quad for \quad T > T_{opt}$$

c_{ex}: exchange coefficient of the sediment phosphorus release
P_{eq}: equilibrium concentration of the sediment phosphorus release
$c_{b/c}$: ratio of algal biomass to carbon

$f(\psi) = 1 - \psi_{min}/\psi$
$f(T)$: temperature limiting factor
T_{min}: minimum temperature for algal growth
T_{max}: maximum temperature for algal growth
T_{opt}: optimal temperature for algal growth
$f(I)$: light limiting factor (see *Table* 5.3)
k_m: mineralization rate
θ_m: temperature factor for mineralization
$Sop(SS)$:sorption as a function of suspended sediments
f_{op}: fraction of organic phosphorus in TP contained in dead phytoplankton
γ: fraction of detritus that is dissolved

Table C.3 Modified Steele's Light Limiting Function for Non-light Inhibition

Conventional Steele's light limiting function is modified to non-inhibiting function as follows.

$$f(I) = \begin{cases} 1 & \text{for } I \geq I_s \quad \text{----------(1)} \\ \frac{I}{I_s}\exp(1-\frac{I}{I_s}) & \text{for } I < I_s \quad \text{----------(2)} \end{cases}$$

where I = light intensity in the water column: $I = I_0 e^{-K_e z}$, z = distance from the water surface, I_s = saturation light intensity, I_0=surface light intensity, K_e = extinction coefficient.

At the depth, where light intensity reaches a saturation light intensity, $I = I_s \quad at \quad h_s \quad \rightarrow \quad I_s = I_0 e^{-K_e h_s}$.

The depth of a saturation light intensity can be induced as,

$$h_s = -\frac{1}{k_e}\ln\frac{I_s}{I_0}$$

Integrating equation (2) over $z = h_s \sim h$ and taking its average, equations (1), (2) can be converted as,

$$\overline{f}_1(I) = 1 \qquad \text{for } z = 0 \sim h_s \qquad \text{---- (3)}$$

$$\overline{f}_2(I) = \frac{e}{k_e(h-h_s)}\left\{\exp(-ae^{-k_e h}) - \exp(-ae^{-k_e h_s})\right\} \qquad \text{for } z = h_s \sim h \qquad \text{---- (4)}$$

where $a = \frac{I_0}{I_s}$

For all the depth, equations (3) and (4) are combined as,

$$\overline{f}(I) = \frac{1}{h}\left\{h_s + (h-h_s)\overline{f}_2(I)\right\} \qquad \text{---- (5)}$$

Table C.4 Suspended Sediment Model Equations (Luettich *et al.*, 1990)

$$\tilde{c} = c_e + c_{bak} + (\tilde{c}_i - c_e - c_{bak}) \exp[-\frac{\beta}{h}(t - t_i)]$$

where

$\tilde{c}$: depth-averaged suspended sediment concentration, $\tilde{c} \equiv \int_{-h}^{0} \bar{c}\, dz$

$\tilde{c}_i$: initial condition of $\tilde{c}$ at $t = t_i$

c_e: equilibrium suspended sediment concentration, $c_e = K[\frac{H - H_C}{H_{ref}}]^n$

H, H_{ref}, H_C: wave height, reference wave height, and critical wave height
n: model parameter
β: settling velocity
c_{bak}: non-settling background suspended sediment concentration
K: model parameter (mg/l)

Wave height equations (CERC, 1974),

$$\frac{gH}{U_{10}^2} = 0.283 \tanh[\alpha] \tanh[\frac{\gamma}{\tanh \alpha}]$$

$$\alpha = 0.53\,(gh / U_{10}^2)^{0.75}$$

$$\gamma = 0.125\,(gF / U_{10}^2)^{0.42}$$

where
g = gravitational acceleration
U_{10}= wind speed at 10m above the water surface
F = effective fetch

Table C.5 Phosphorus Concentrations in the Sediment of Lake Balaton (Dobolyi, 1995)

Average values of 11 sediment samples in 1978

Sampling depth cm	CDB extracted P μg/g	NaOH extracted P μg/g	HCL extracted P μg/g	Total Extracted P μg/g	Total P μg/g
0-5	229	20.2	227	476	618
5-10	232	19.4	216	468	626
10-15	195	19.0	239	453	593
15-20	172	19.9	261	453	580
20-25	141	16.4	281	438	567
25-30	138	14.2	273	425	551

Average values of 11 sediment samples in 1995

Sampling depth cm	CDB extracted P μg/g	NaOH extracted P μg/g	HCL extracted P μg/g	Total Extracted P μg/g	Total P μg/g
0-5	61.8	248	269	557	788
5-10	61.0	187	296	526	758
10-15	63.4	145	288	483	746
15-20	59.9	103	327	495	692
20-25	56.1	108	307	472	725
25-30	54.5	99.5	318	473	675

Table C.6 Parameter Values for Completely-mixed Biogeochemical Model Calculations

Descriptions	symbol in equations	terms in graphs	unit	standard value	Reference
maximum cell quota	q_{max}	*psi_max*	ND	0.018	Shafik *et al.*, 1987
minimum cell quota	q_{min}	*psi_min*	ND	0.002	Shafik *et al.*, 1987
maximum P uptake rate	k_u	*p_up_max*	1/day	1.5	Shafik *et al.*, 1987
half-saturation constant for P uptake	P_{1k}	*half_sat*	mg/m^3	18.0	Shafik *et al.*, 1987
mineralization rate	k_{m0}	*R_mineral*	1/day	0.04	Tezuka,1989
temperature correction factor for mineralization	θ_m	*T_mineral*	ND	1.18	Tezuka,1989
death rate	d_{p0}	*R_mortal*	1/day	0.092	Bowie *et al.*, 1985
temperature correction factor for death	θ_p	*T_mortal*	ND	1.04	Bowie *et al.*, 1985
maximum specific growth rate	μ_{max}	*Growth_max*	1/day	1.8	Shafik *et al.*, 1987
surfase area of Keszthely bay	A	-	km^2	38	Herodek *et al.*, 1988
settling rate of algal biomass	v_{s3}	*Ws-bmass*	m/d	0.01	Sommer,1984
settling rate of detritus	v_{s4}	*Ws-det*	m/d	0.05	Sommer,1984
fraction of organic-P in dead algal-P	f_{op}	*Fop*	ND	0.7	Tezuka,1989
fraction of detritus that is dissolved	r	*gamma*	ND	0.1	Tezuka,1989
initial slope of P-I curve	α	*alpha*	mg C/mg Chla/ly	2.6	Balaton Limnol.Res.Inst., 1996
biomass carbon ratio	C_{bc}	*P/C ratio*	mg d.w./mg C	0.02	IBP,1971
equilibrium concentration of PO_4-P in the sediment	*P_eq*	*P_eq*	mg P/m^3	30	Istvanovics *et al.*, 1989
exchange coefficient of sediment P-release	*C_ex*	*C_ex*	1/day	0.15	
P-desorption rate	$\Delta C/ss$	*P_release*	mg P/g DM	0.008	Gelencser *et al.*, 1982
			ND=no unit		

Table C.7 Parameters for Sensitivity Study

Case I

ψ_{min} (mg P/mg DW)	ψ_{max} (mg P/mg DW)	μ_{max} (1/day)	Case No.	Figure No.
0.0015	0.018	1.7	I-1	F.1
0.0020		1.8	I-2	F.2
0.0025		2.0	I-3	F.3
0.0030		2.1	I-4	F.4
0.0035		2.2	I-5	F.5

Case II

ψ_{min} (mg P/mg DW)	ψ_{max} (mg P/mg DW)	μ_{max} (1/day)	Case No.	Figure No.
0.002	0.010	1.80	II-1	F.6
	0.015	1.80	II-2	F.7
	0.020	1.80	II-3	F.8
	0.025	1.80	II-4	F.9
	0.030	1.80	II-5	F.10

Case III

k_u (mg P/mg DW/day)	P_{1k} (mg P/m^3)	Case No.	Figure No.
1.5	10	III-1	F.11
3.0	40	III-2	F.12
6.0	60	III-3	F.13
9.0	80	III-4	F.14

Case IV

$\Delta C/ss$ (mg P/g DM)	Case No.	Figure No.	Peq (mg P/m^3)	Case No.	Figure No.	Cex (1/day)	Case No.	Figure No.
0.004	IV-1	F.15	10	IV-5	F.19	0.05	IV-9	F.23
0.008	IV-2	F.16	30	IV-6	F.20	0.15	IV-10	F.24
0.02	IV-3	F.17	50	IV-7	F.21	0.3	IV-11	F.25
0.1	IV-4	F.18	100	IV-8	F.22	0.5	IV-12	F.26

Case V

k_u (mg P/mg DW/day)	P_{1k} (mg P/m^3)	Fop	Case No.	Figure No.
0.5	3.0	0.7	V-1	F.27
	5.0		V-2	F.28
	8.0		V-3	F.29
	3.0	0.9	V-4	F.30
	5.0		V-5	F.31
	8.0		V-6	F.32
1.5	18.0	0.7	V-7	F.33
	40.0		V-8	F.34
	80.0		V-9	F.35
	18.0	0.9	V-10	F.36
	40.0		V-11	F.37
	80.0		V-12	F.38

Case VI

Topt(° C)	Tmin(° C)	Case No.	Figure No.
28	18	VI-1	F.39
	19	VI-2	F.40
29	18	VI-3	F.41
	19	VI-4	F.42
30	18	VI-5	F.43
	19	VI-6	F.44

Case VII

Constant depth (m)	Constant volume	Case No.	Figure No.
1.98	7.17×10^7	VII-1	F.45
2.42	8.77×10^7	VII-2	F.46

Table C.8 Two Dimensional Mass Transport Equations

$$\frac{\partial C_i}{\partial t} + \frac{\partial\left((q_x/H)C_i\right)}{\partial x} + \frac{\partial\left((q_y/H)C_i\right)}{\partial y}$$

$$= -\frac{\partial M_x}{\partial x} - \frac{\partial M_y}{\partial y} \pm R_i \quad ; i = 1, 4 \cdots\cdots (1)$$

$$C_i = \int_{-h}^{\eta} c_i dz = \bar{c}_i H \cdots\cdots (2)$$

$$M_x = -E_{xx} H \frac{\partial \bar{c}_i}{\partial x} - E_{xy} H \frac{\partial \bar{c}_i}{\partial y} \cdots (3)$$

$$M_y = -E_{yx} H \frac{\partial \bar{c}_i}{\partial x} - E_{yy} H \frac{\partial \bar{c}_i}{\partial y} \cdots (4)$$

where

C_i =consituent concentration per unit area

$\bar{c}_i$ =depth average concentration

$H = h + \eta$; h = depth, η = surface elevaton

R_i=internal reactive source/sink;

E_{xx}, E_{xy} =longitudinal and lateral dispersion coefficient.

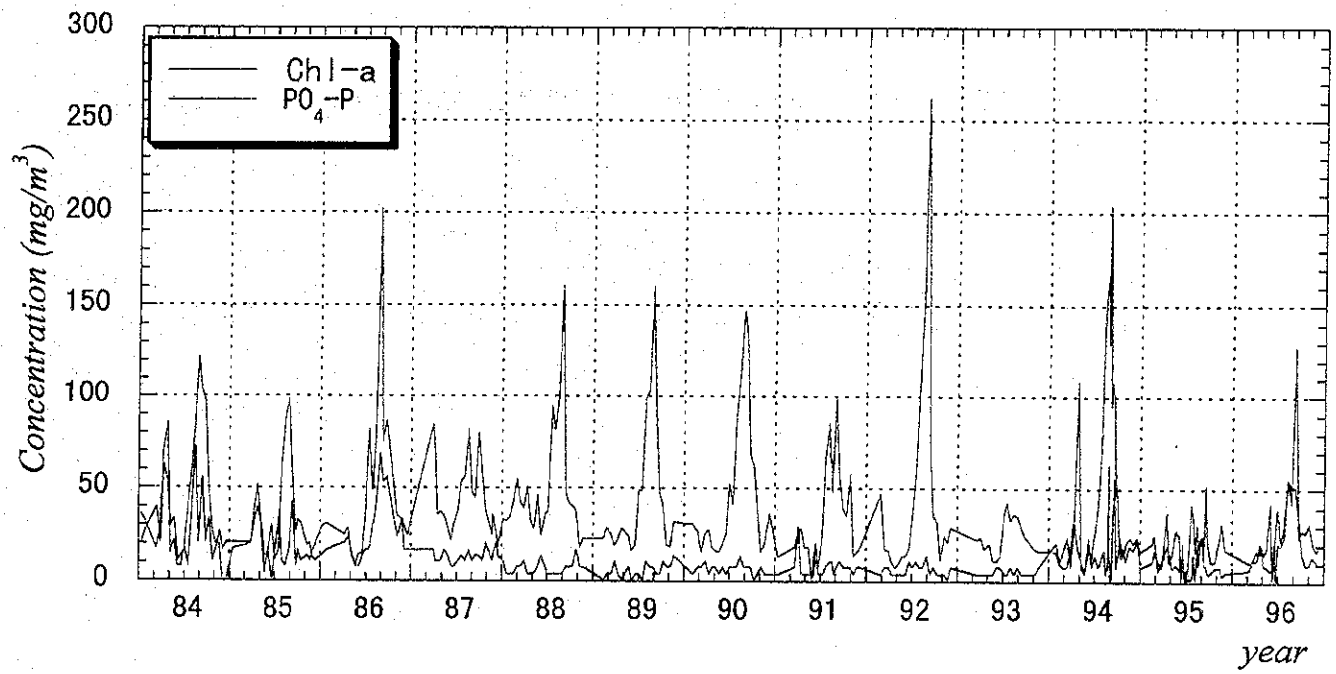

Figure C.1 Water Quality Transition during 1984-1996 in Keszthely Bay (KDT-KÖFE)

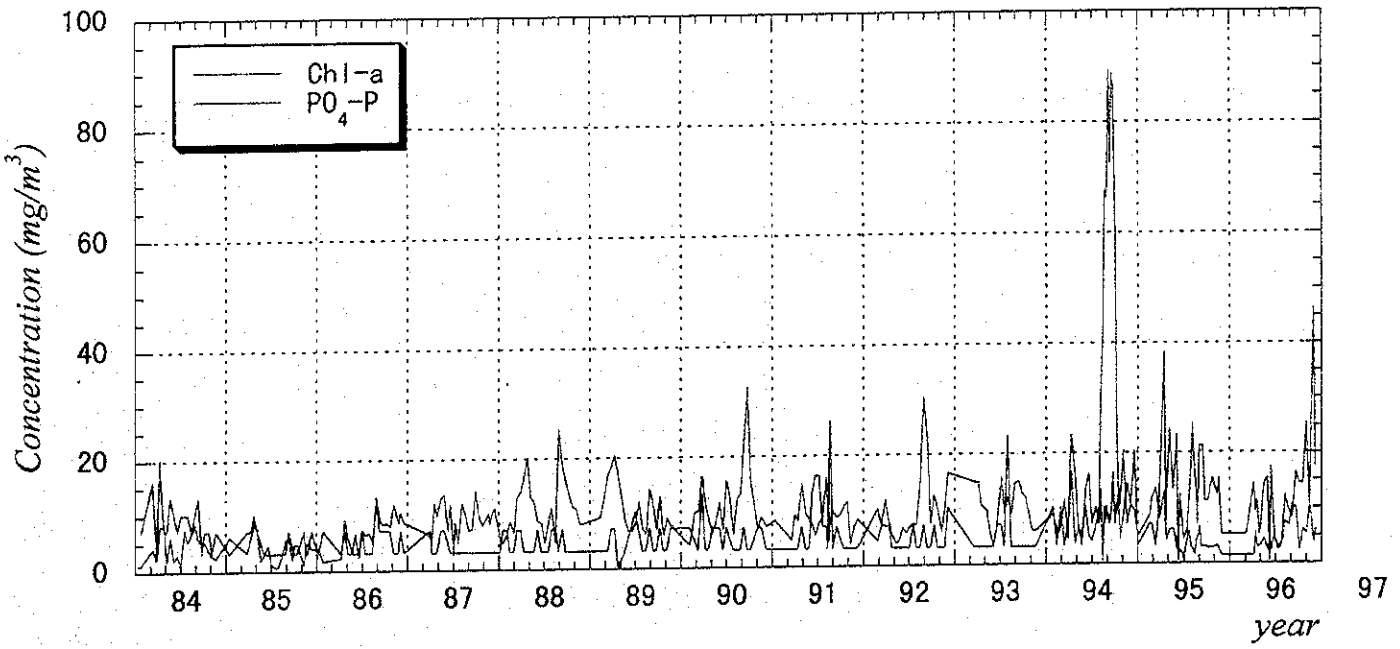

Figure C.2 Water Quality Transition during 1984-1996 in Siófok Basin (KDT-KÖFE)

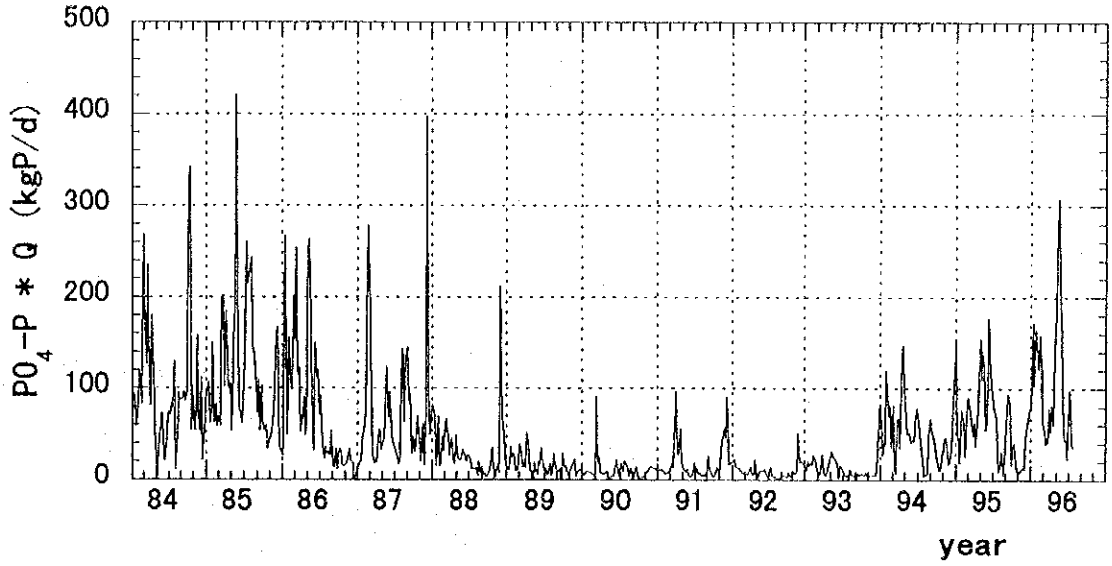

(a) PO_4-P loading from Zala river

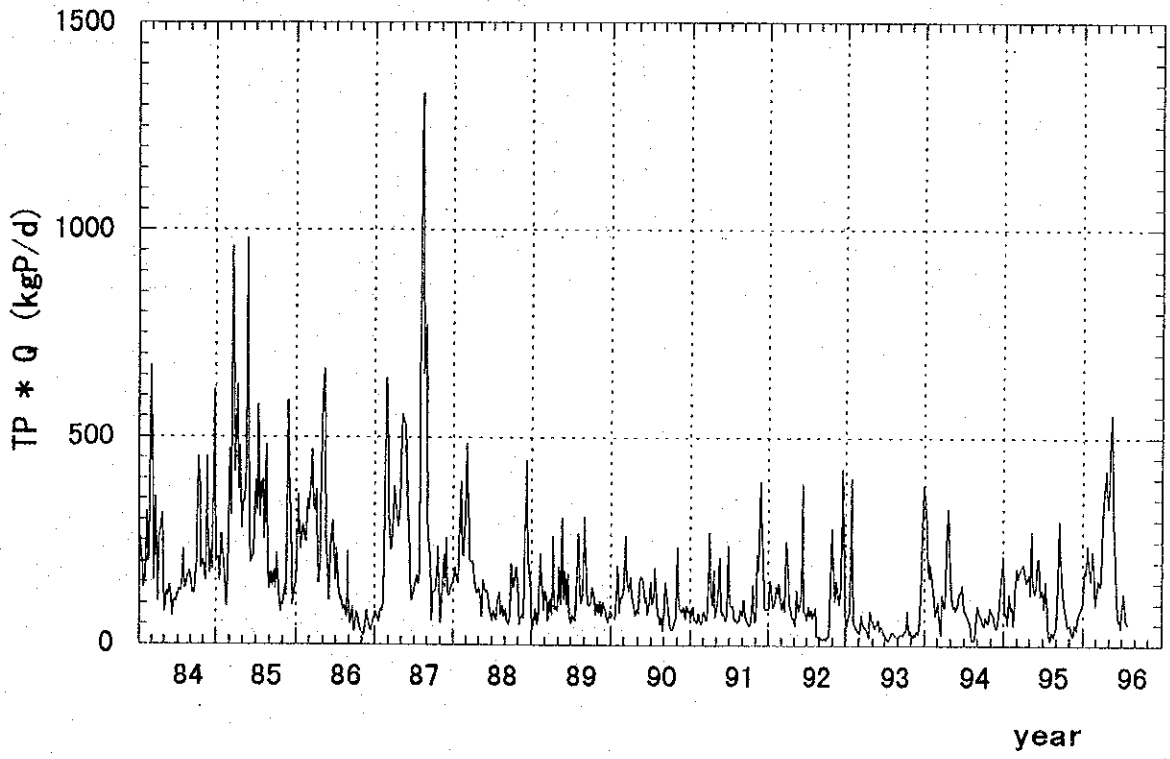

(b) Total phosphorus (TP) loading from Zala river

Figure C.3 PO_4-P and TP Loads from Zala River

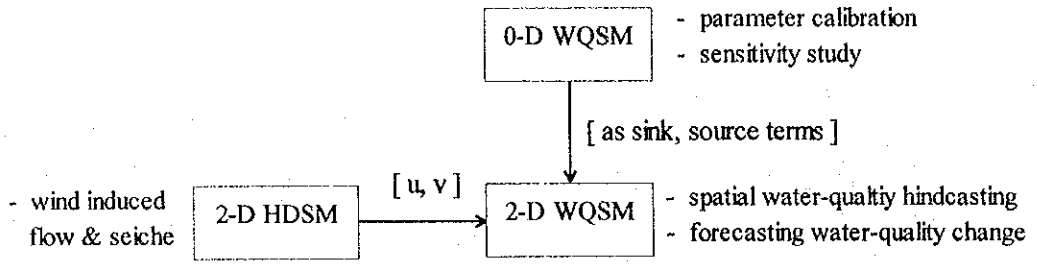

Figure C.4 Conceptual Structure of WQSM

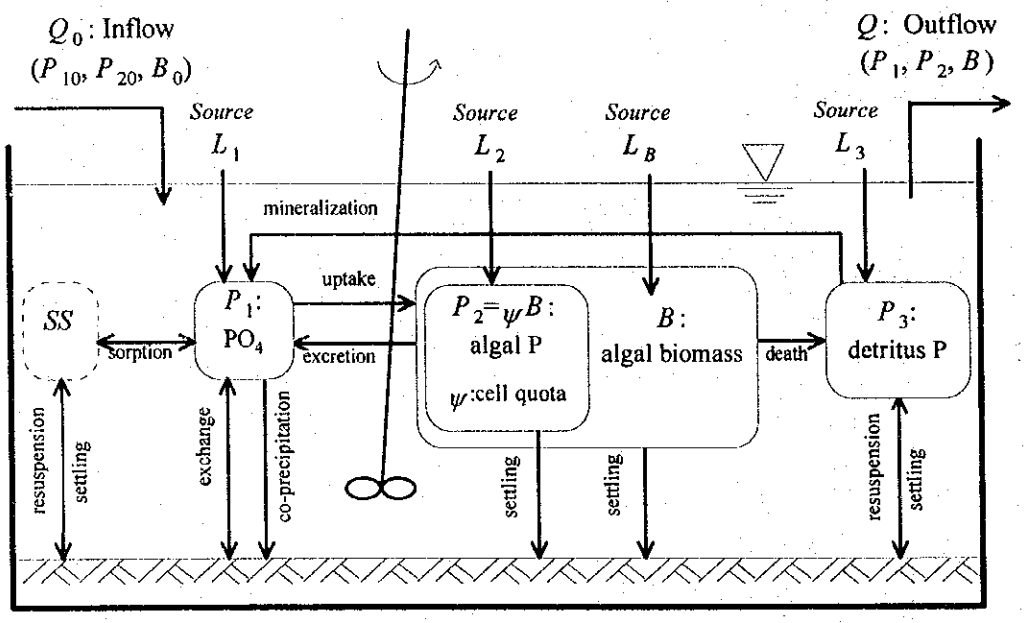

Figure C.5 Conceptual Structure of 0-D WQSM

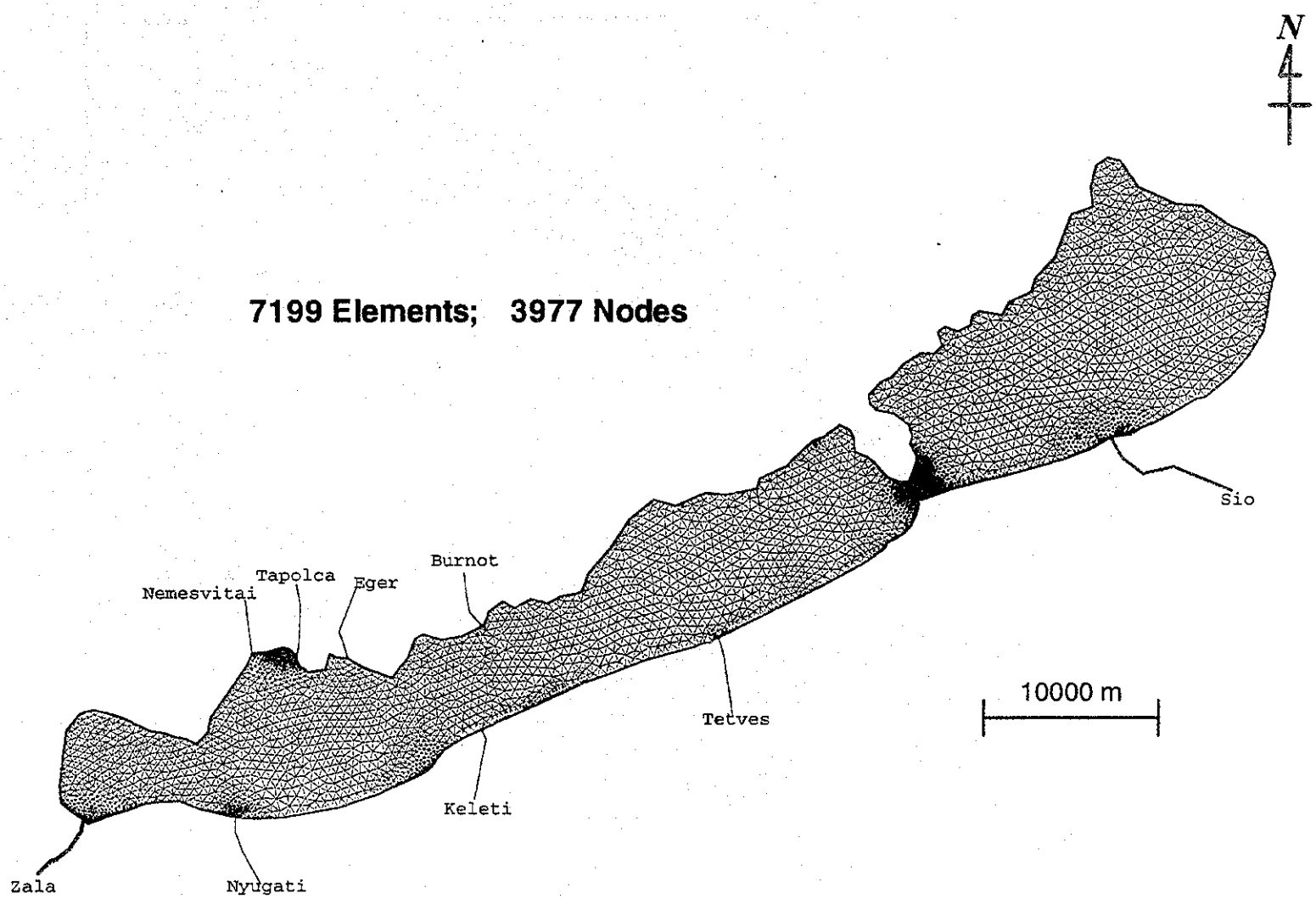

Figure C.6 Finite Element Mesh for Lake Balaton

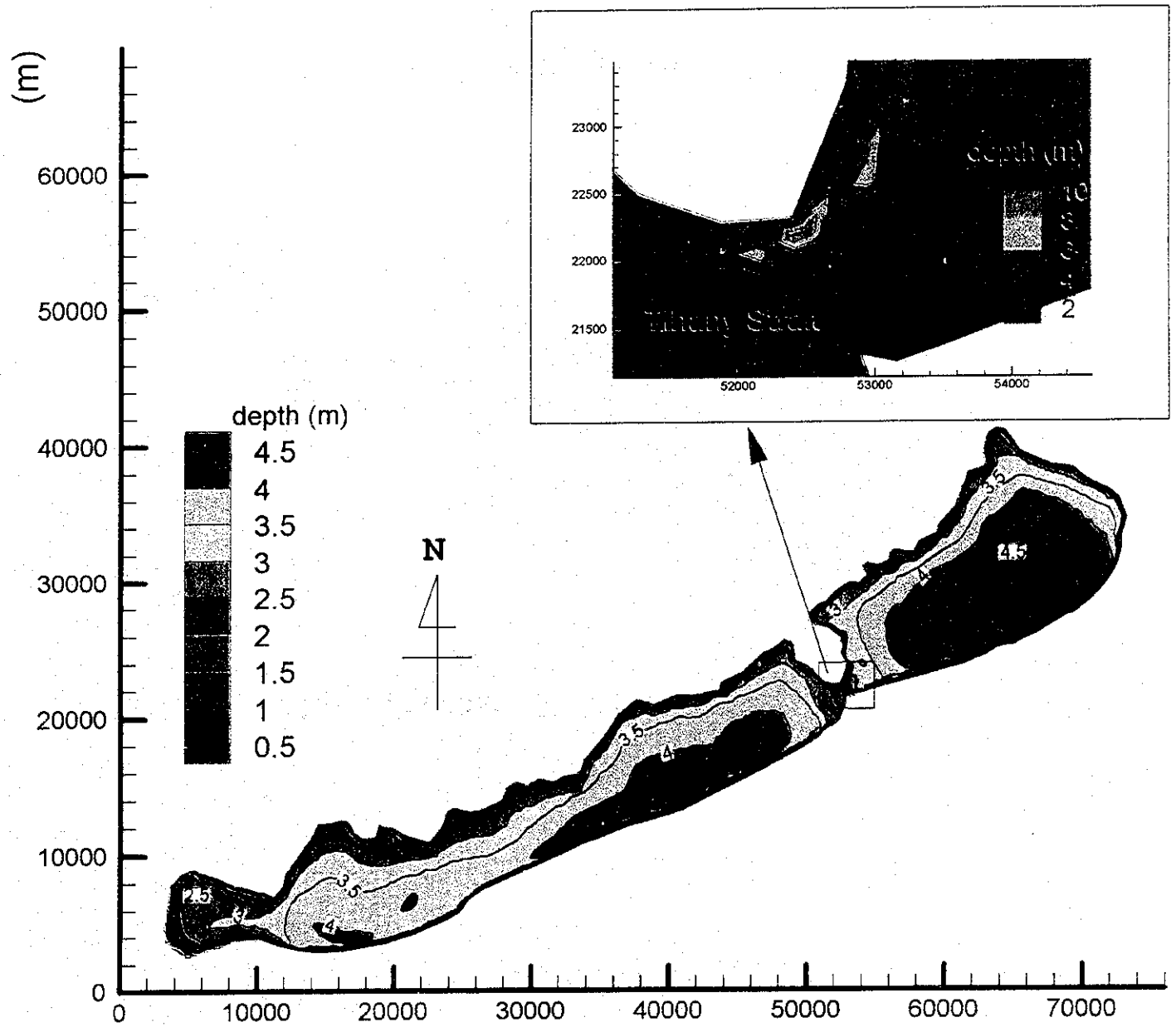

Figure C.7 Depth Contours of Lake Balaton

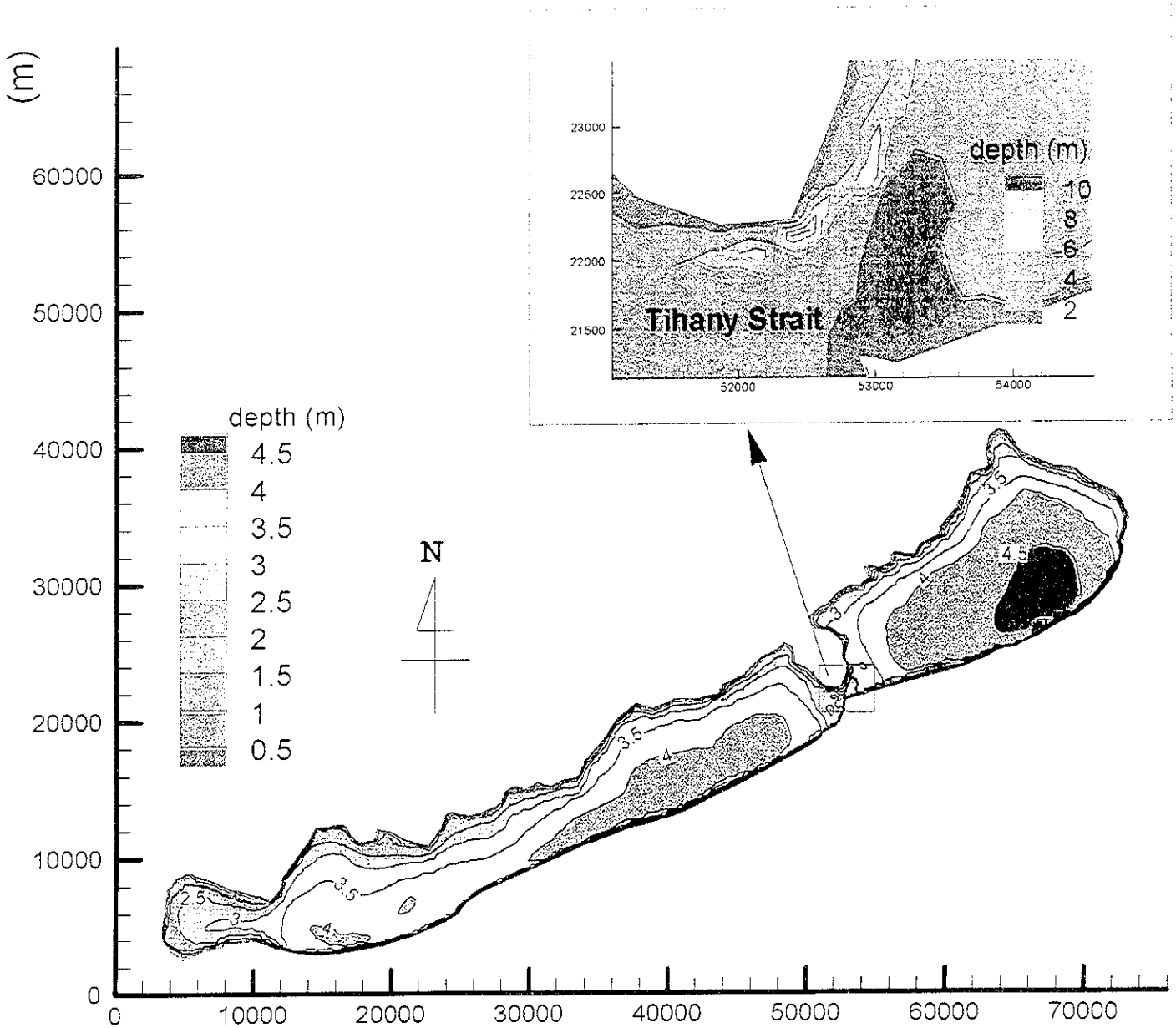

Figure C.7 Depth Contours of Lake Balaton

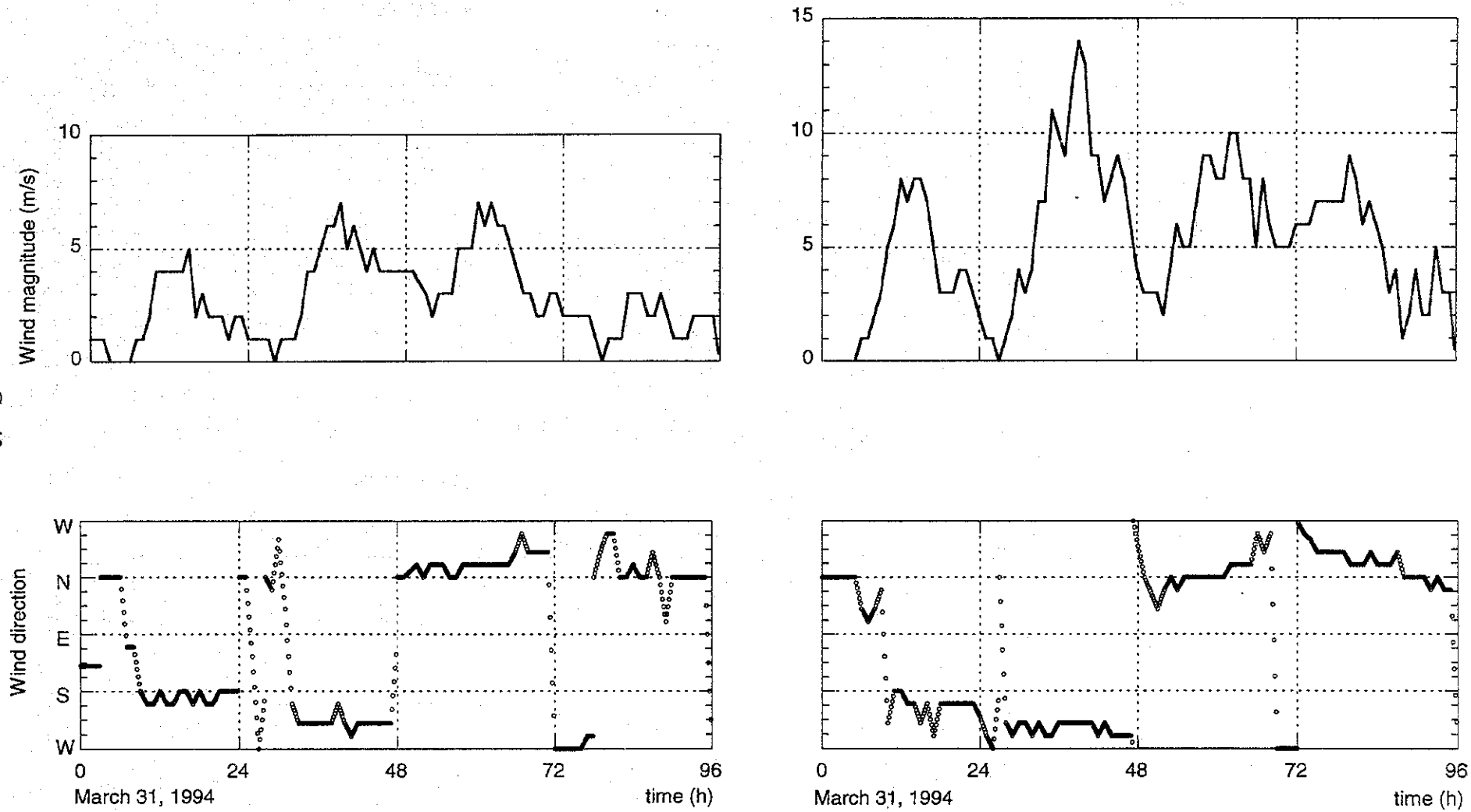

(a) Kestzthely

(b) Siofok

Figure C.8 Wind Speed and Direction during Storm Event, 31 March - 3 April, 1994 (OMSZ)

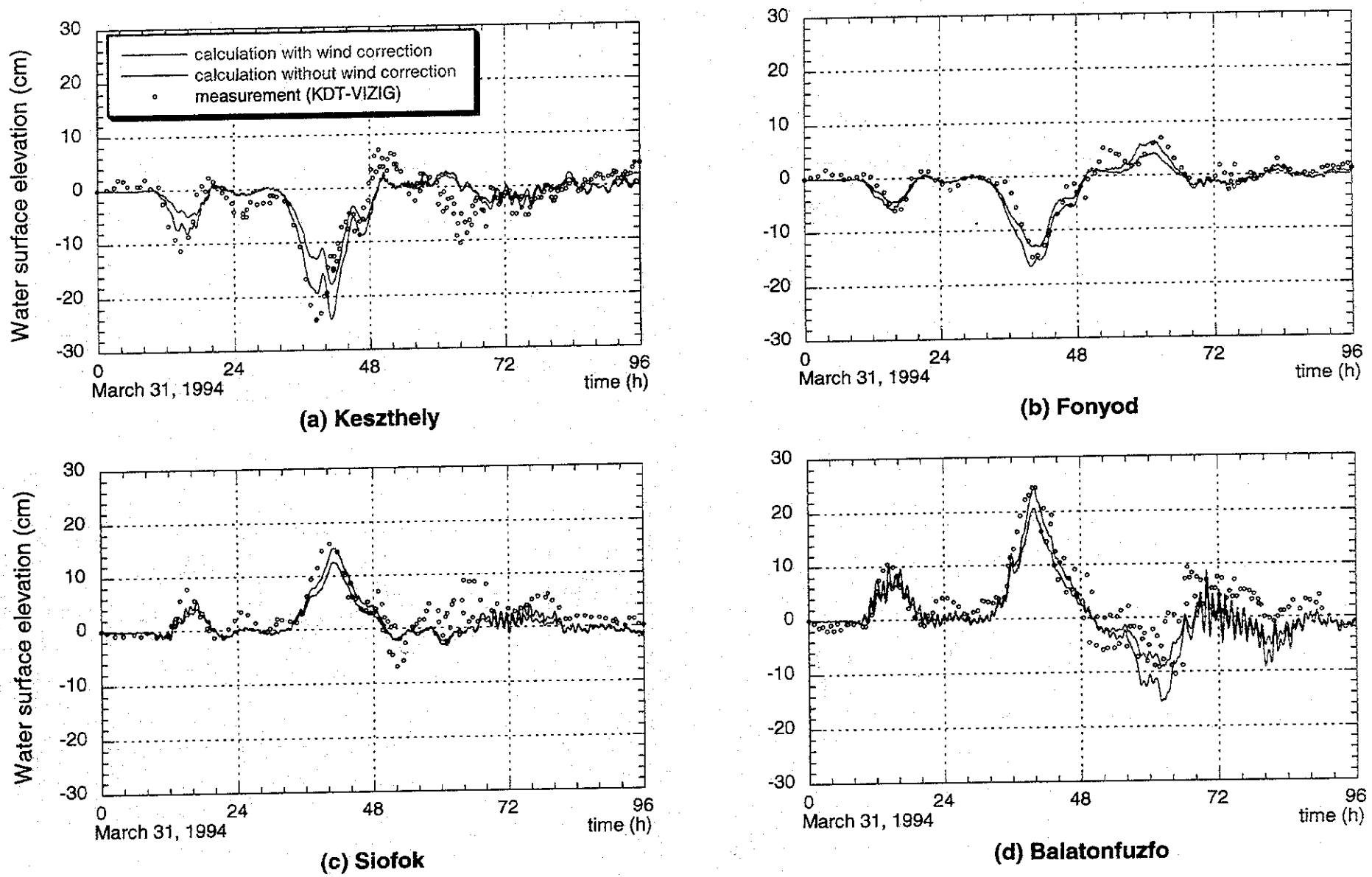

Figure C.9 Sensitivity of Predicted Seiche to Wind Speed Correction

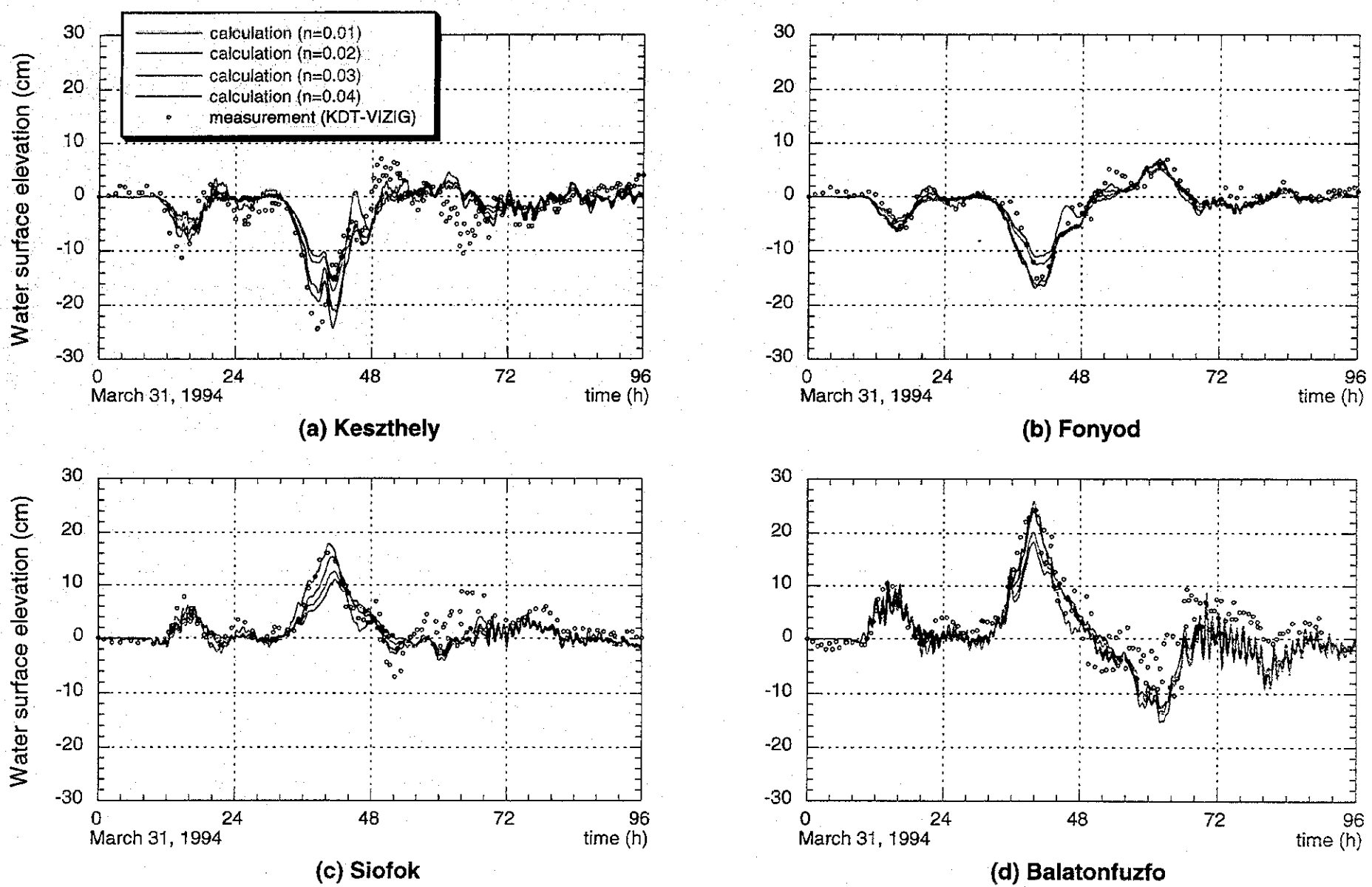

Figure C.10 Sensitivity of Predicted Seiche to Manning's Roughness Coefficient

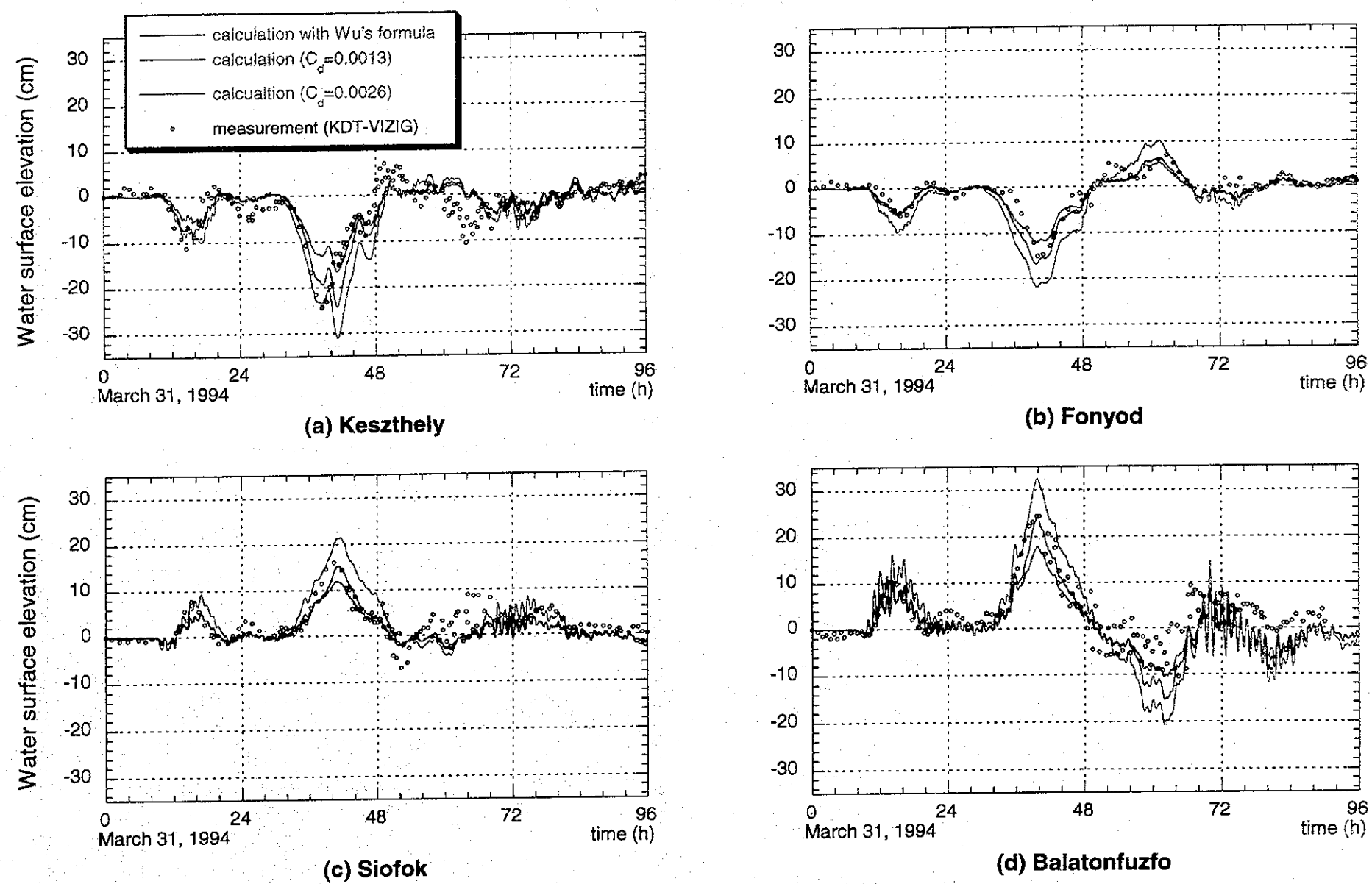

Figure C.11 Sensitivity of Predicted Seiche to Wind Shear Drag Coefficient

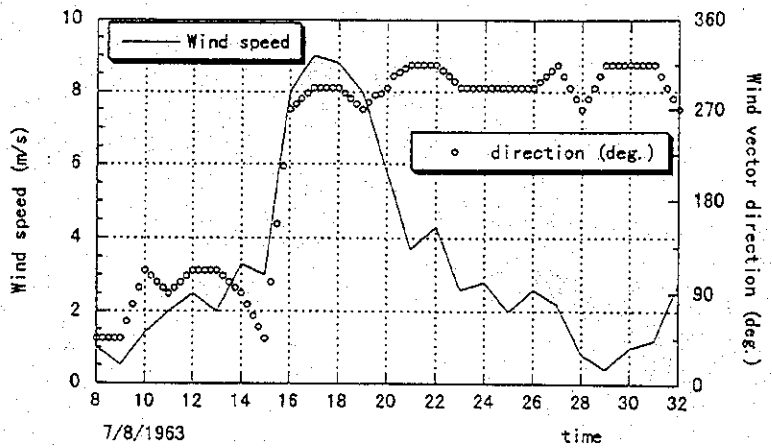

(c) Wind speed and direction

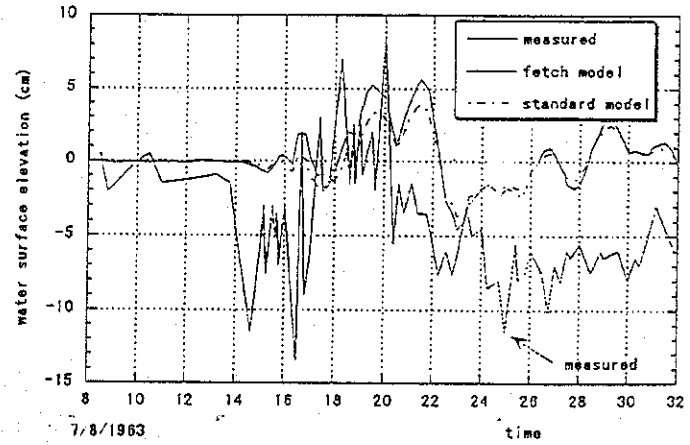

(a) Water surface elevation at Keszthely

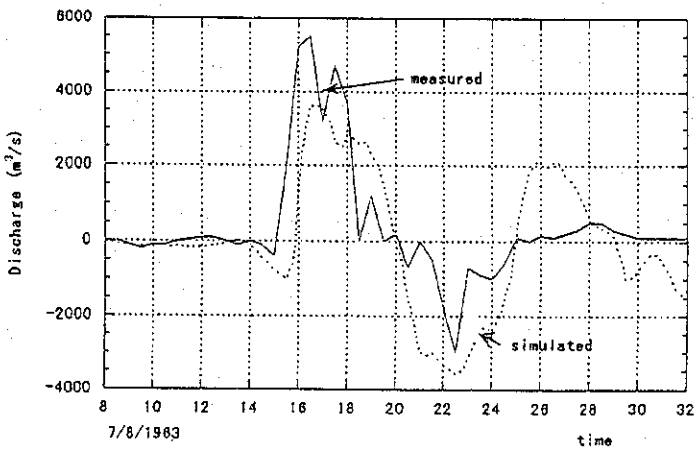

(d) Discharge at Tihany strait

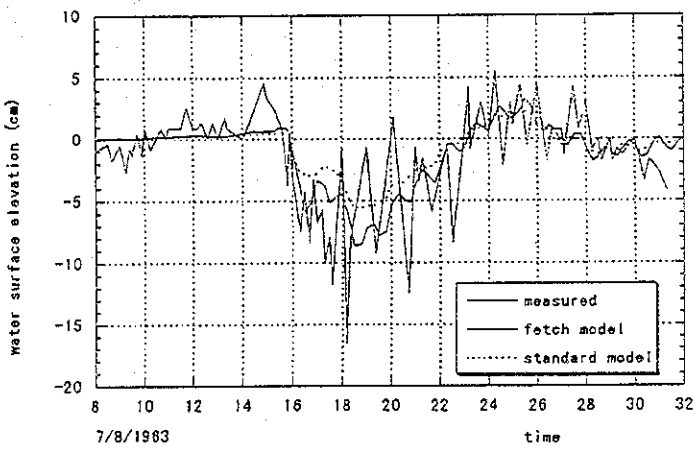

(b) Water surface elevation at Balatonkenese

Figure C.12 Water Surface Elevation and Discharge Time-series during Storm Event, 8-9 July, 1963 (measured data from Muszkálay)

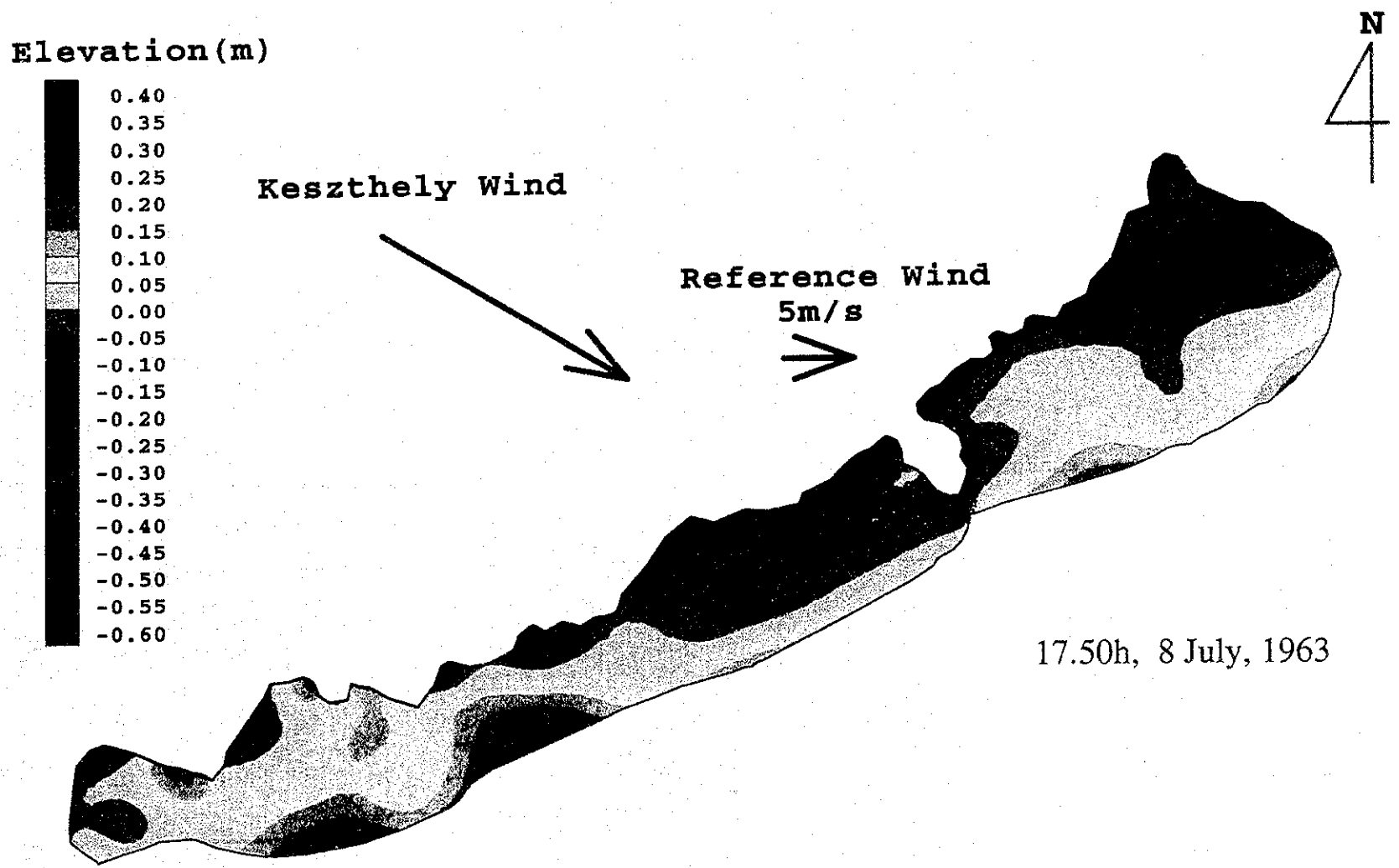

Figure C.13 Water Surface Elevation during Storm Event, 8-9 July, 1963

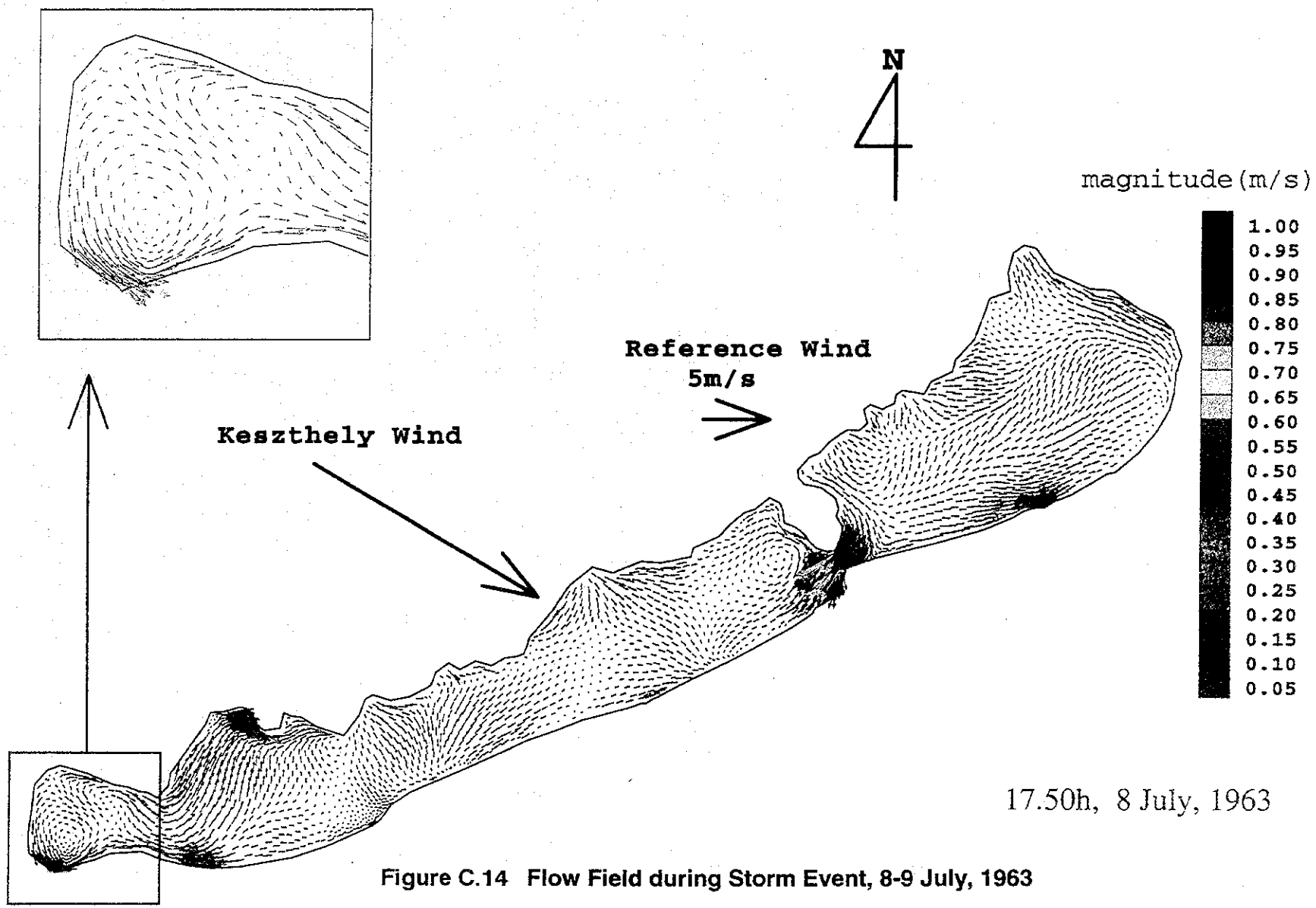

Figure C.14 Flow Field during Storm Event, 8-9 July, 1963

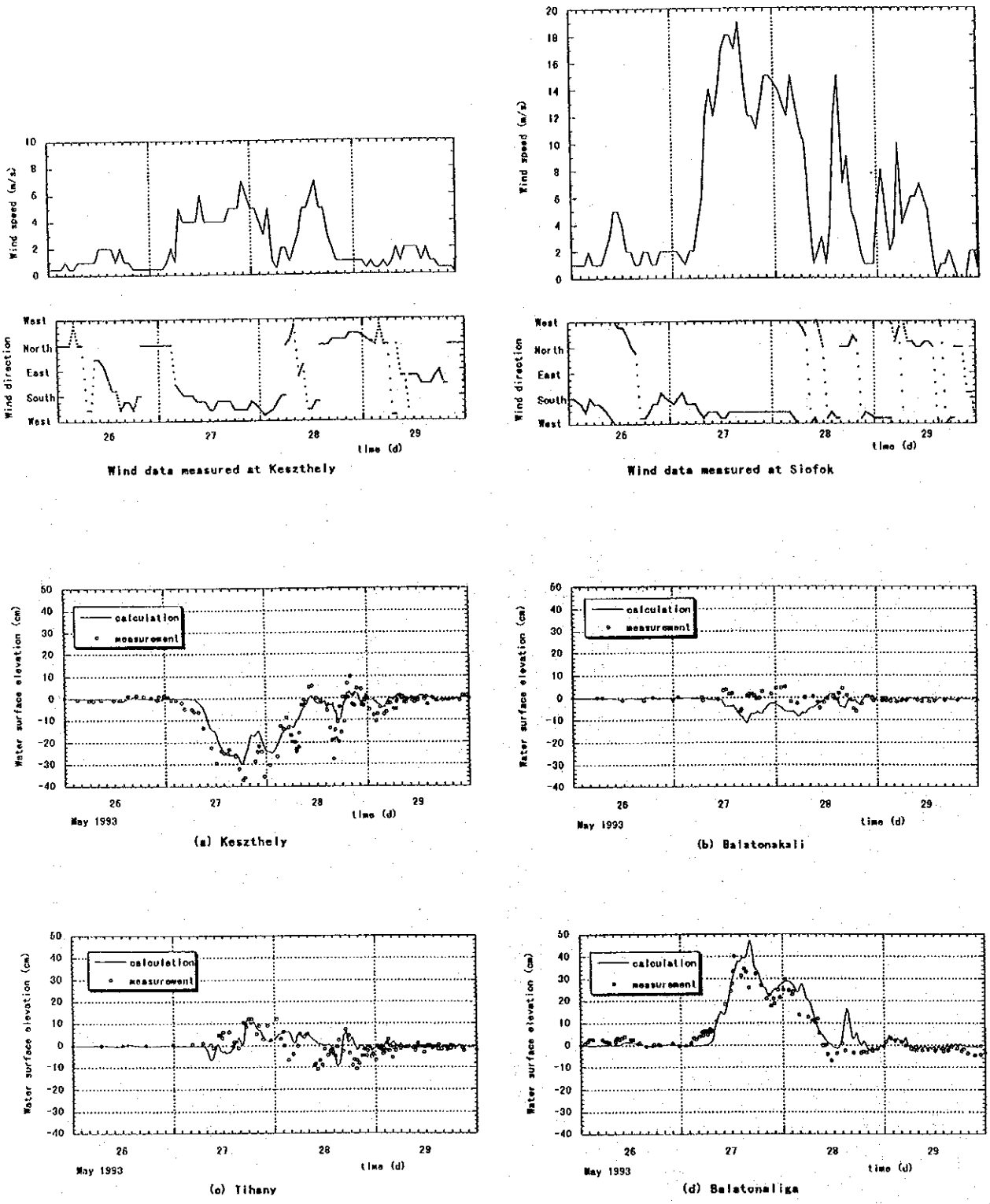

Figure C.15 Time-series of Water Surface Elevation during Storm Event, 26-30 May, 1993 (measured data from KDT-KÖFE)

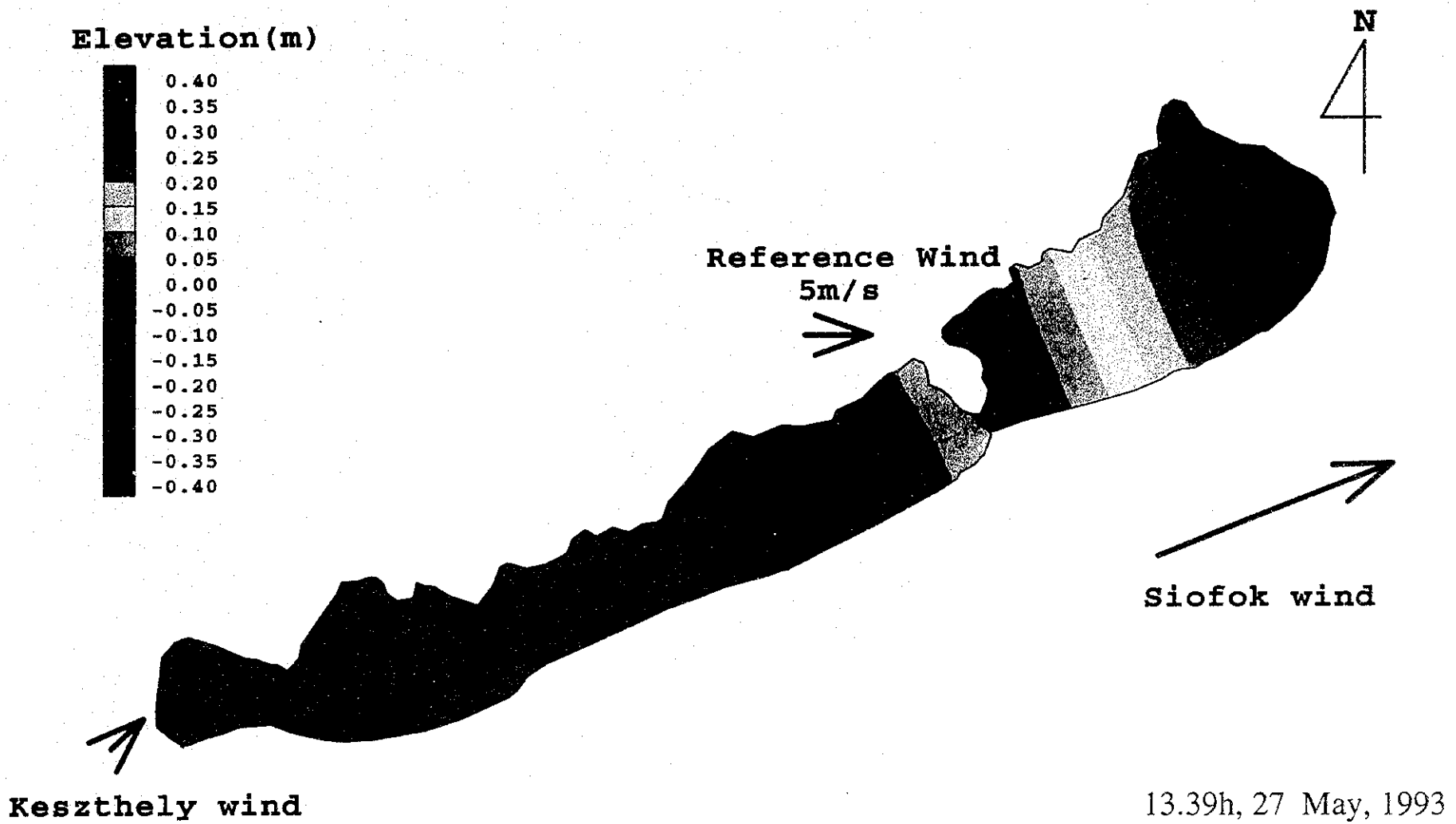

Figure C.16 Water Surface Elevation during Storm Event, 26-30 May, 1993

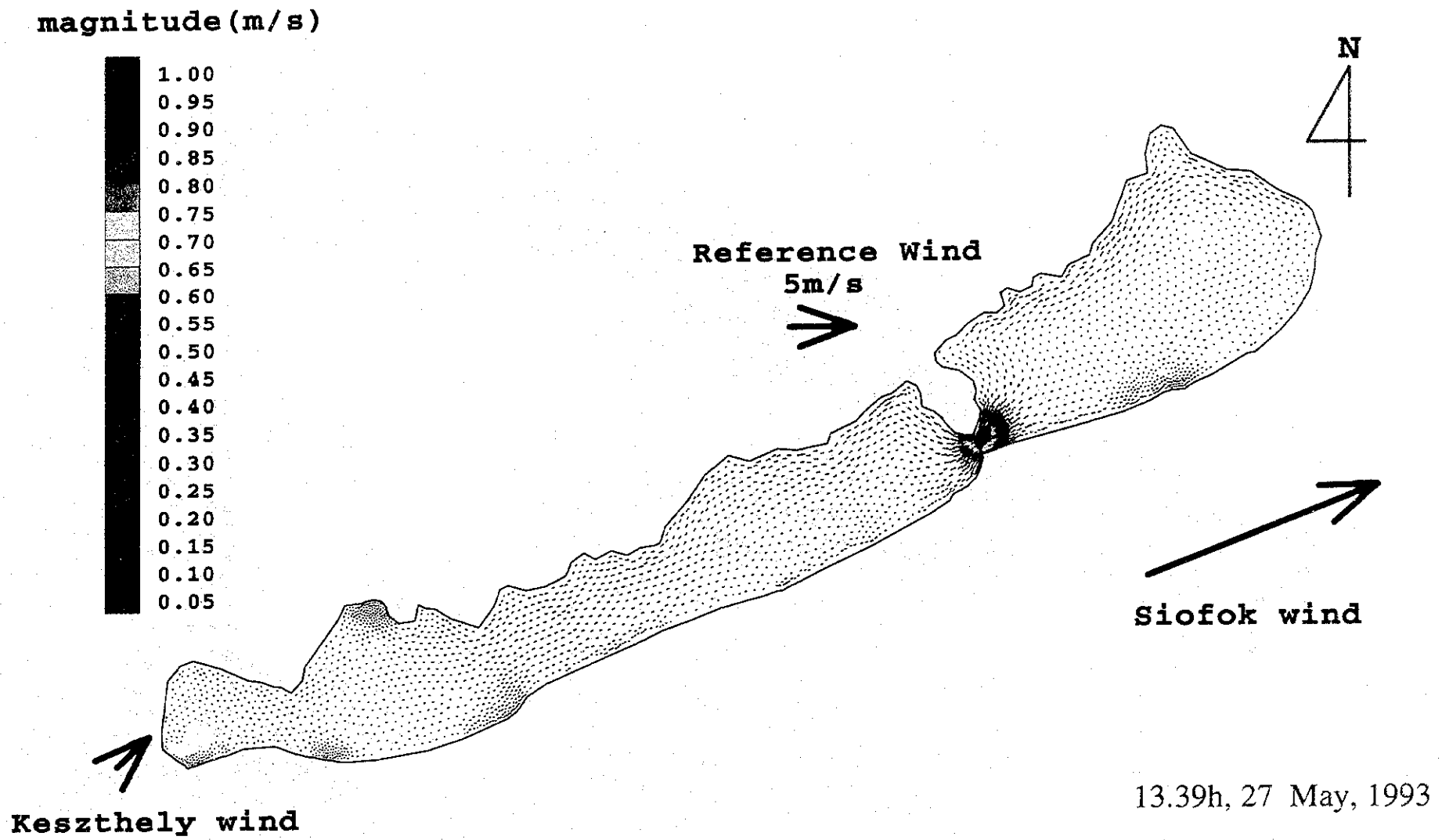

Figure C.17 Flow Field during Storm Event, 26-30 May, 1993

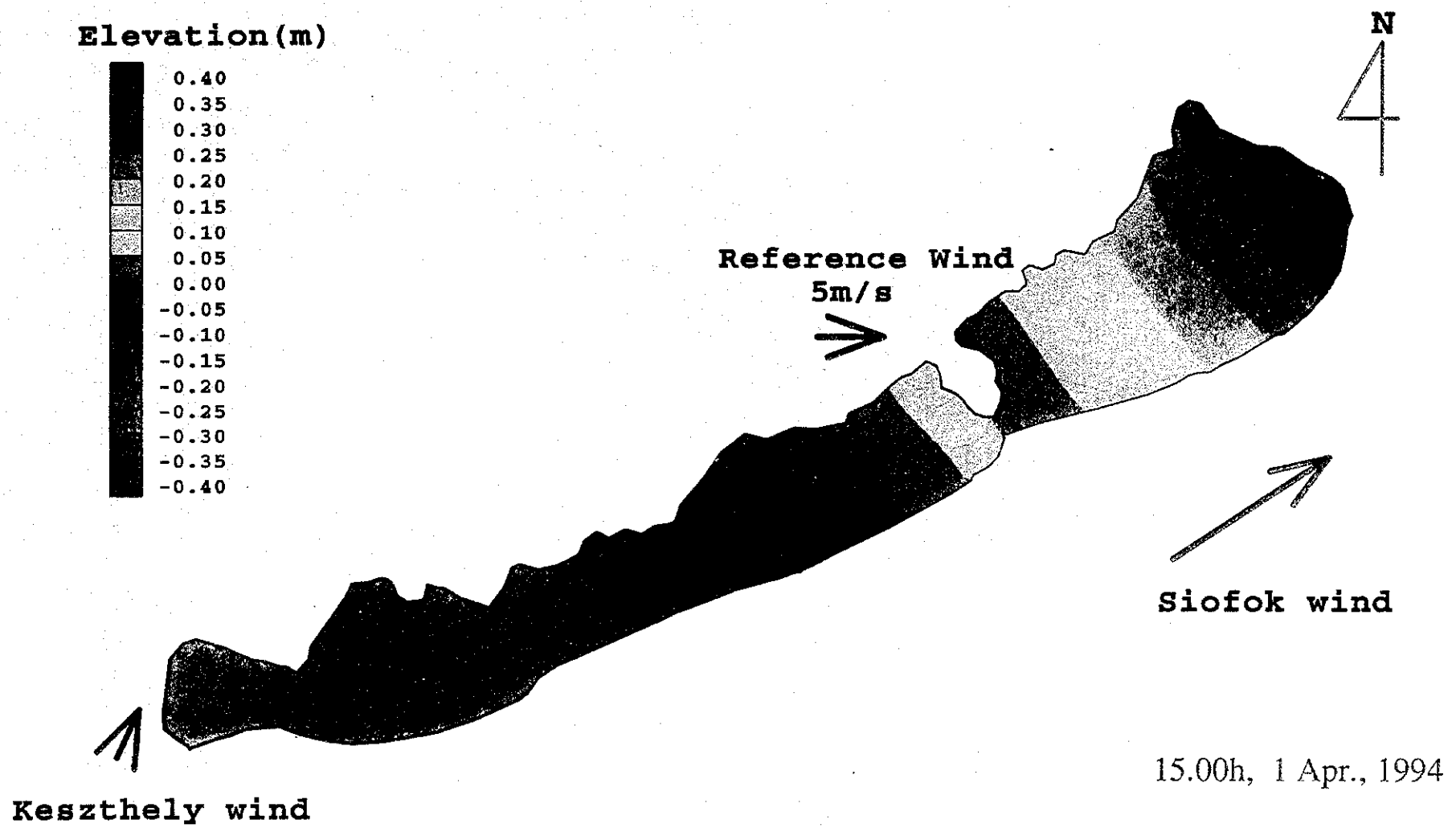

Figure C.18 Water Surface Elevation during Storm Event, 31 March-3 April, 1994

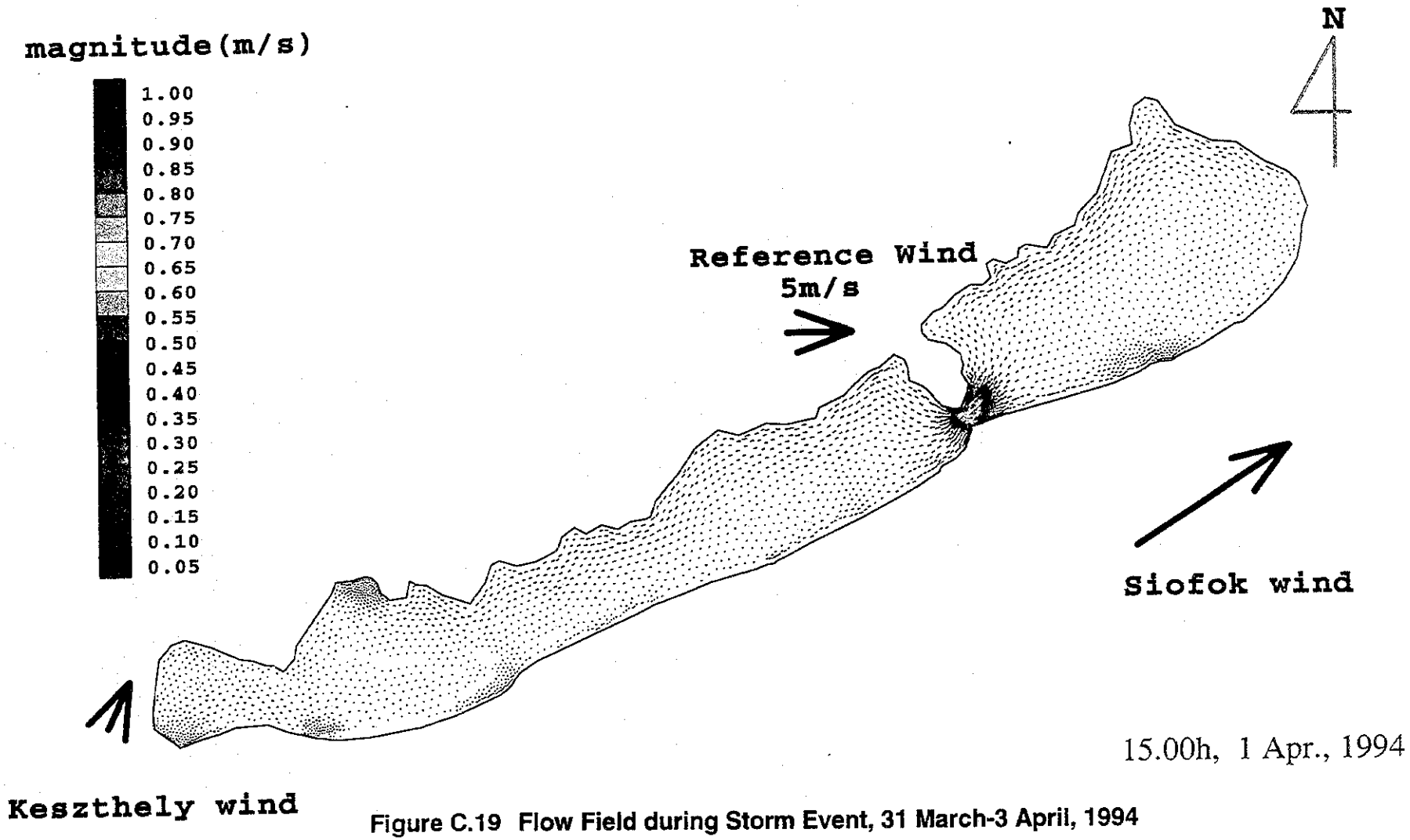

Figure C.19 Flow Field during Storm Event, 31 March-3 April, 1994

Mixing Analysys : 1994

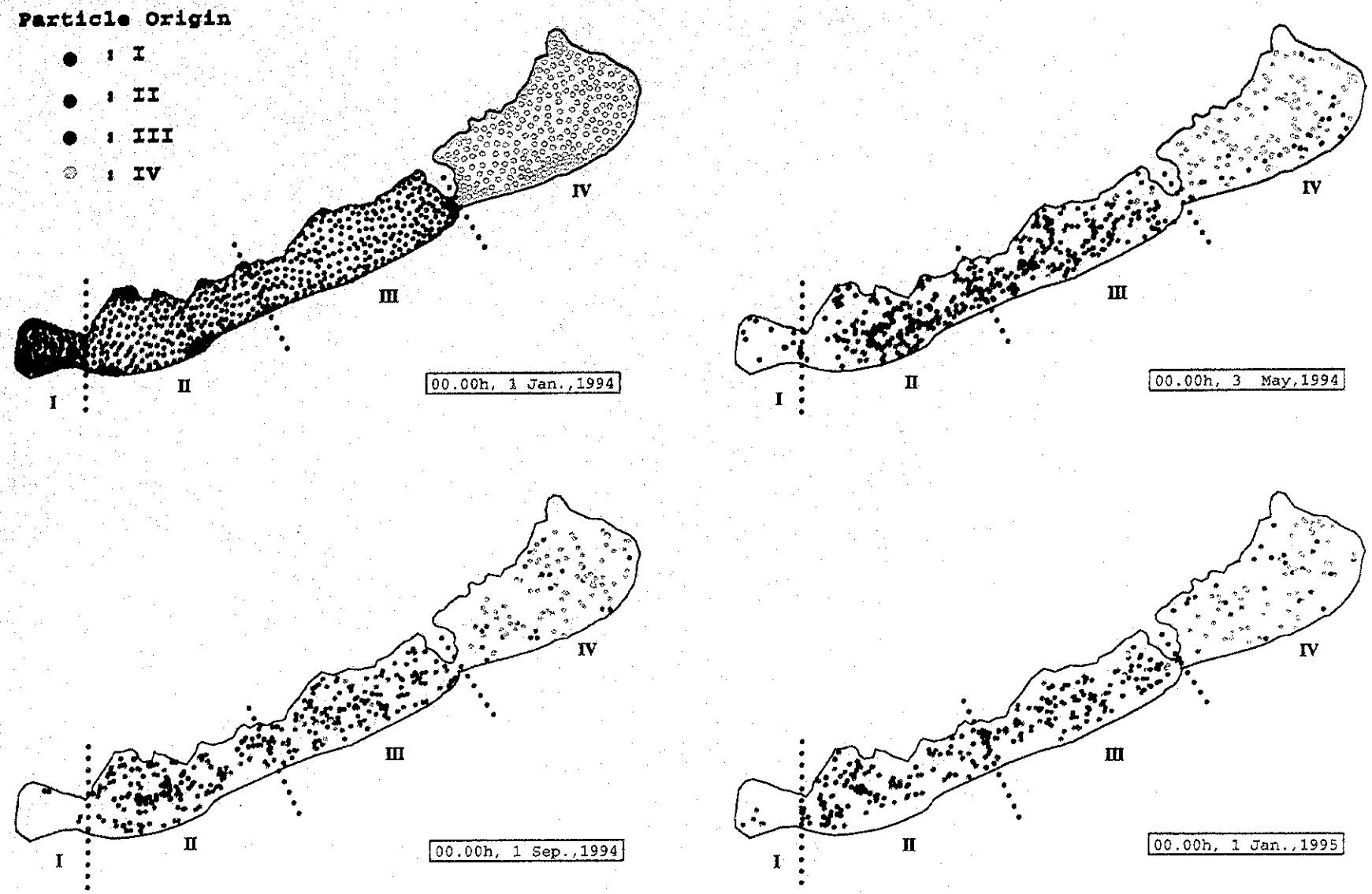

Figure C.20 Particle Tracking during 1994

Mixing Analysys : 1995

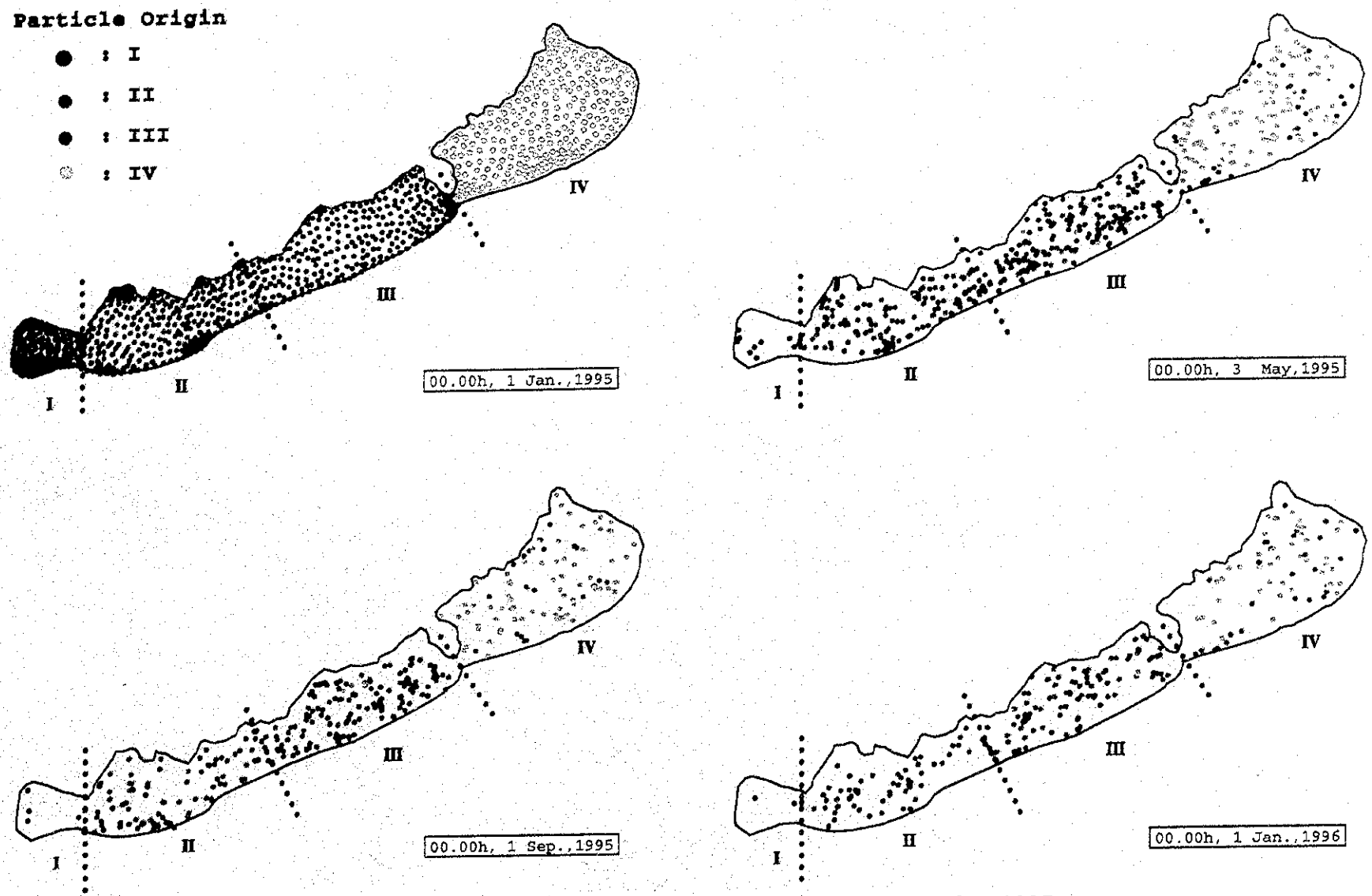

Figure C.21 Particle Tracking during 1995

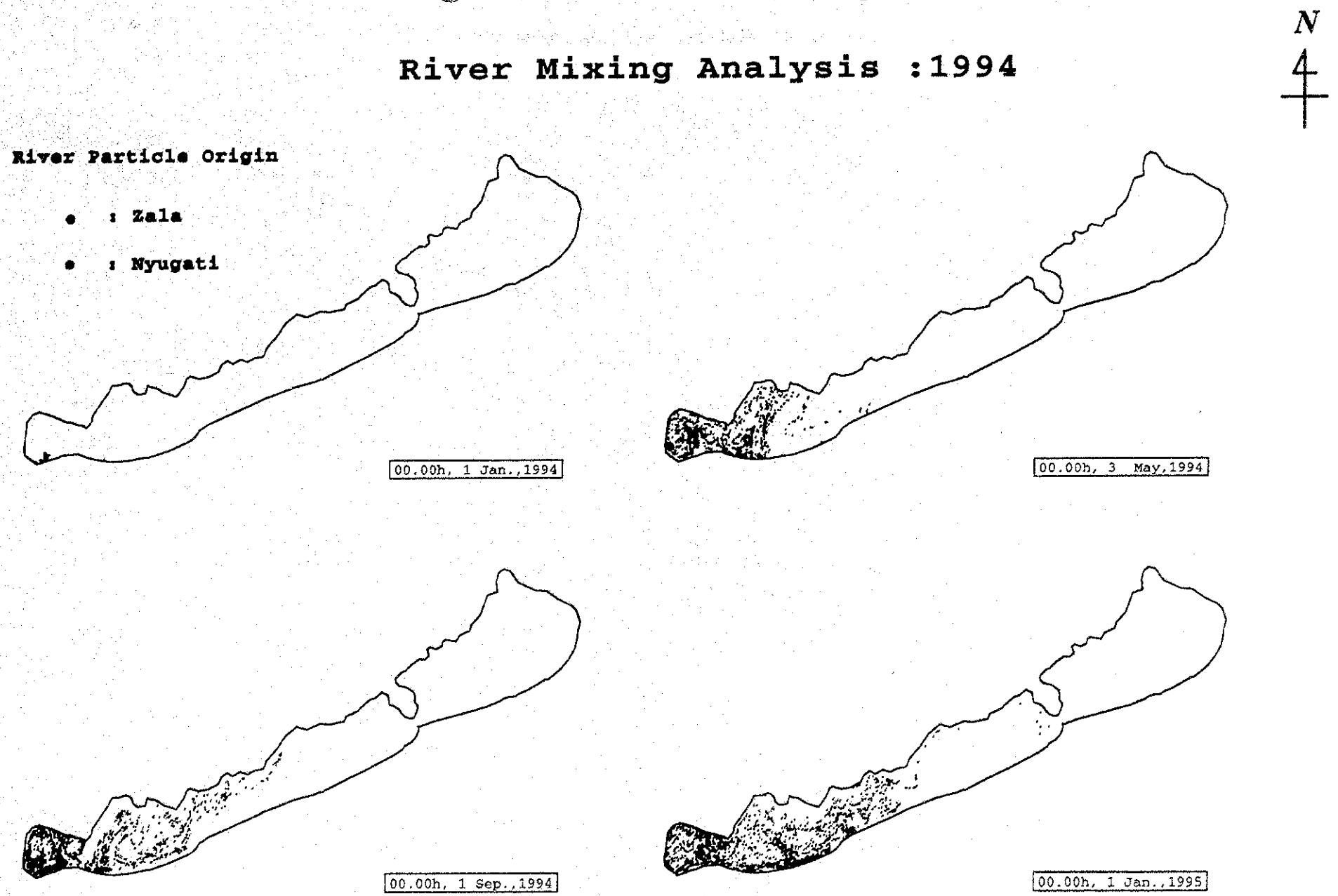

Figure C.22 River Particle Tracking during 1994

River Mixing Analysis :1995

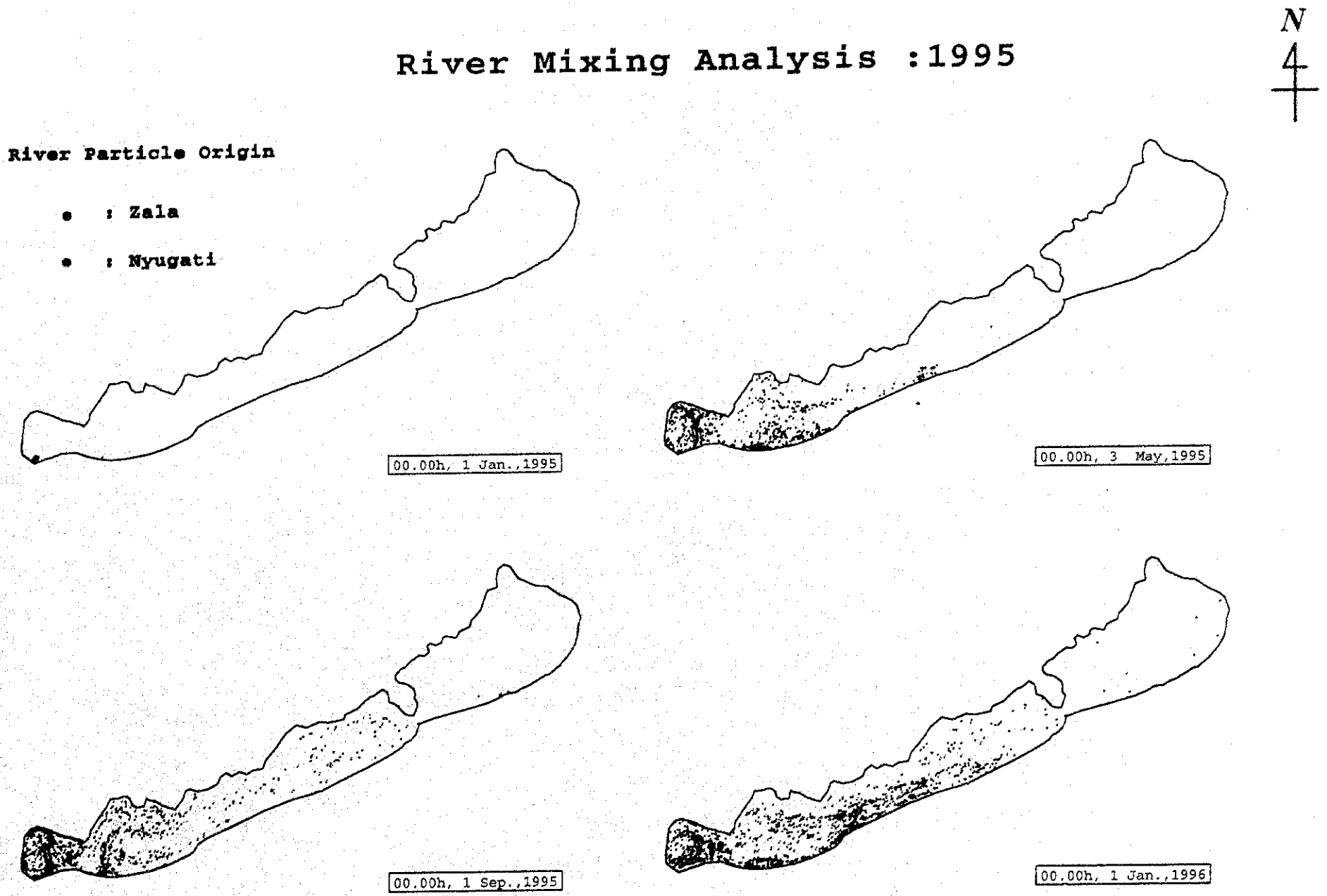

Figure C.23 River Particle Tracking during 1995

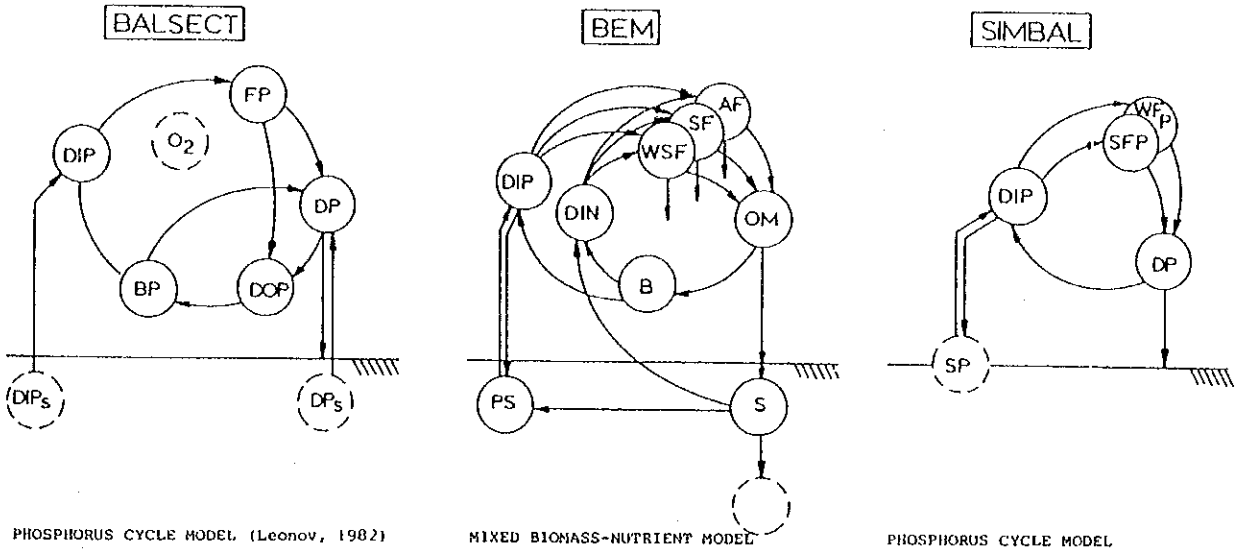

PHOSPHORUS CYCLE MODEL (Leonov, 1982)

FP : Phytoplankton P
DP : Particulate detritus P
DOP: Dissolved organic P
BP : Bacteria P
DIP: Dissolved inorganic P

MIXED BIOMASS-NUTRIENT MODEL (Kutas and Herodek, 1982)

AF : Autumn phytoplankton biomass
SF : Summer phytoplankton biomass
WSF: Winter and spring phytoplankton
OM : Organic material (detritus)
B : Bacteria biomass
DIN: Dissolved inorganic N
DIP: Dissolved inorganic P

PHOSPHORUS CYCLE MODEL (Van Straten, 1980)

WFP: Cold water phytoplankton P
SFP: Warm water phytoplankton P
DP : Detritus P
DIP: Dissolved inorganic P

DP_s : Detritus P in the sediment
DIP_s : Dissolved inorganic P in sediment

PS : Exchangeable P in sediment
S : Organic material in sediment

SP : Adsorbed exchangeable P

Figure C.24 Structure of Previous Balaton Phytoplankton Dynamics Models (van Straten, 1983)

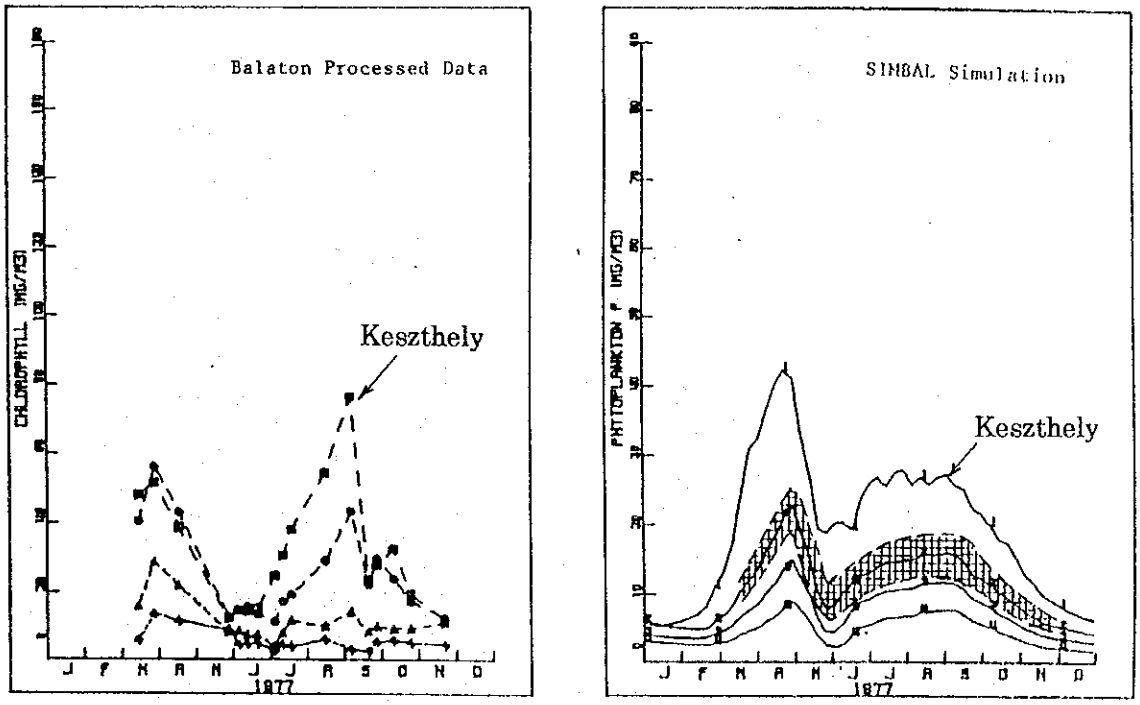

Figure C.25 Results from SIMBAL for Four Basins of Lake Balaton (van Straten, 1980)

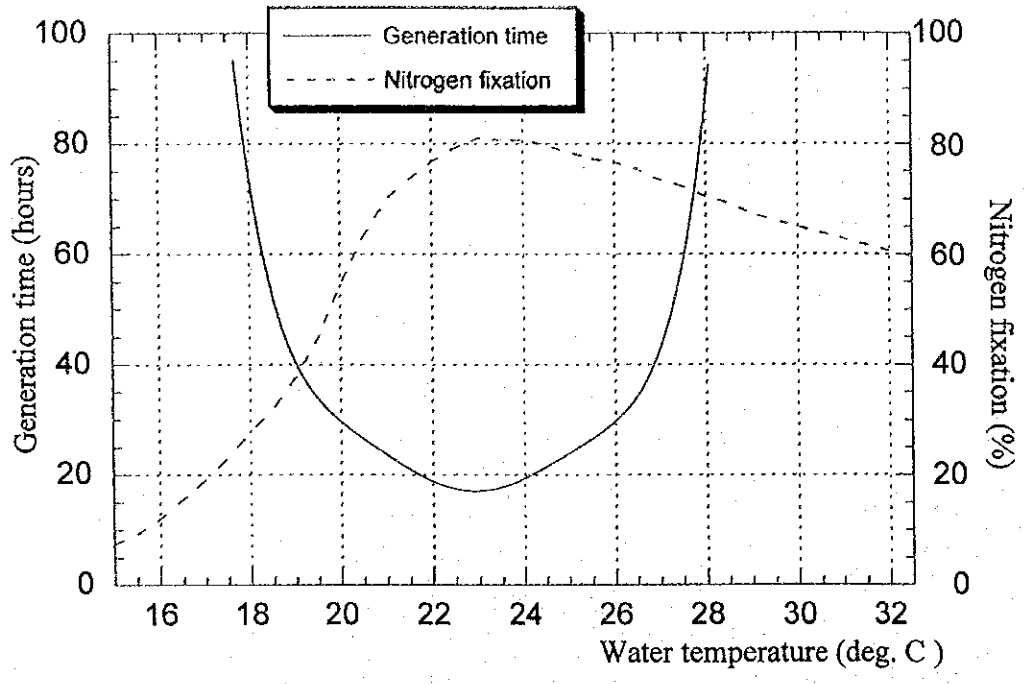

Figure C.26 Growth Characteristics of *C. raciborskii* (KDT-KÖFE, 1988)

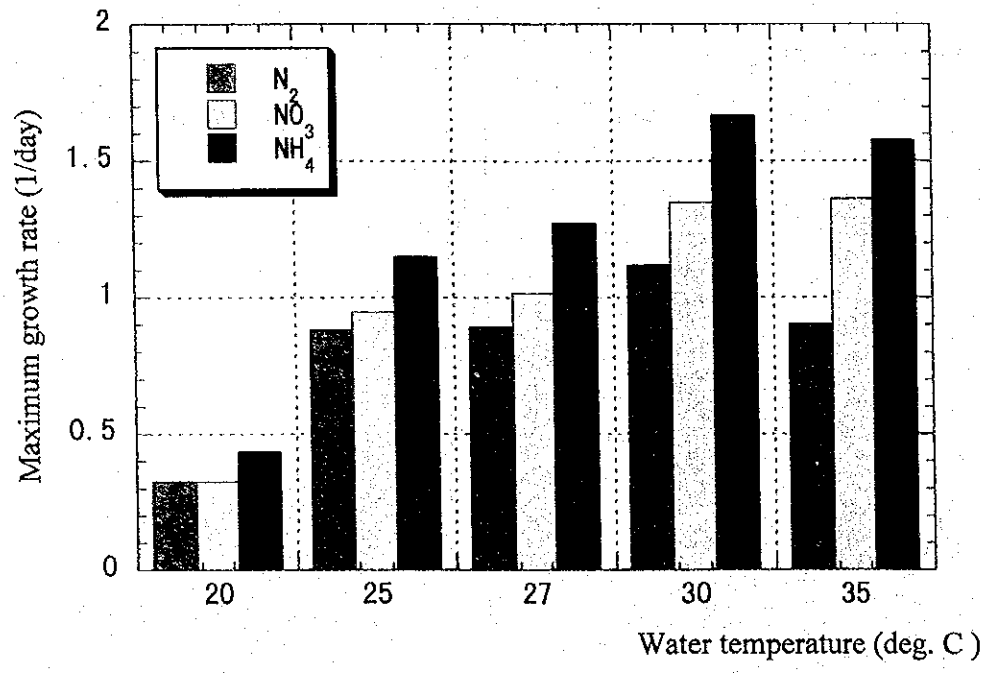

Figure C.27 Growth Rate of *C. raciborskii* with Different N-sources (Shafik *et al.*, 1997)

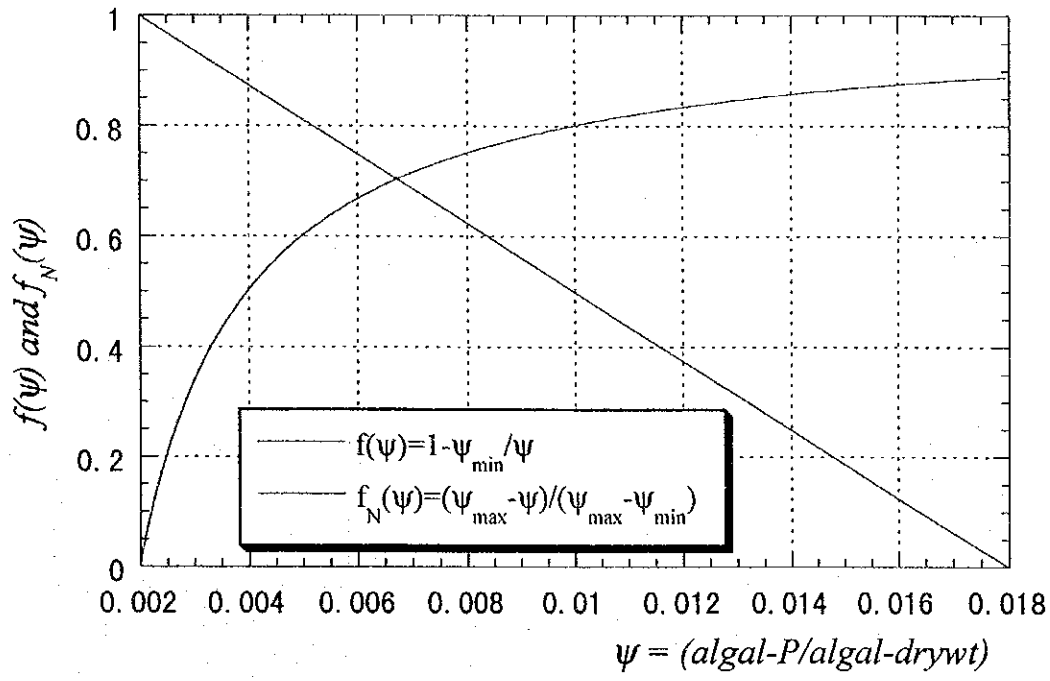

Figure C.28 Characteristics of Cell Quota Function

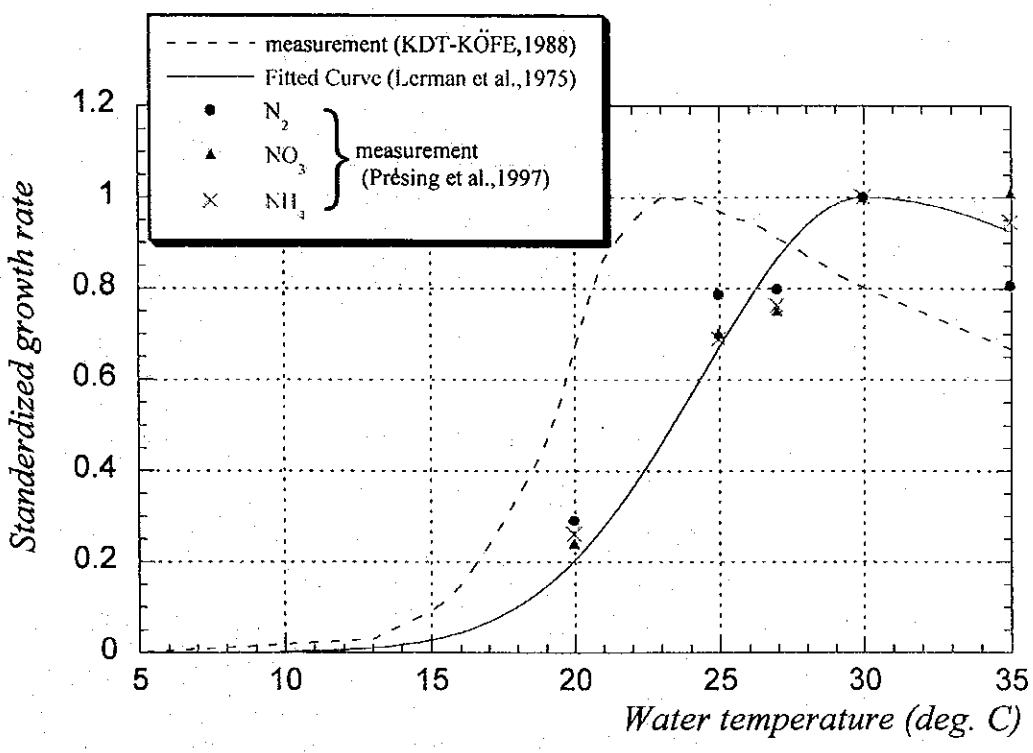

Figure C.29 Normalized Growth Rate of *C. raciborskii* with Different Nitrogen Sources

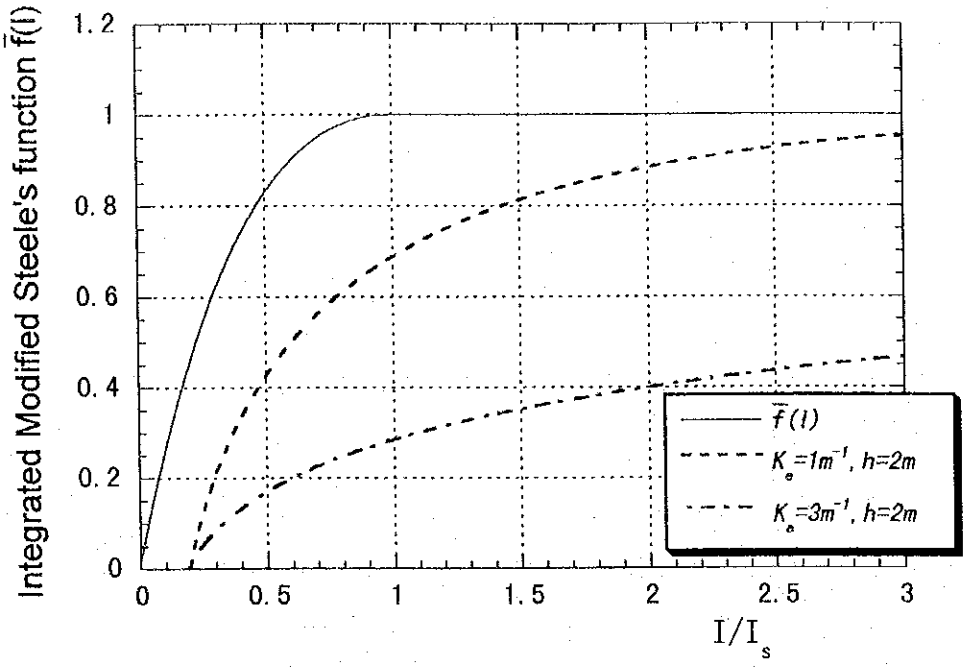

Figure C.30 Characteristics of Integrated Modified Steele's Light Limiting Function

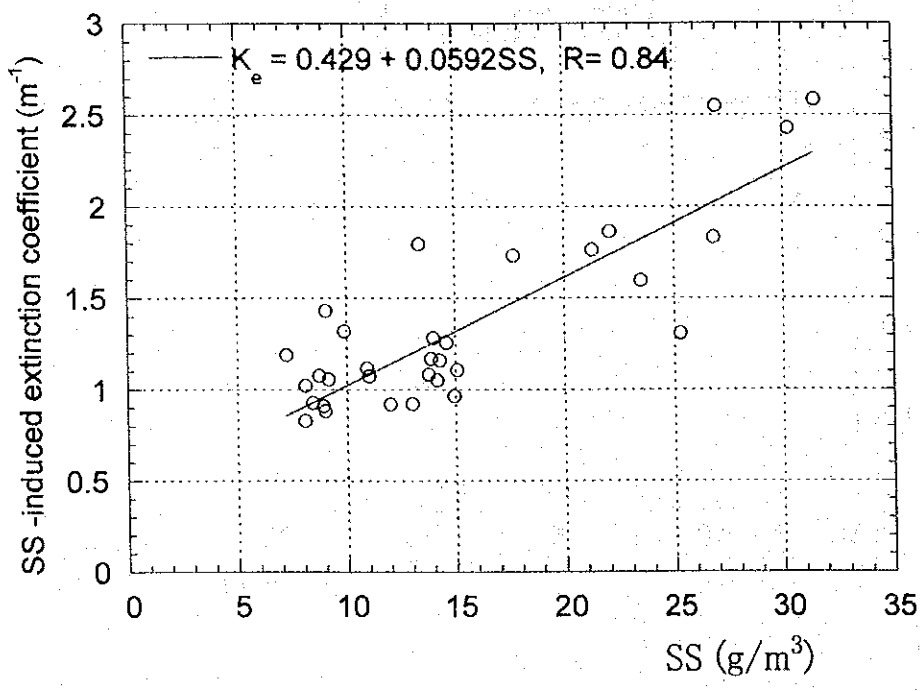

Figure C.31 Extinction coefficients as a Function of Suspended Sediments at Lake Balaton

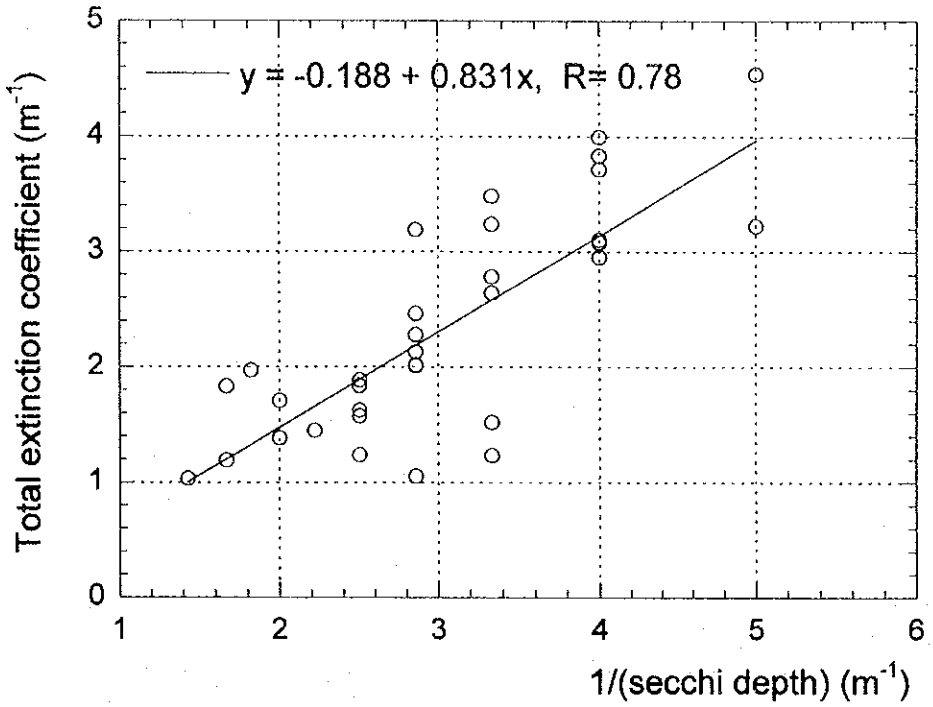

Figure C.32 Secci Depths Correlation with Estimated Extinction Coefficients

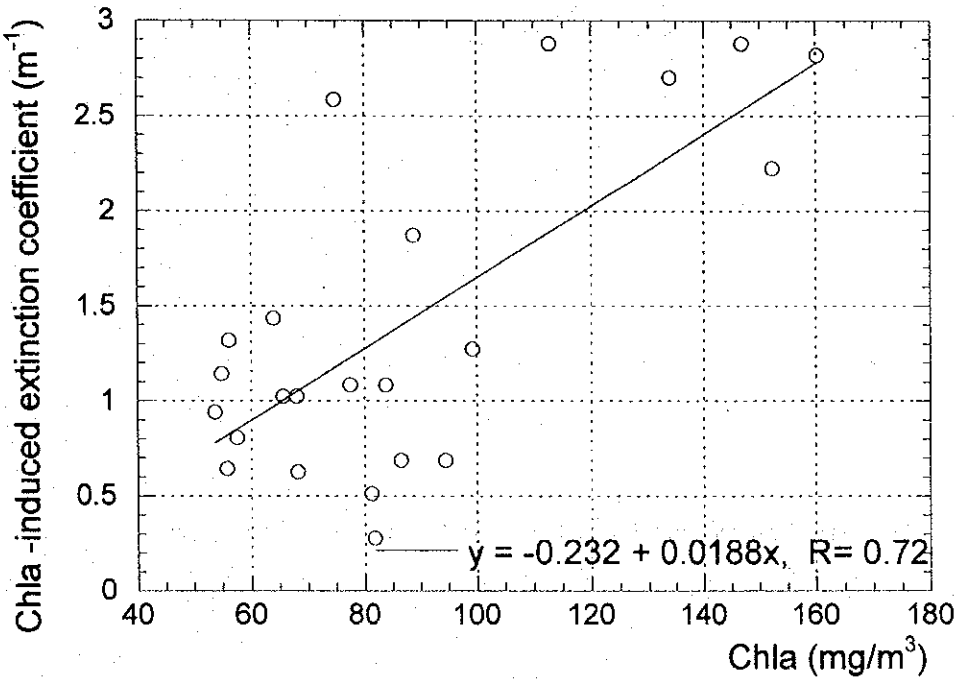

Figure C.33 Extinction Coefficients as a Function of *Chla*

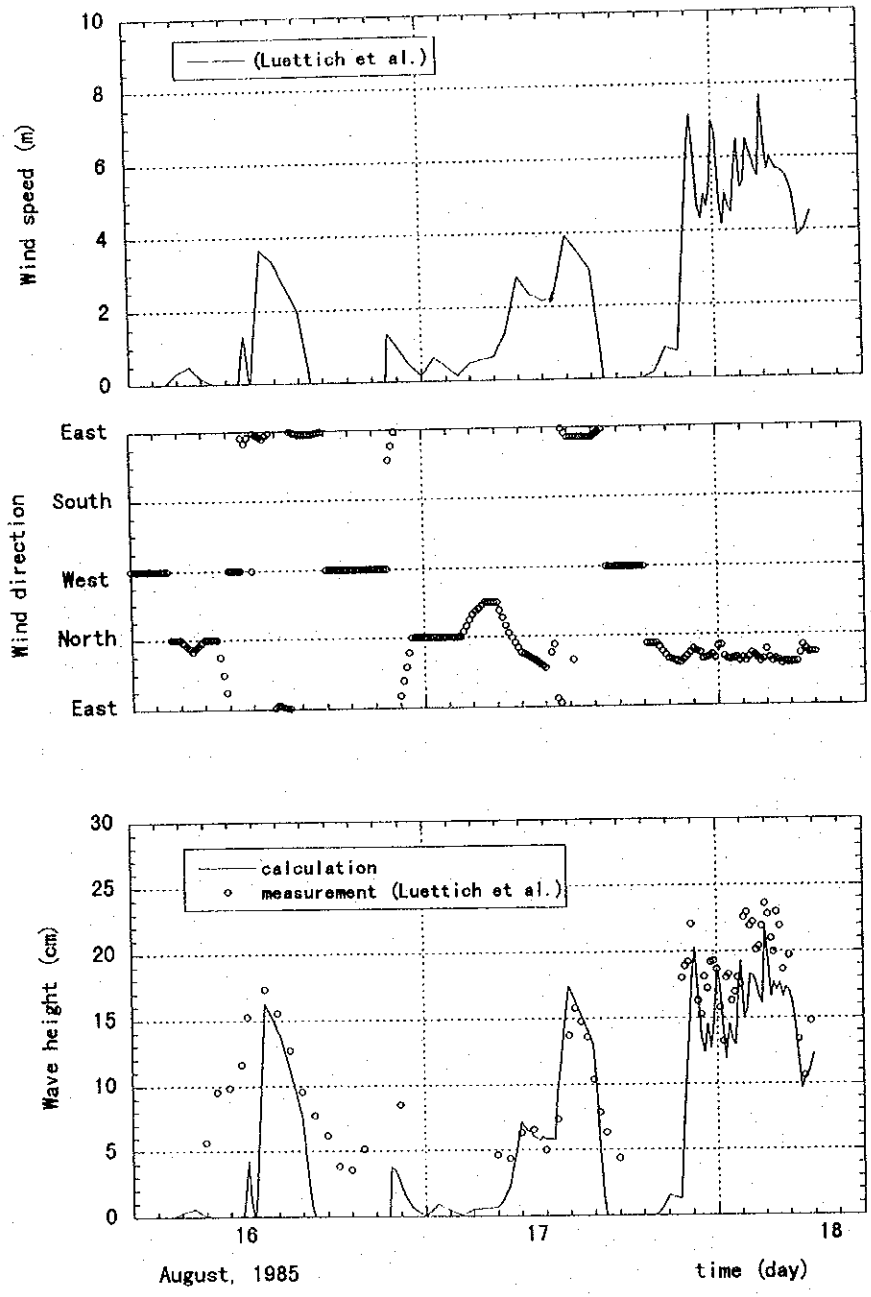

Figure C.34 Wave Height Hindcast in Keszthley Bay

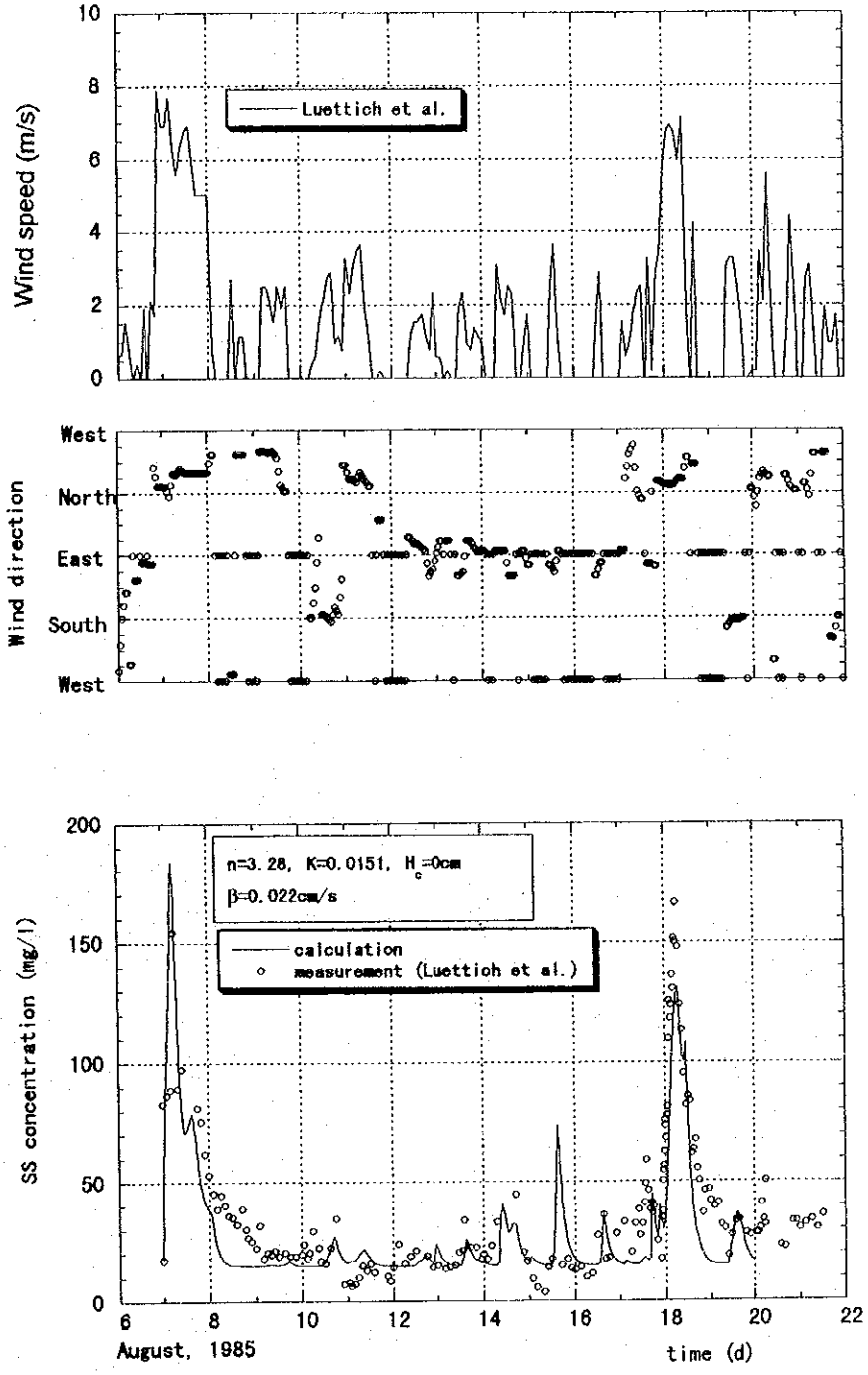

Figure C.35 Suspended Sediments Hindcast in Keszthley Bay

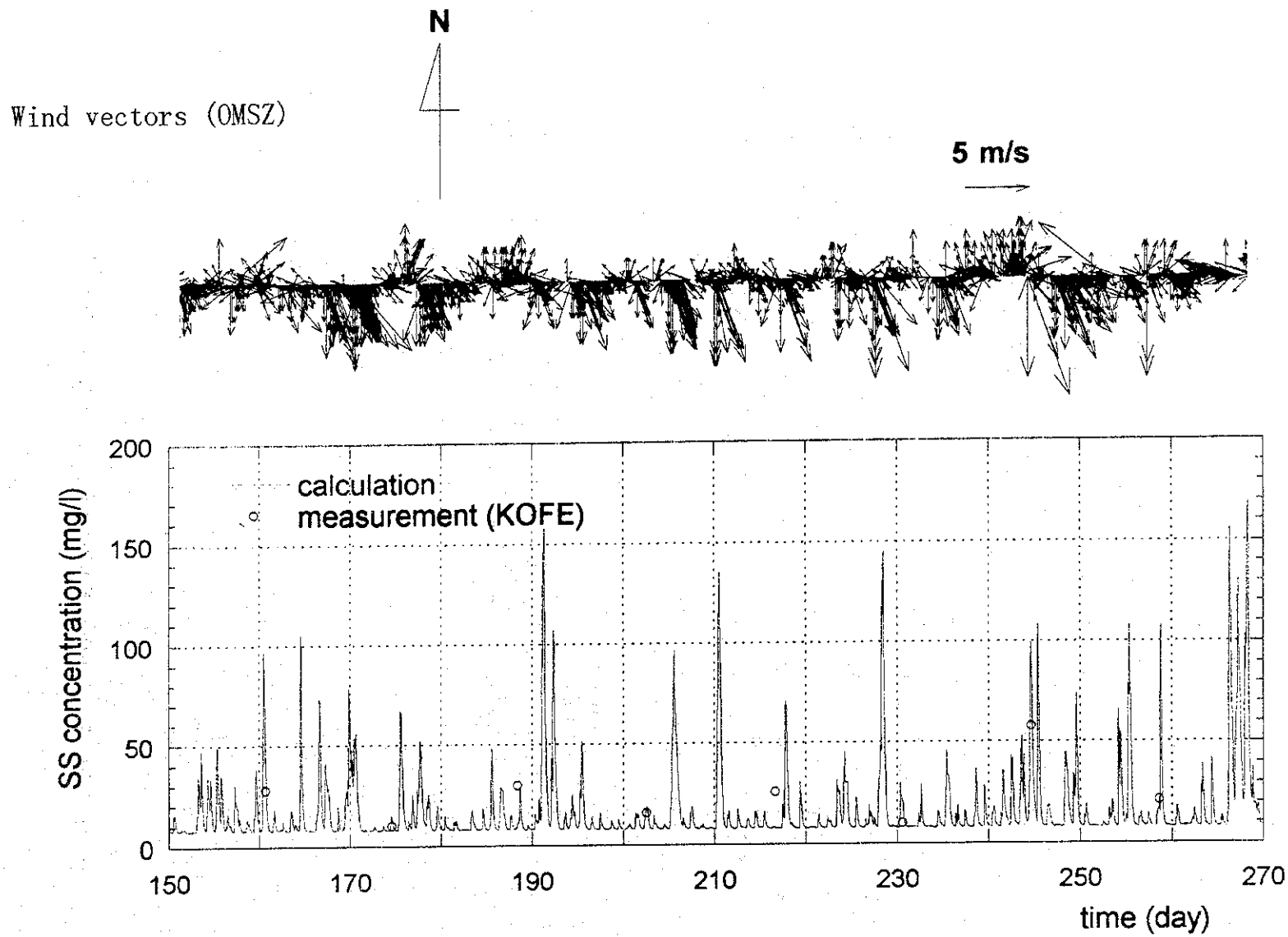

Figure C.36 Suspended Sediments Hindcast in Keszthley Bay in 1992

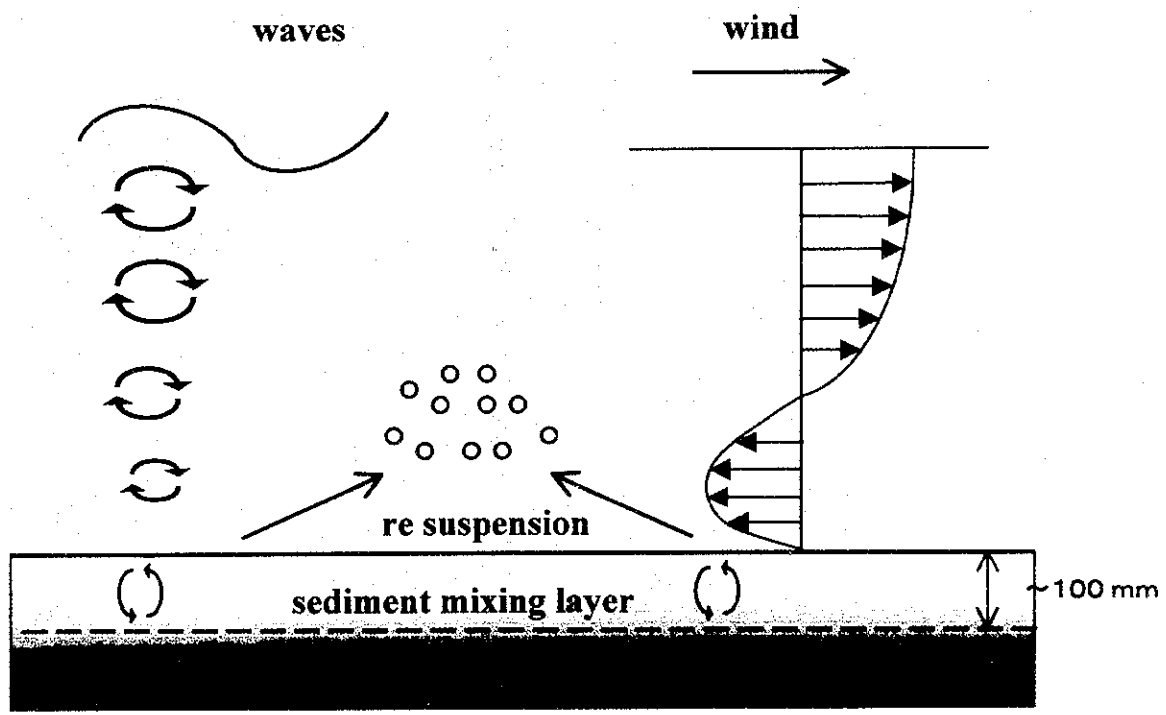

Time required for sedimentation of mixing layer

$$= \frac{\text{mixing depth}}{\text{sedimentation rate}} = \frac{\sim 100\text{mm}}{\sim 3\text{mm}/\text{year}} = 33 \text{ year}$$

Figure C.37 Physical Mechanism of Sediment Re-suspension and Mixing Layer Thickness

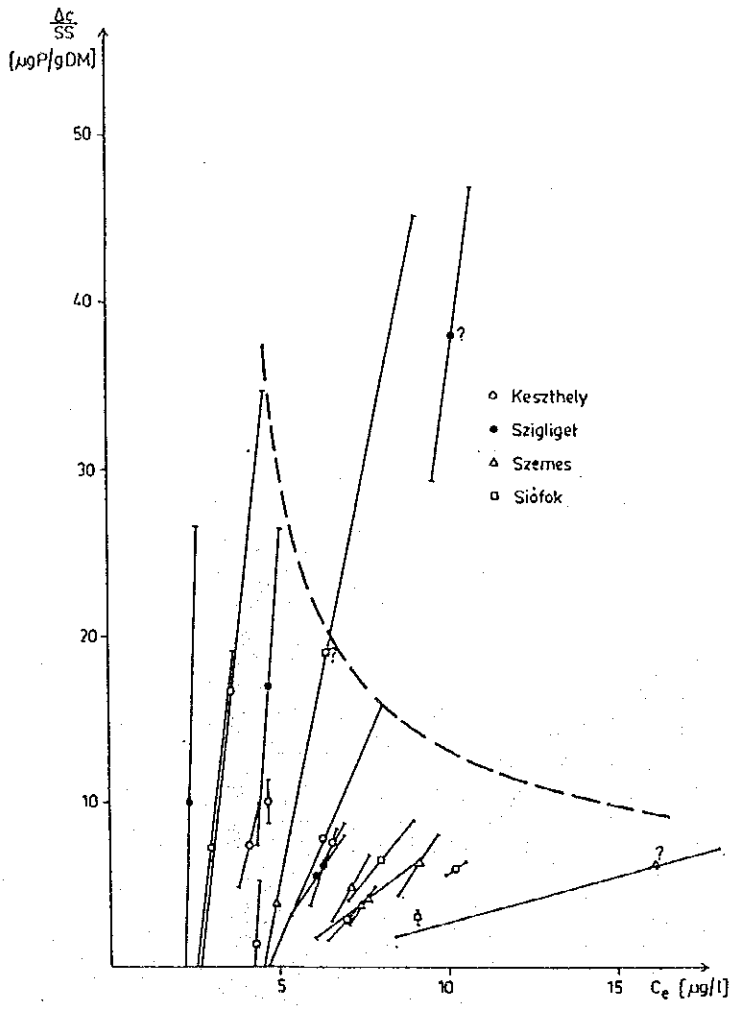

Figure C.38 Results of Desorption Experiment (Gelencser, *et al.*, 1982)

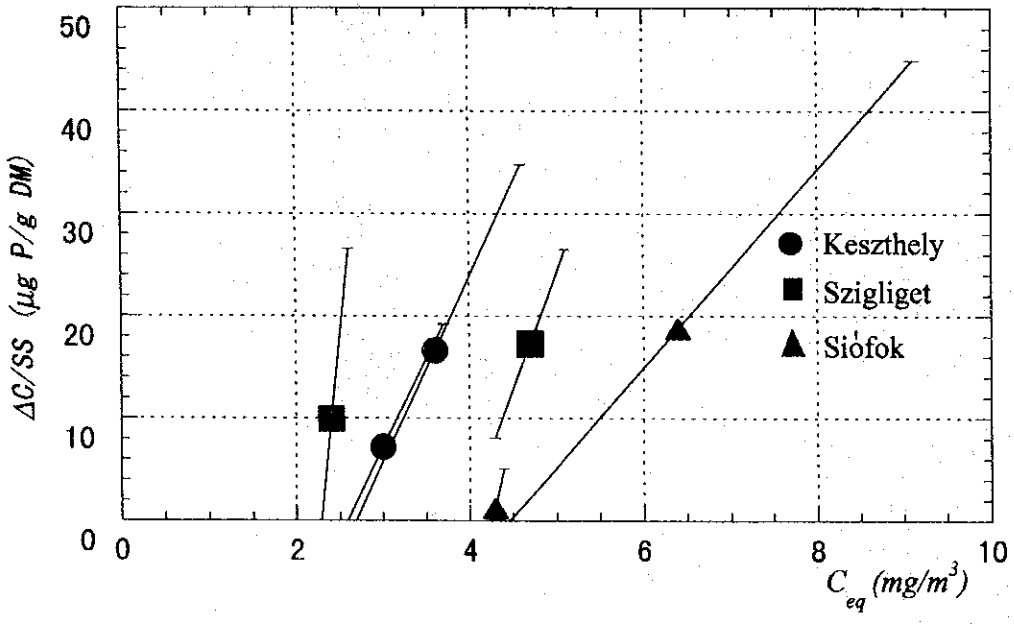

Figure C.39 Desorption Rates for SS < 180 mg/m^3 (Gelencser, *et al.*, 1982)

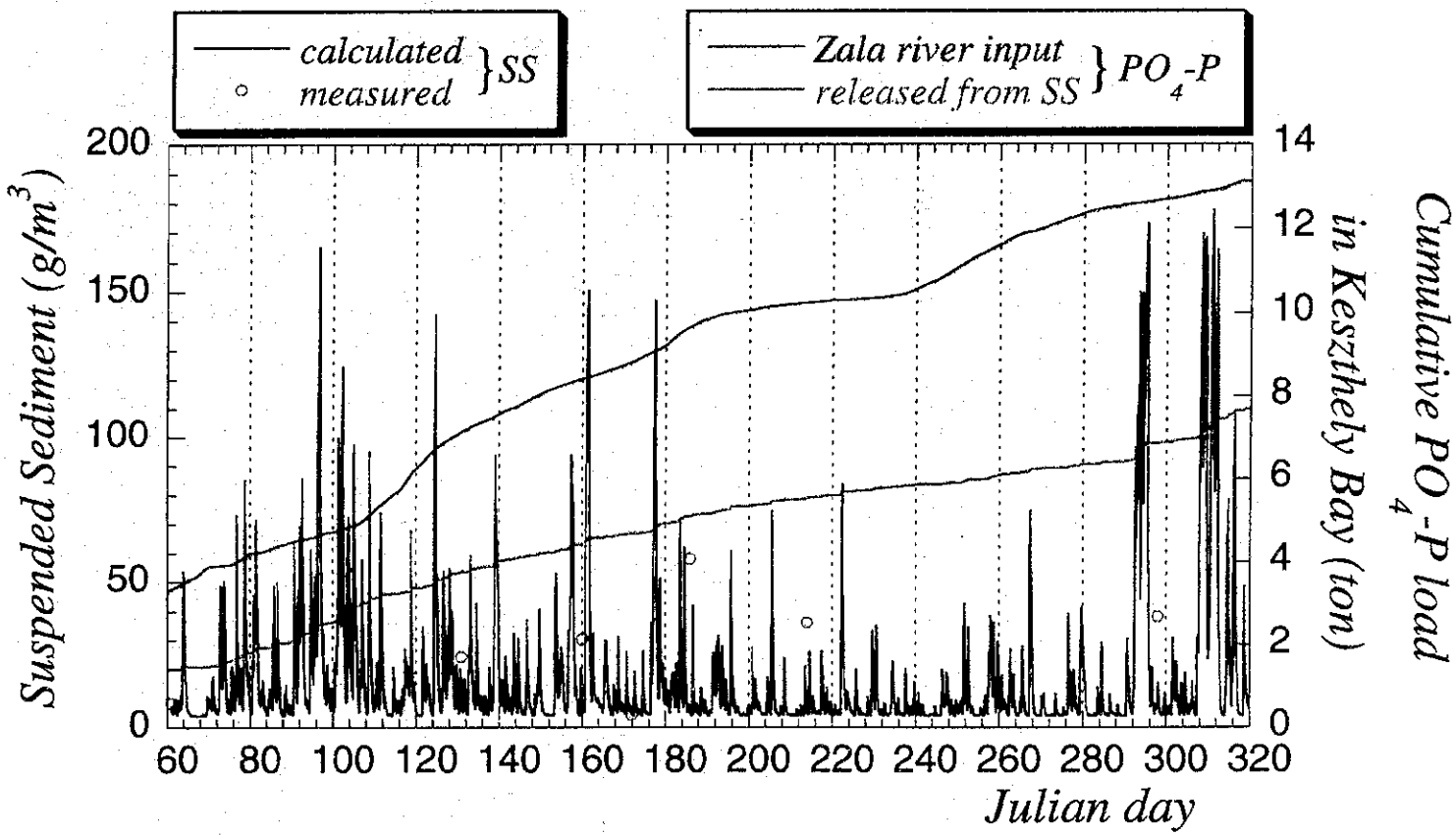

Figure C.40 Suspended Sediments and PO_4-P Loads in Keszthley Bay in 1994

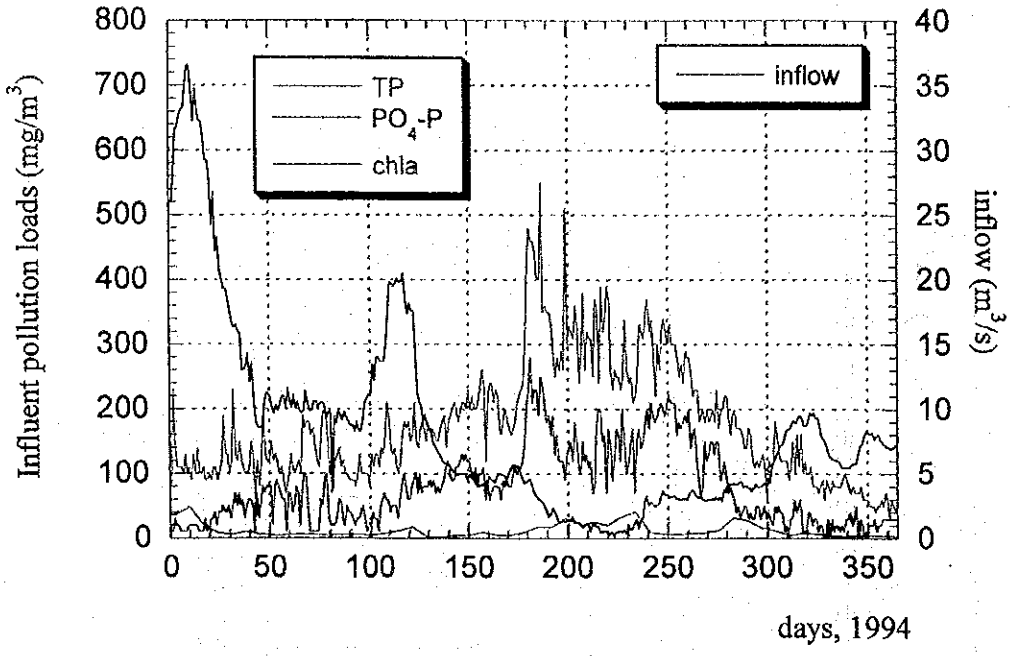

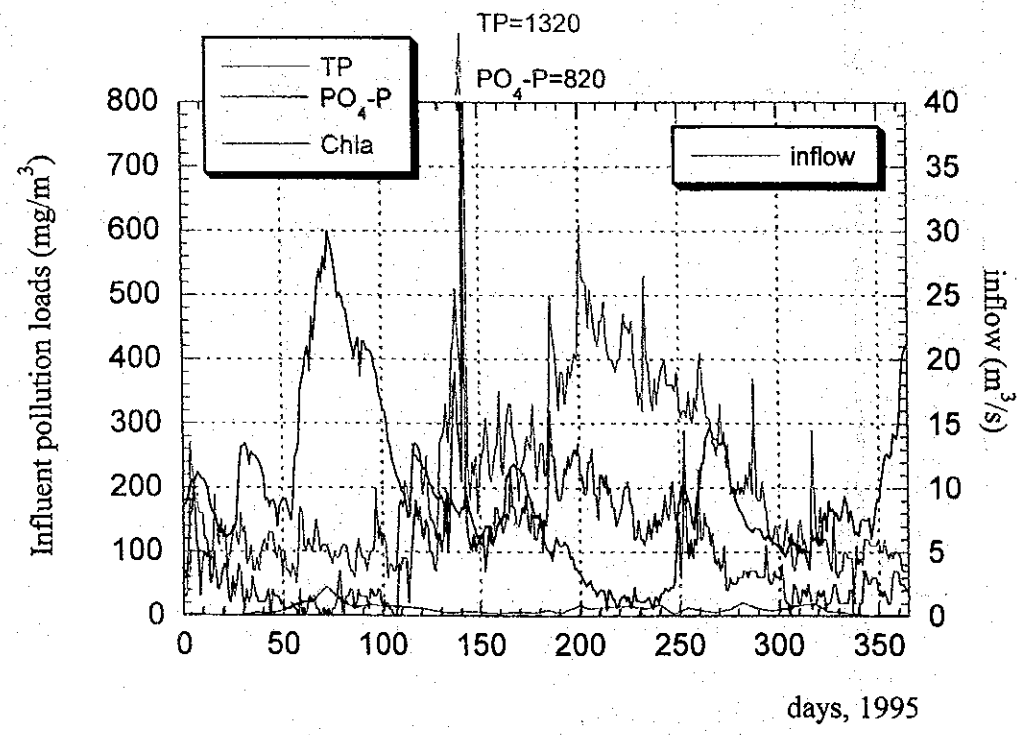

Figure C.41 Water-Quality and -Quantity of Zala River in 1994 and 1995

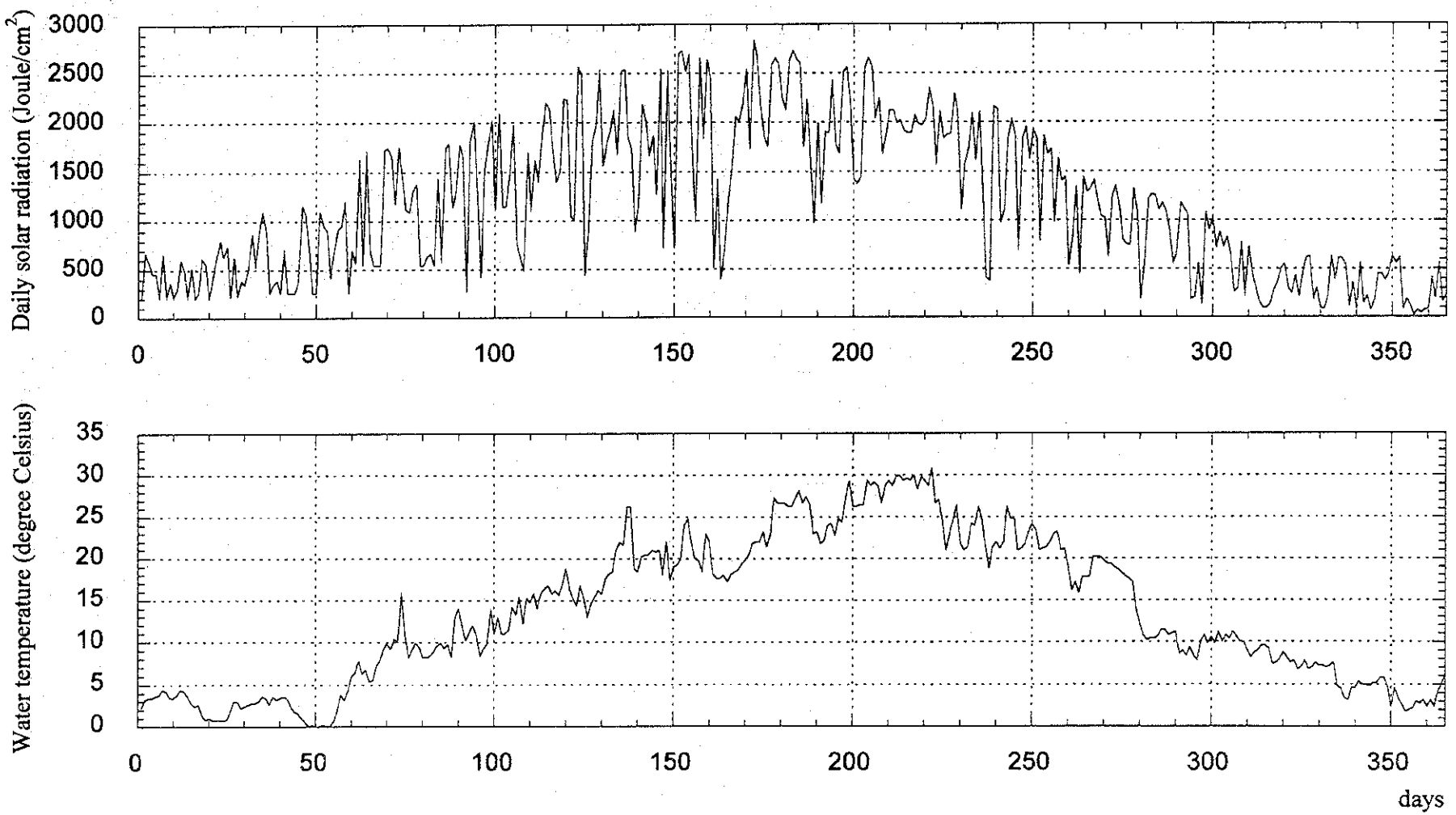

Figure C.42 Daily Solar Radiation and Water Temperature in 1994 (OMSZ and KDT-VIZIG)

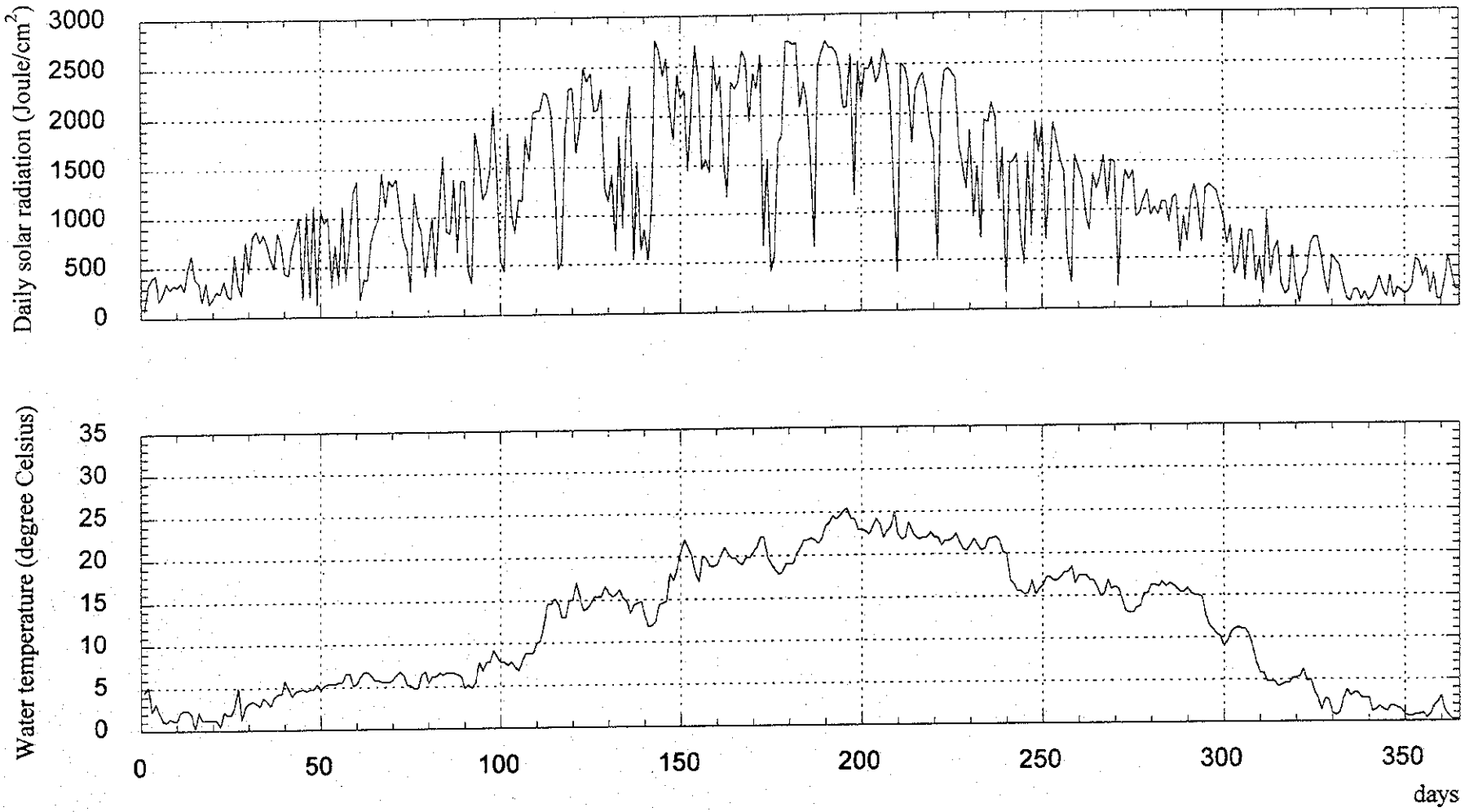

Figure C.43 Daily Solar Radiation and Water Temperature in 1995 (OMSZ and KDT-VIZIG)

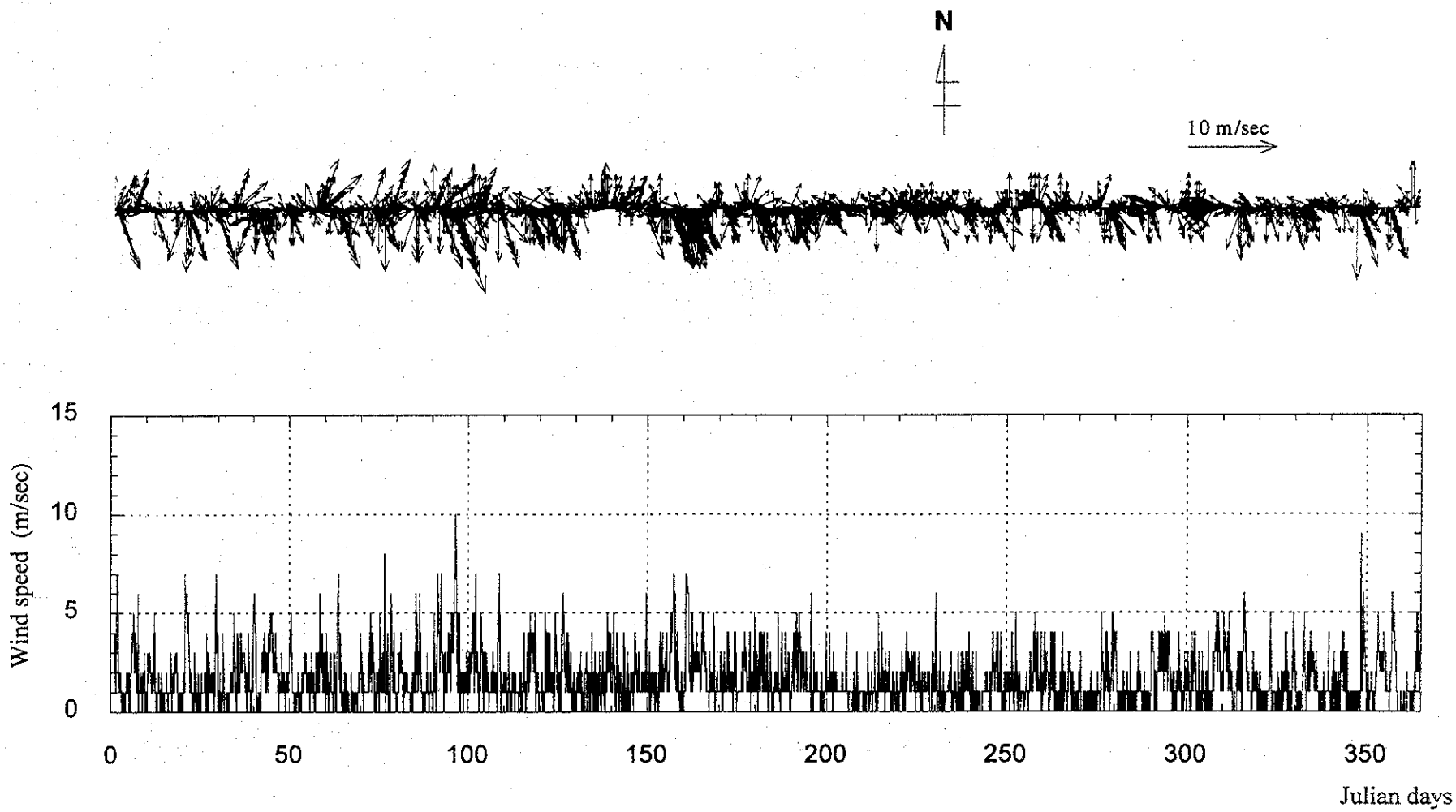

Figure C.44 Wind-vector and Wind-speed at the Keszthely weather station, 1994 (OMSZ)

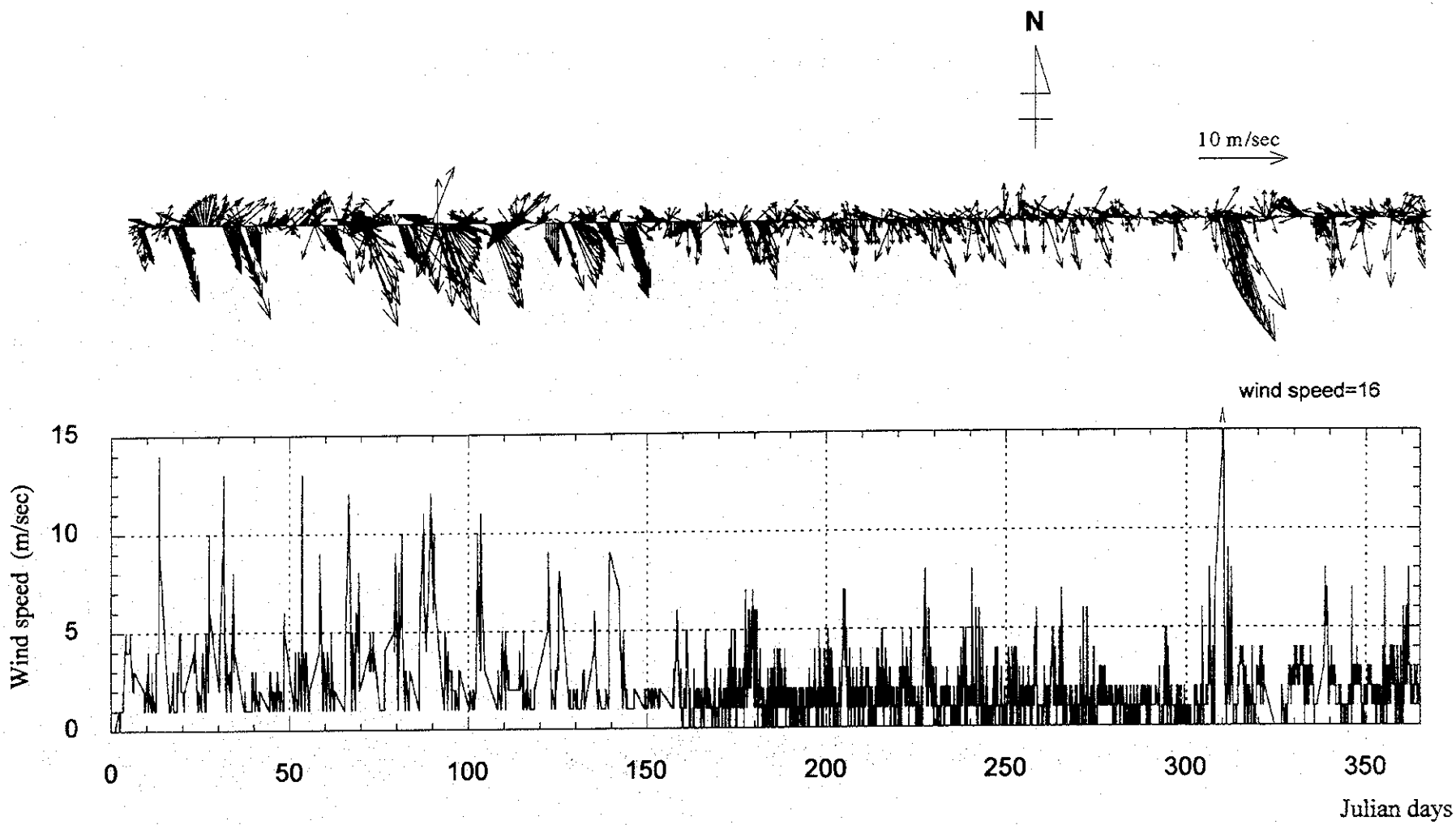

Figure C.45 Wind-vector and Wind-speed at the Keszthely weather station, 1995 (OMSZ)

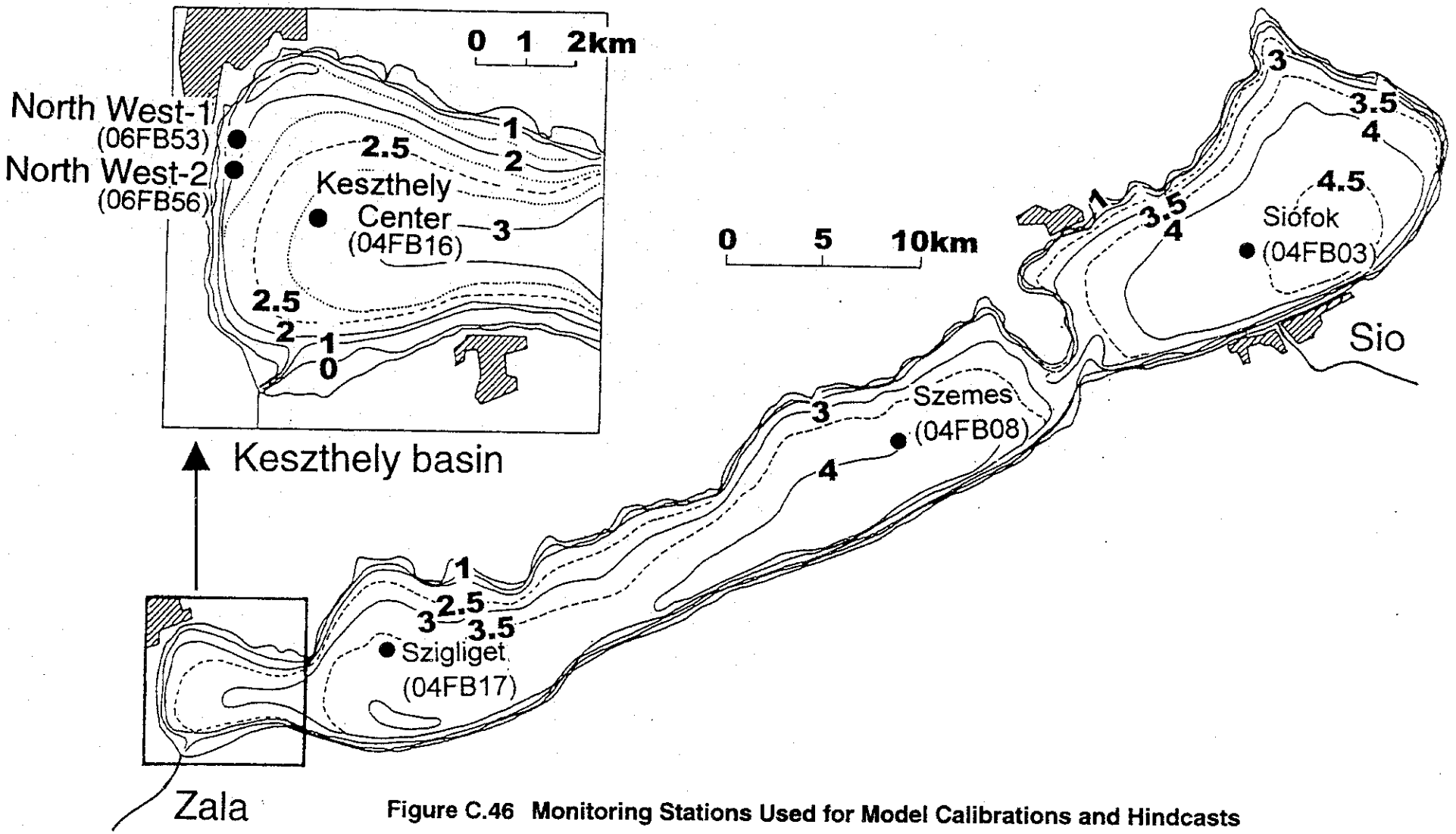

Figure C.46 Monitoring Stations Used for Model Calibrations and Hindcasts

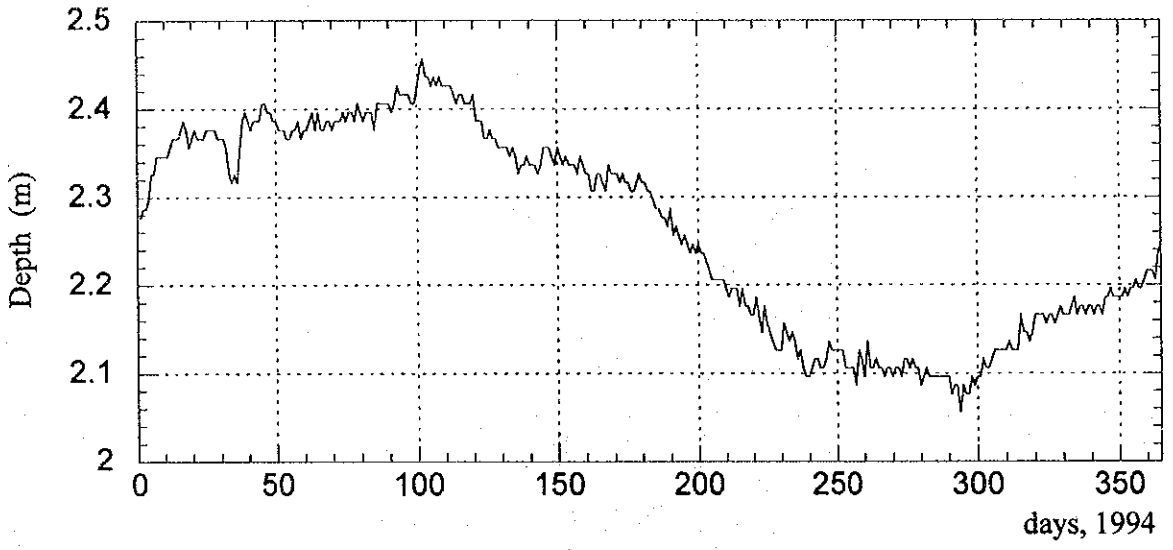

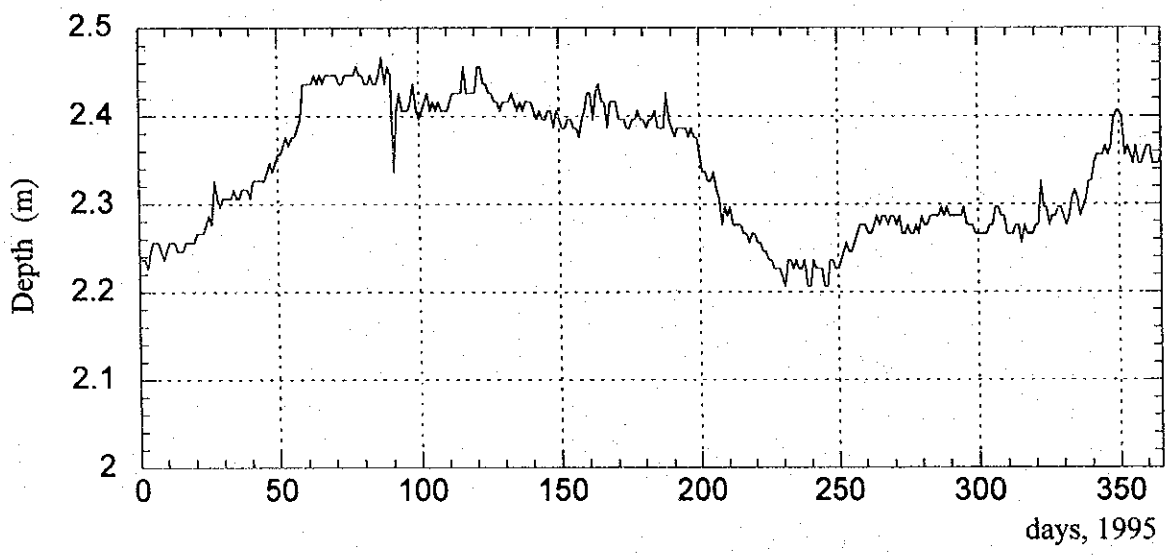

Figure C.47 Average Water Depth of Keszthely Bay in 1994 and 1995 (KDT-VIZIG)

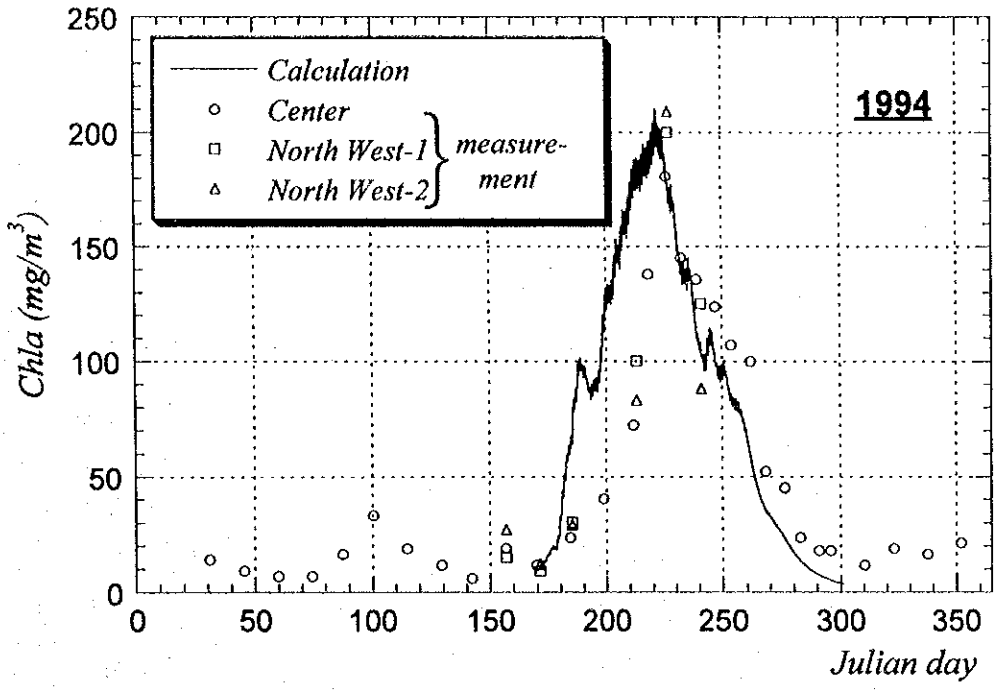

Figure C.48 Chlorophyll-a Hindcast Comapred with Measurements (Présing and KDT-KÖFE) in 1994

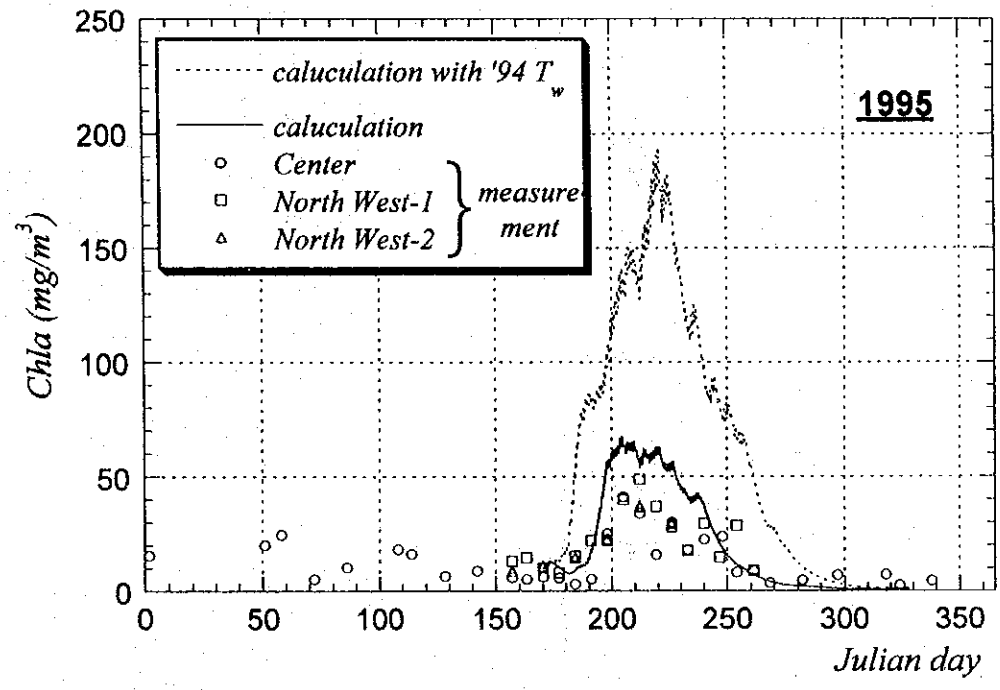

Figure C.49 Chlorophyll-a Hindcast Comapred with Measurements (KDT-KÖFE) in 1995

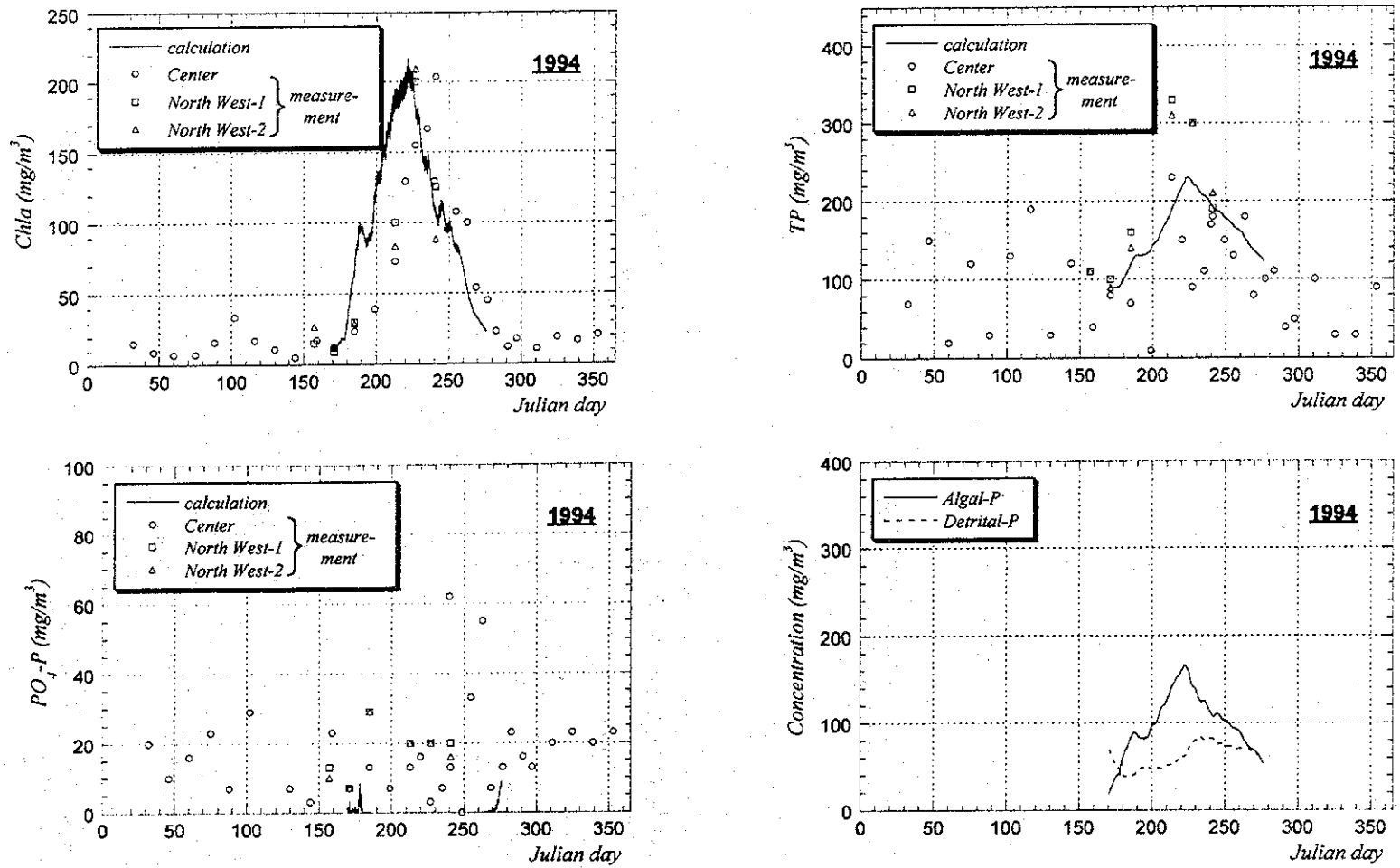

P_up_max = 1.500 half_sat =18.000 R_mineral = 0.040 T_mineral = 1.180
R_mortal = 0.092 T_mortal = 1.040 Growth_max= 1.700 Fop = 0.700

alph = 2.600 Ws-det = 0.100 Ws-bmass = 0.050 L_A/D = 13.30
gamma = 0.100 C_ex = 0.150 P_eq =30.000 P_release = 0.008

psi_min =0.0015 psi_max = 0.018 B/C ratio = 2.11 P/C ratio = 0.02
Saturation PAR = 4.50 CCHL_const = Light_function = non-inhibited
f(1)-0 = 7.000 f(2)-0 =90.000 f(3)-0 =11.100 f(4)-0 = 0.0

SS-0 = 8.0 kyear = 1994 Jday_start= 171 Jday_end = 300
deltat = 0.005

Figure C.50 Sensitivity Analysis of Model Parameters, Case I-1

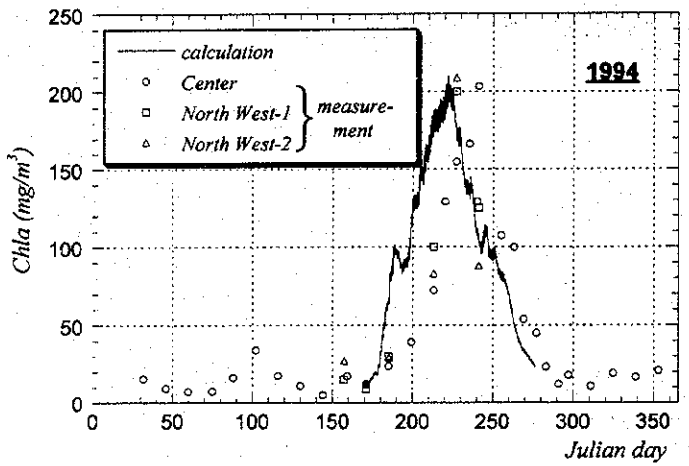

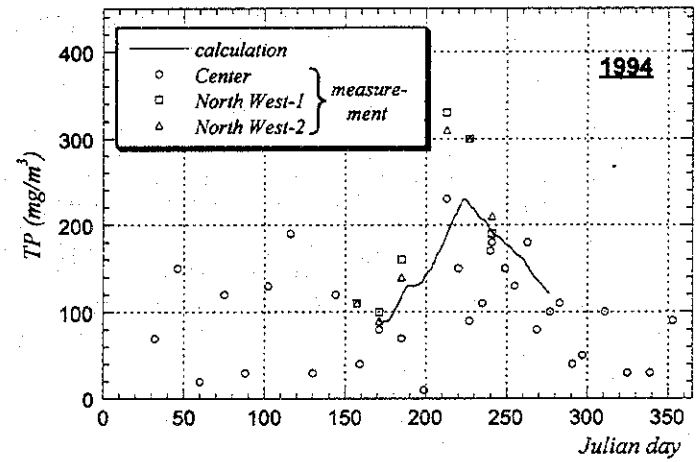

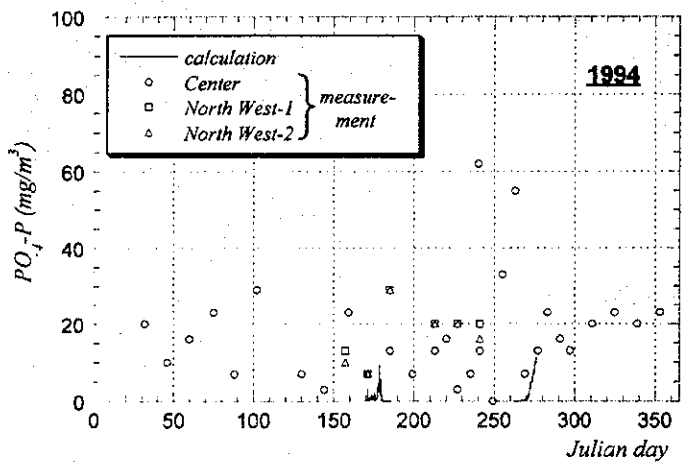

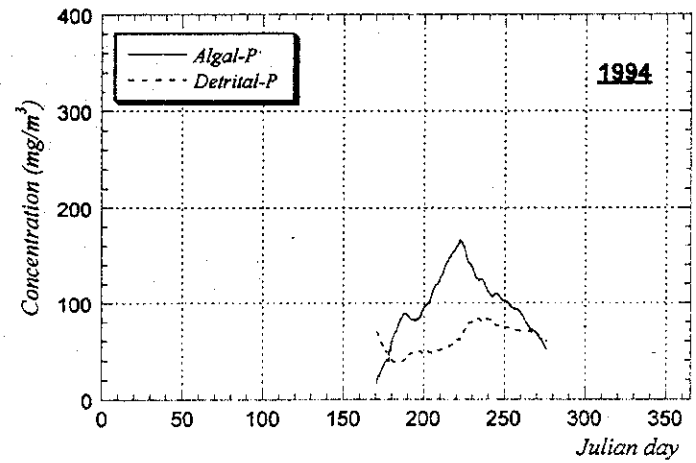

P_up_max = 1.500 half_sat =18.000 R_mineral = 0.040 T_mineral = 1.180
R_mortal = 0.092 T_mortal = 1.040 Growth_max= 1.800 Fop = 0.700

alph = 2.600 Ws-det = 0.100 Ws-bmass = 0.050 L_A/D = 13.30
gamma = 0.100 C_ex = 0.150 P_eq =30.000 P_release = 0.008

psi_min =0.002 psi_max = 0.018 B/C ratio = 2.11 P/C ratio = 0.02
Saturation PAR = 4.50 CCHL_const = Light_function = non-inhibited
f(1)-0 = 7.000 f(2)-0 =90.000 f(3)-0 =11.100 f(4)-0 = 0.0

SS-0 = 8.0 kyear = 1994 Jday_start= 171 Jday_end = 300
deltat = 0.005

Figure C.51 Sensitivity Analysis of Model Parameters, Case I-2

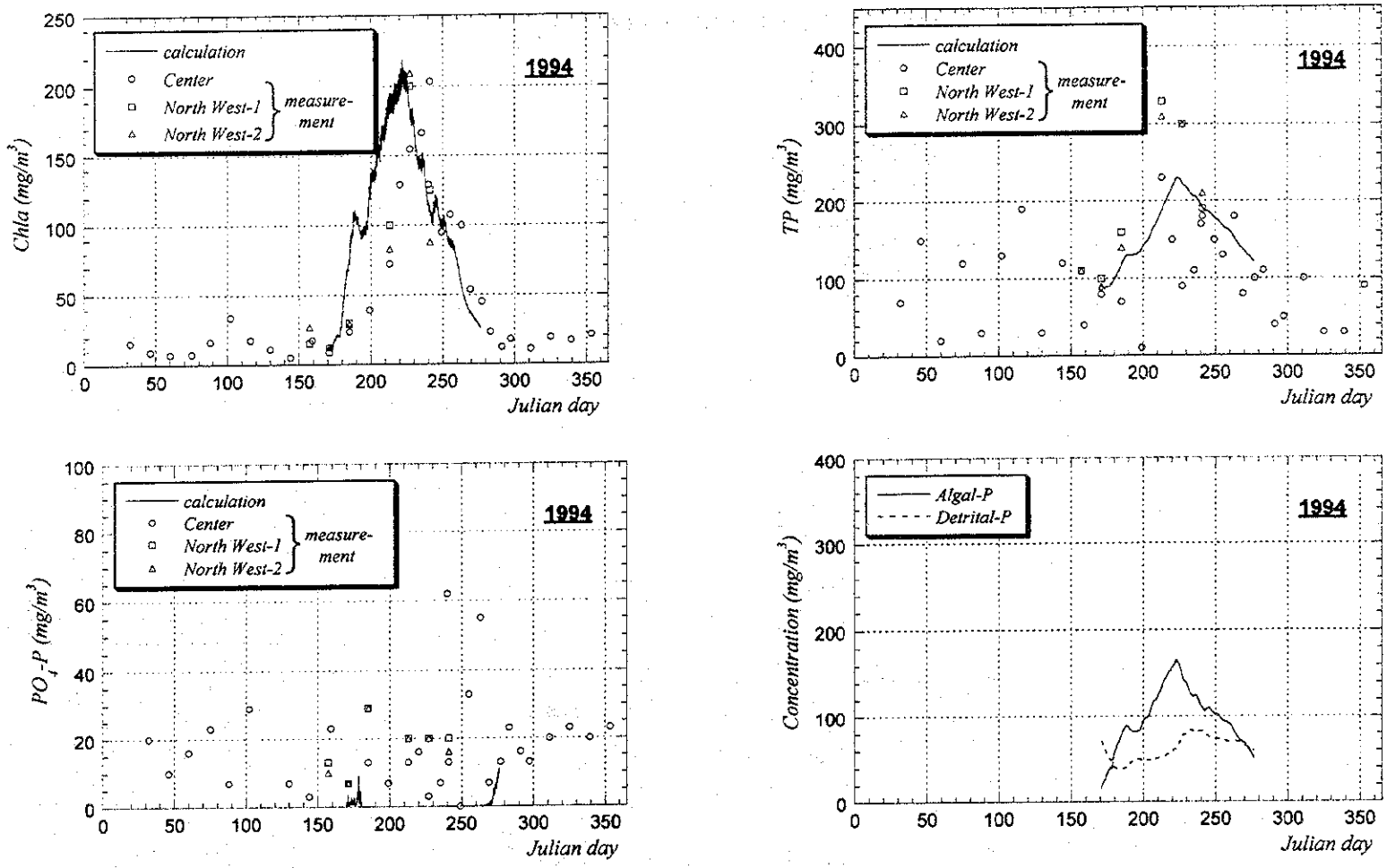

P_up_max = 1.500 half_sat =18.000 R_mineral = 0.040 T_mineral = 1.180
R_mortal = 0.092 T_mortal = 1.040 Growth_max= 2.000 Fop = 0.700

alph = 2.600 Ws-det = 0.100 Ws-bmass = 0.050 L_A/D = 13.30
gamma = 0.100 C_ex = 0.150 P_eq =30.000 P_release = 0.008

psi_min =0.0025 psi_max = 0.018 B/C ratio = 2.11 P/C ratio = 0.02
Saturation PAR = 4.50 CCHL_const = Light_function = non-inhibited
f(1)-0 = 7.000 f(2)-0 =90.000 f(3)-0 =11.100 f(4)-0 = 0.0

SS-0 = 8.0 kyear = 1994 Jday_start= 171 Jday_end = 300
deltat = 0.005

Figure C.52 Sensitivity Analysis of Model Parameters, Case I-3

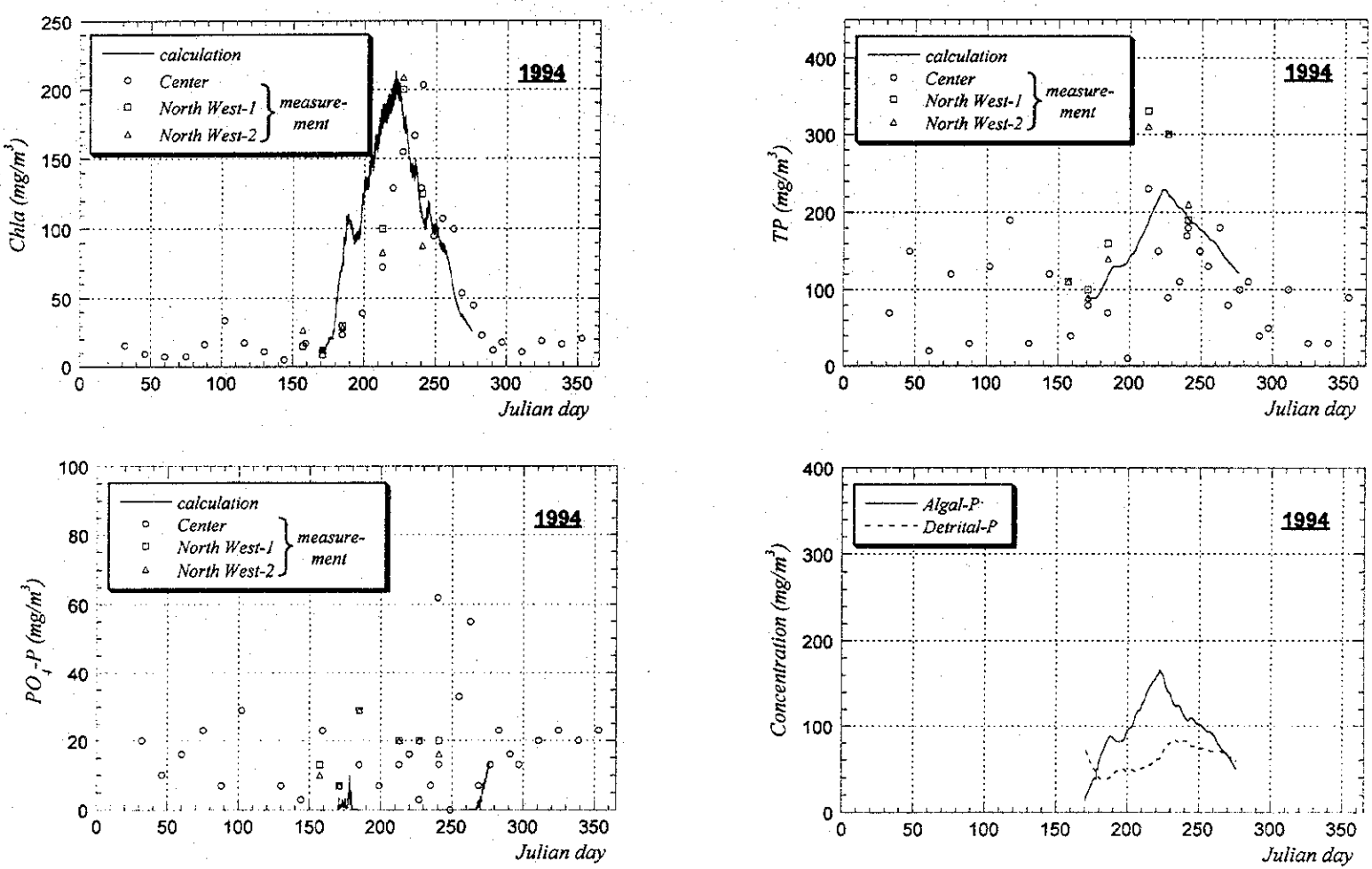

P_up_max = 1.500 half_sat =18.000 R_mineral = 0.040 T_mineral = 1.180
R_mortal = 0.092 T_mortal = 1.040 Growth_max= 2.100 Fop = 0.700

alph = 2.600 Ws-det = 0.100 Ws-bmass = 0.050 L_A/D = 13.30
gamma = 0.100 C_ex = 0.150 P_eq =30.000 P_release = 0.008

psi_min =0.003 psi_max = 0.018 B/C ratio = 2.11 P/C ratio = 0.02
Saturation PAR = 4.50 CCHL_const = Light_function = non-inhibited
f(1)-0 = 7.000 f(2)-0 =90.000 f(3)-0 =11.100 f(4)-0 = 0.0

SS-0 = 8.0 kyear = 1994 Jday_start= 171 Jday_end = 300
deltat = 0.005

Figure C.53 Sensitivity Analysis of Model Parameters, Case I-4

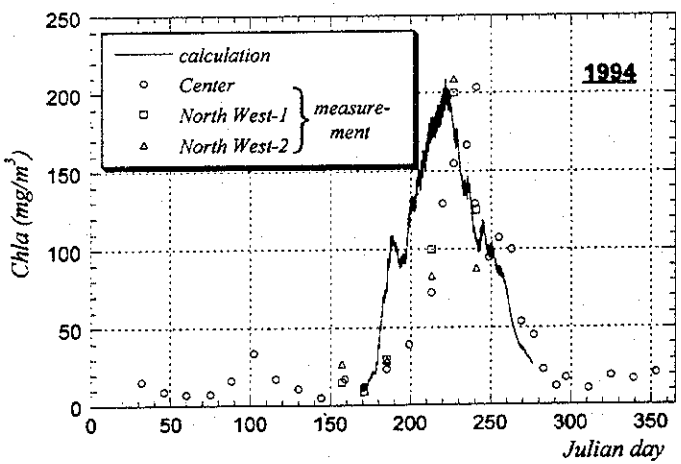

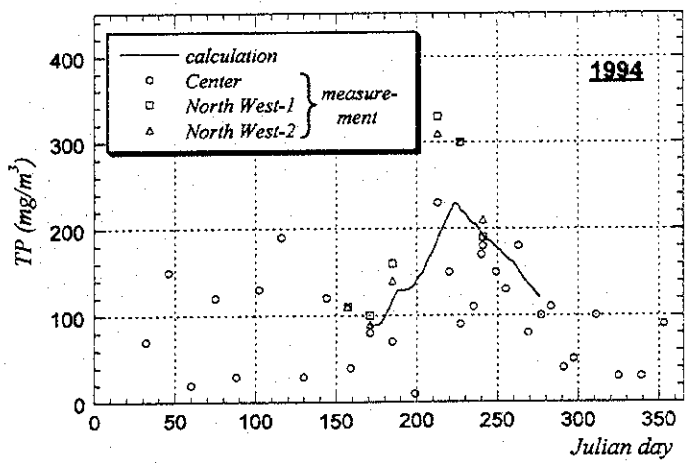

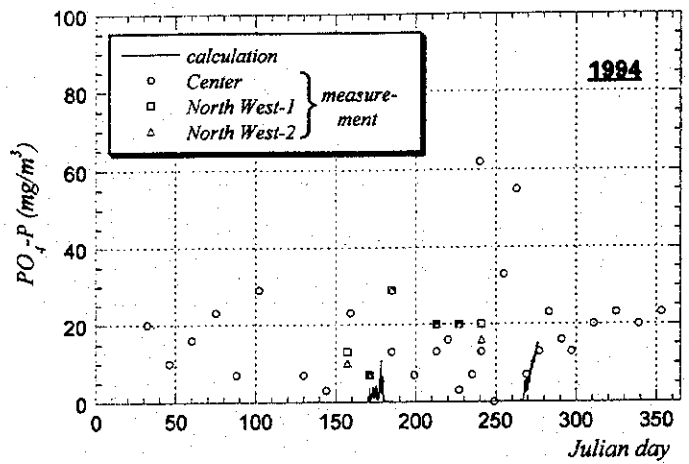

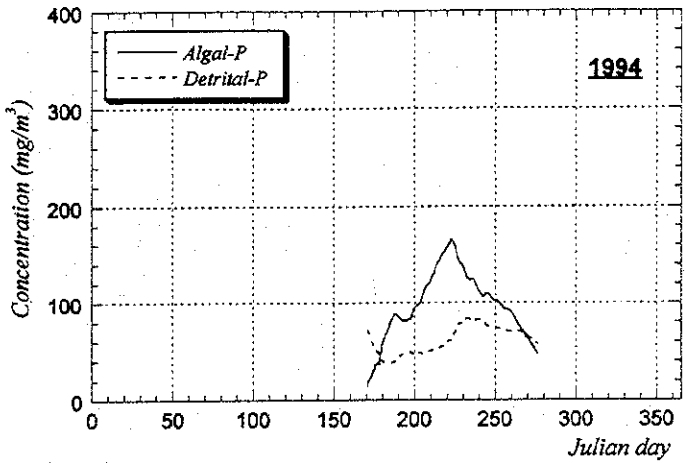

P_up_max = 1.500 half_sat =18.000 R_mineral = 0.040 T_mineral = 1.180
R_mortal = 0.092 T_mortal = 1.040 Growth_max= 2.200 Fop = 0.700
alph = 2.600 Ws-det = 0.100 Ws-bmass = 0.050 L_A/D = 13.30
gamma = 0.100 C_ex = 0.150 P_eq =30.000 P_release = 0.008
psi_min =0.0035 psi_max = 0.018 B/C ratio = 2.11 P/C ratio = 0.02
Saturation PAR = 4.50 CCHL_const = non-inhibited
f(1)-0 = 7.000 f(2)-0 =90.000 f(3)-0 =11.100 f(4)-0 = 0.0
SS-0 = 8.0 kyear = 1994 Jday_start= 171 Jday_end = 300
deltat = 0.005

Figure C.54 Sensitivity Analysis of Model Parameters, Case I-5

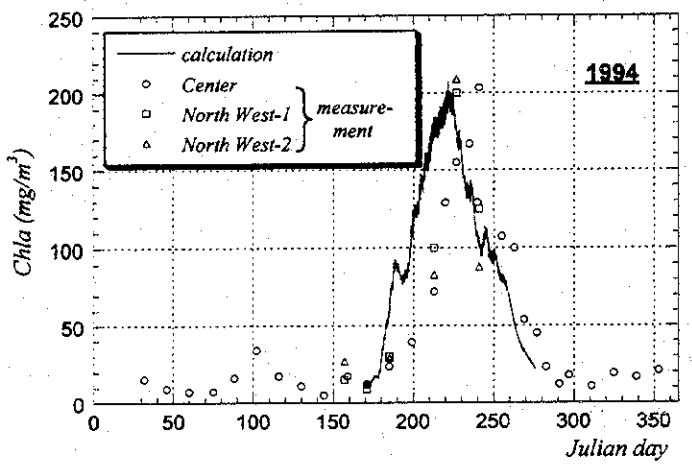

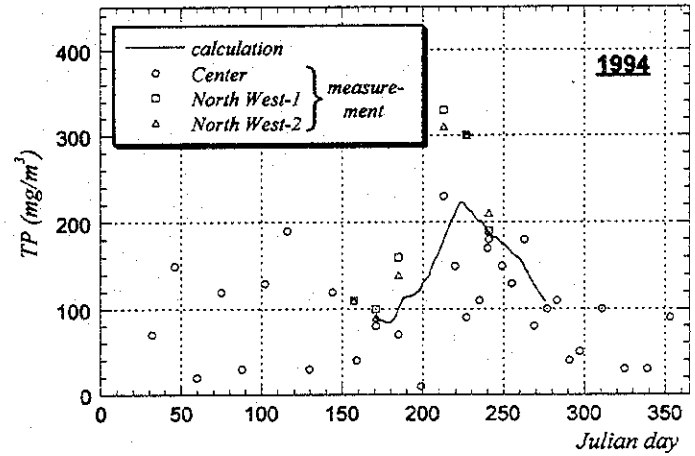

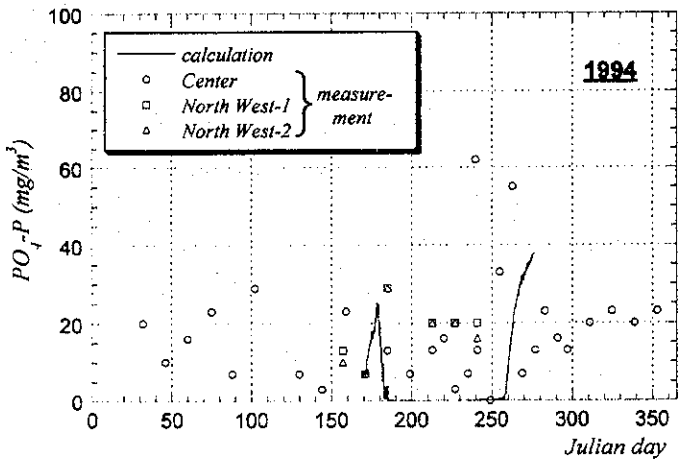

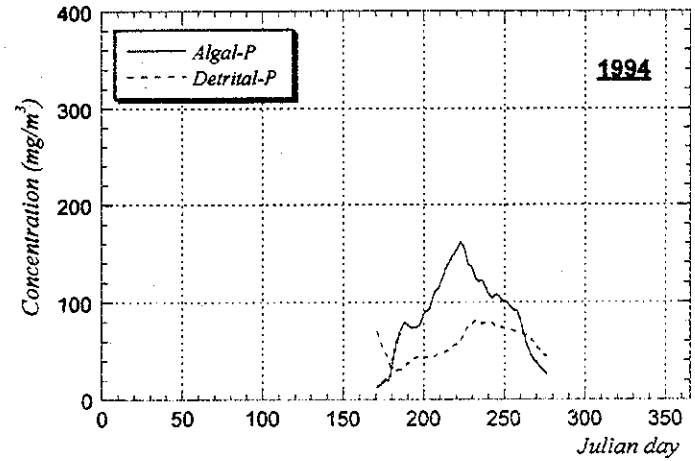

P_up_max = 1.500 half_sat =18.000 R_mineral = 0.040 T_mineral = 1.180
R_mortal = 0.092 T_mortal = 1.040 Growth_max= 1.800 Fop = 0.700
alph = 2.600 Ws-det = 0.100 Ws-bmass = 0.050 L_A/D = 13.30
gamma = 0.100 C_ex = 0.150 P_eq =30.000 P_release = 0.008
psi_min =0.0020 psi_max = 0.010 B/C ratio = 2.11 P/C ratio = 0.02
Saturation PAR = 4.50 CCHL_const =Light_function = non-inhibited
f(1)-0 = 7.000 f(2)-0 =90.000 f(3)-0 =11.100 f(4)-0 = 0.0
SS-0 = 8.0 kyear = 1994 Jday_start= 171 Jday_end = 300
deltat = 0.005

Figure C.55 Sensitivity Analysis of Model Parameters, Case II-1

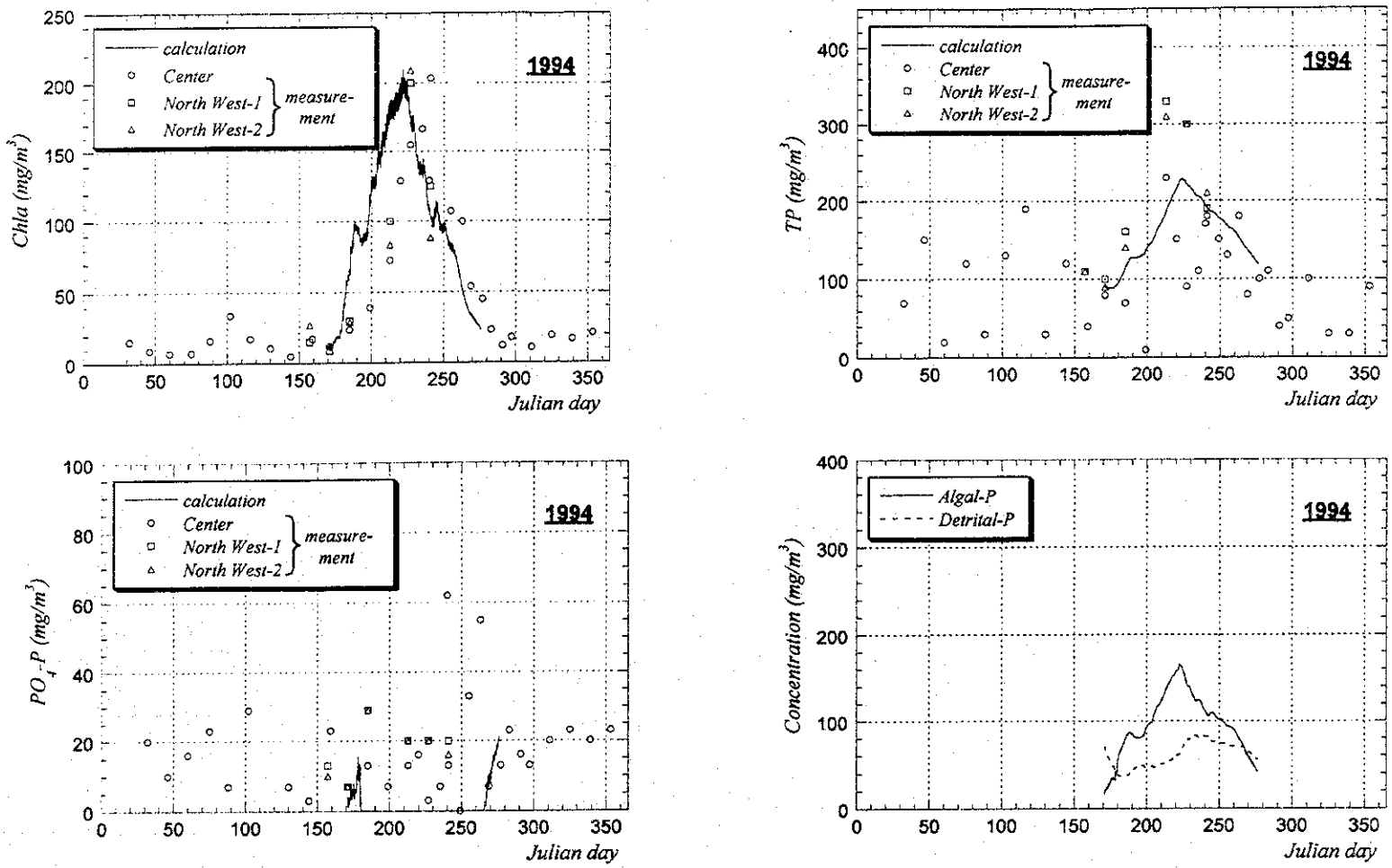

P_up_max = 1.500 half_sat =18.000 R_mineral = 0.040 T_mineral = 1.180
R_mortal = 0.092 T_mortal = 1.040 Growth_max= 1.800 Fop = 0.700

alph = 2.600 Ws-det = 0.100 Ws-bmass = 0.050 L_A/D = 13.30
gamma = 0.100 C_ex = 0.150 P_eq =30.000 P_release = 0.008

psi_min =0.002 psi_max = 0.015 B/C ratio = 2.11 P/C ratio = 0.02
Saturation PAR = 4.50 CCHL_const = Light_function = non-inhibited
f(1)-0 = 7.000 f(2)-0 =90.000 f(3)-0 =11.100 f(4)-0 = 0.0

SS-0 = 8.0 kyear = 1994 Jday_start= 171 Jday_end = 300
deltat = 0.005

Figure C.56 Sensitivity Analysis of Model Parameters, Case II-2

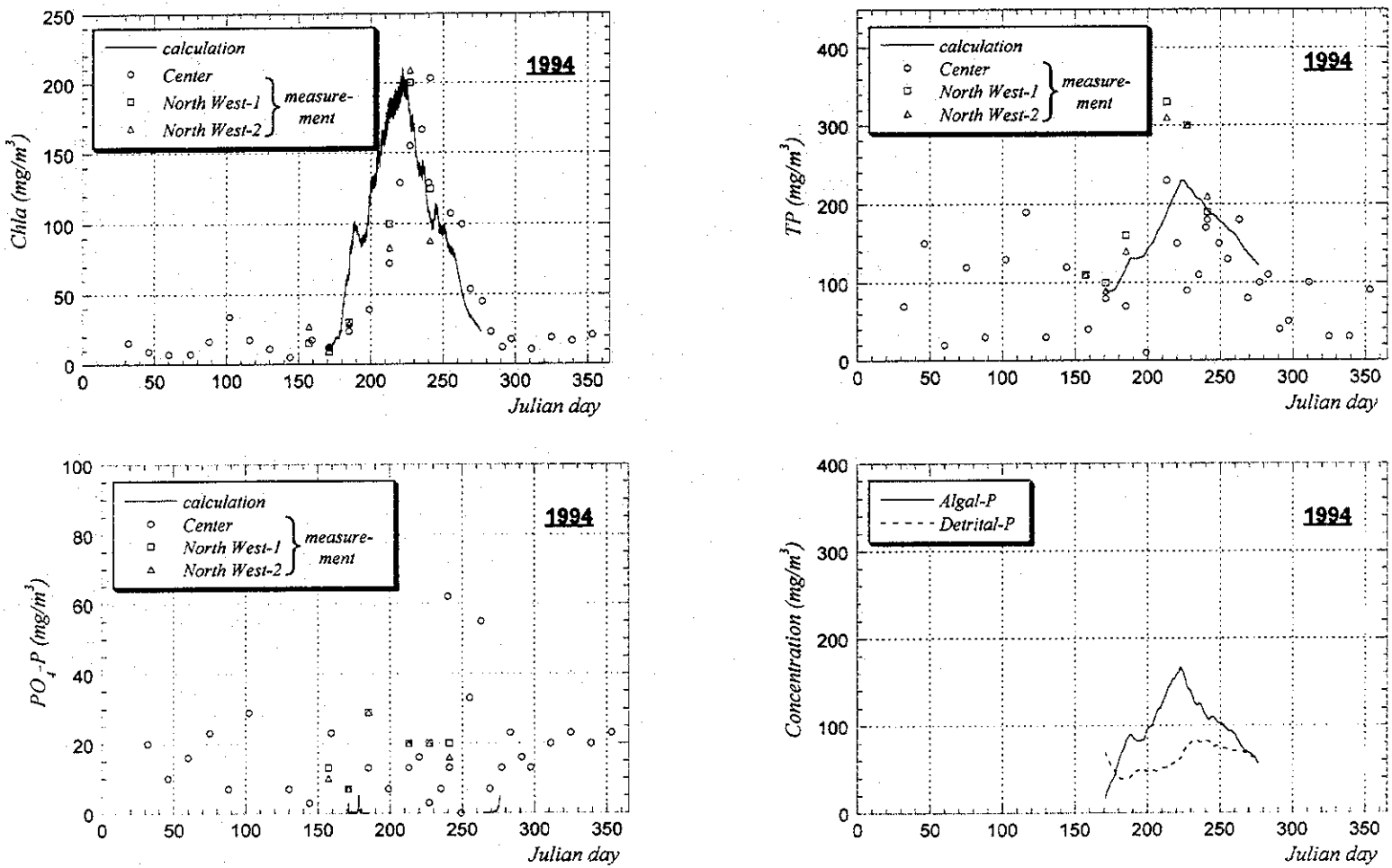

P_up_max = 1.500 half_sat =18.000 R_mineral = 0.040 T_mineral = 1.180
R_mortal = 0.092 T_mortal = 1.040 Growth_max= 1.800 Fop = 0.700

alph = 2.600 Ws-det = 0.100 Ws-bmass = 0.050 L_A/D = 13.30
gamma = 0.100 C_ex = 0.150 P_eq =30.000 P_release = 0.008

psi_min =0.002 psi_max = 0.02 B/C ratio = 2.11 P/C ratio = 0.02
Saturation PAR = 4.50 CCHL_const = Light_function = non-inhibited
f(1)-0 = 7.000 f(2)-0 =90.000 f(3)-0 =11.100 f(4)-0 = 0.0

SS-0 = 8.0 kyear = 1994 Jday_start= 171 Jday_end = 300
deltat = 0.005

Figure C.57 Sensitivity Analysis of Model Parameters, Case II-3

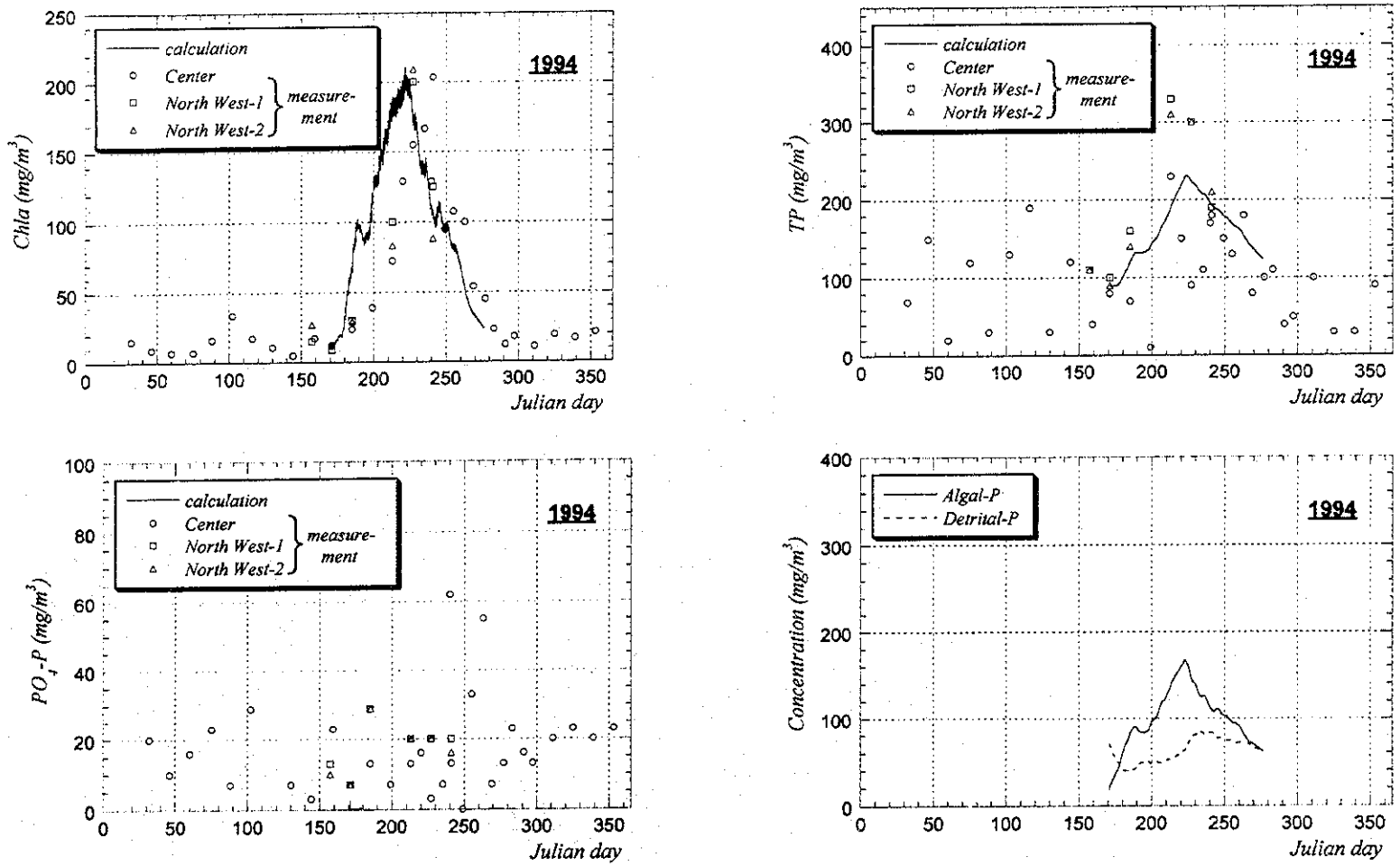

P_up_max = 1.500 half_sat =18.000 R_mineral = 0.040 T_mineral = 1.180
R_mortal = 0.092 T_mortal = 1.040 Growth_max= 1.800 Fop = 0.700

alph = 2.600 Ws-det = 0.100 Ws-bmass = 0.050 L_A/D = 13.30
gamma = 0.100 C_ex = 0.150 P_eq =30.000 P_release = 0.008

psi_min =0.002 psi_max = 0.025 B/C ratio = 2.11 P/C ratio = 0.02
Saturation PAR = 4.50 CCHL_const = Light_function = non-inhibited
f(1)-0 = 7.000 f(2)-0 =90.000 f(3)-0 =11.100 f(4)-0 = 0.0

SS-0 = 8.0 kyear = 1994 Jday_start= 171 Jday_end = 300
deltat = 0.005

Figure C.58 Sensitivity Analysis of Model Parameters, Case II-4

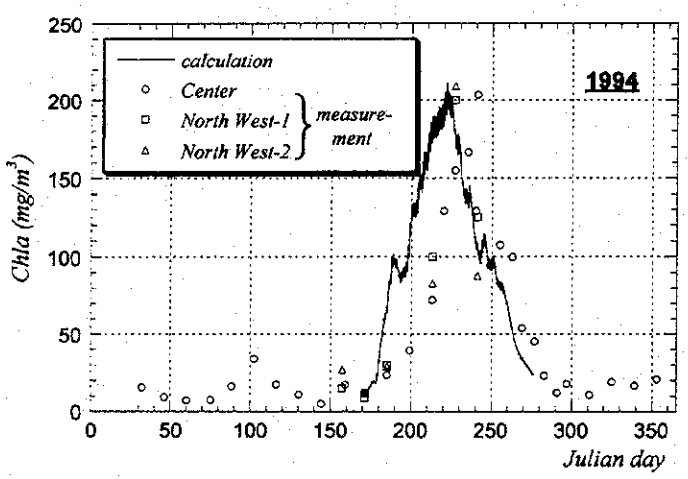

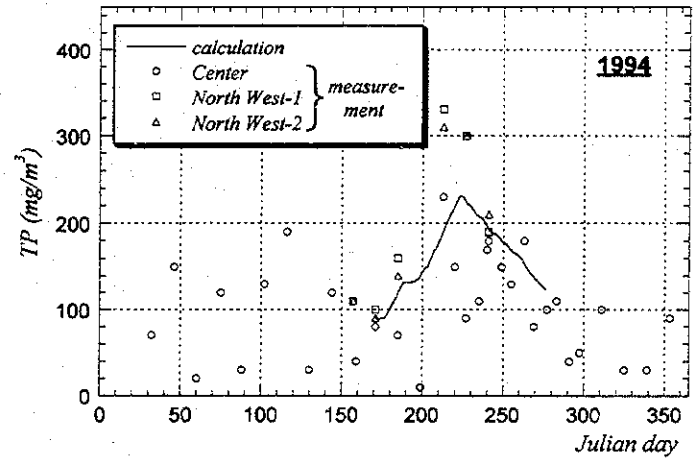

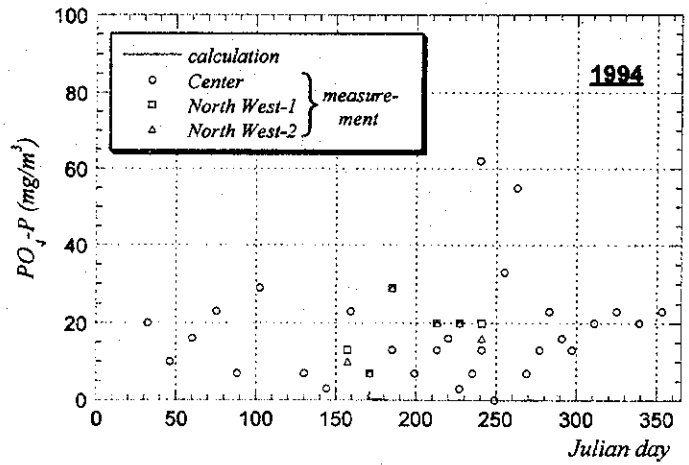

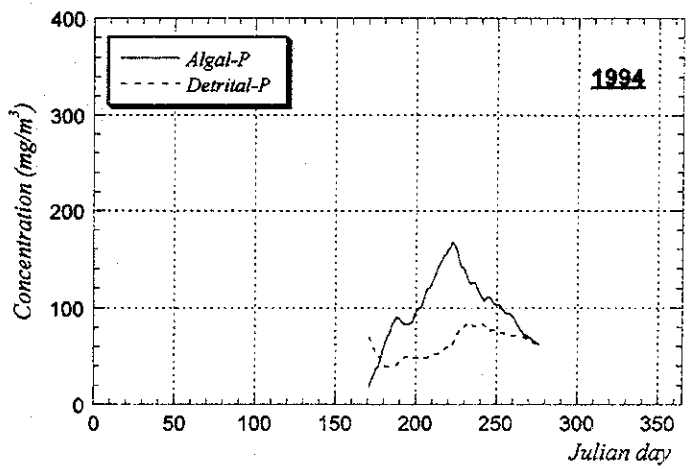

P_up_max = 1.500 half_sat =18.000 R_mineral = 0.040 T_mineral = 1.180
R_mortal = 0.092 T_mortal = 1.040 Growth_max= 1.800 Fop = 0.700
alph = 2.600 Ws-det = 0.100 Ws-bmass = 0.050 L_A/D = 13.30
gamma = 0.100 C_ex = 0.150 P_eq =30.000 P_release = 0.008
psi_min =0.0020 psi_max = 0.030 B/C ratio = 2.11 P/C ratio = 0.02
Saturation PAR = 4.50 CCHL_const =Light_function = non-inhibited
f(1)-0 = 7.000 f(2)-0 =90.000 f(3)-0 =11.100 f(4)-0 = 0.0
SS-0 = 8.0 kyear = 1994 Jday_start= 171 Jday_end = 300
deltat = 0.005

Figure C.59 Sensitivity Analysis of Model Parameters, Case II-5

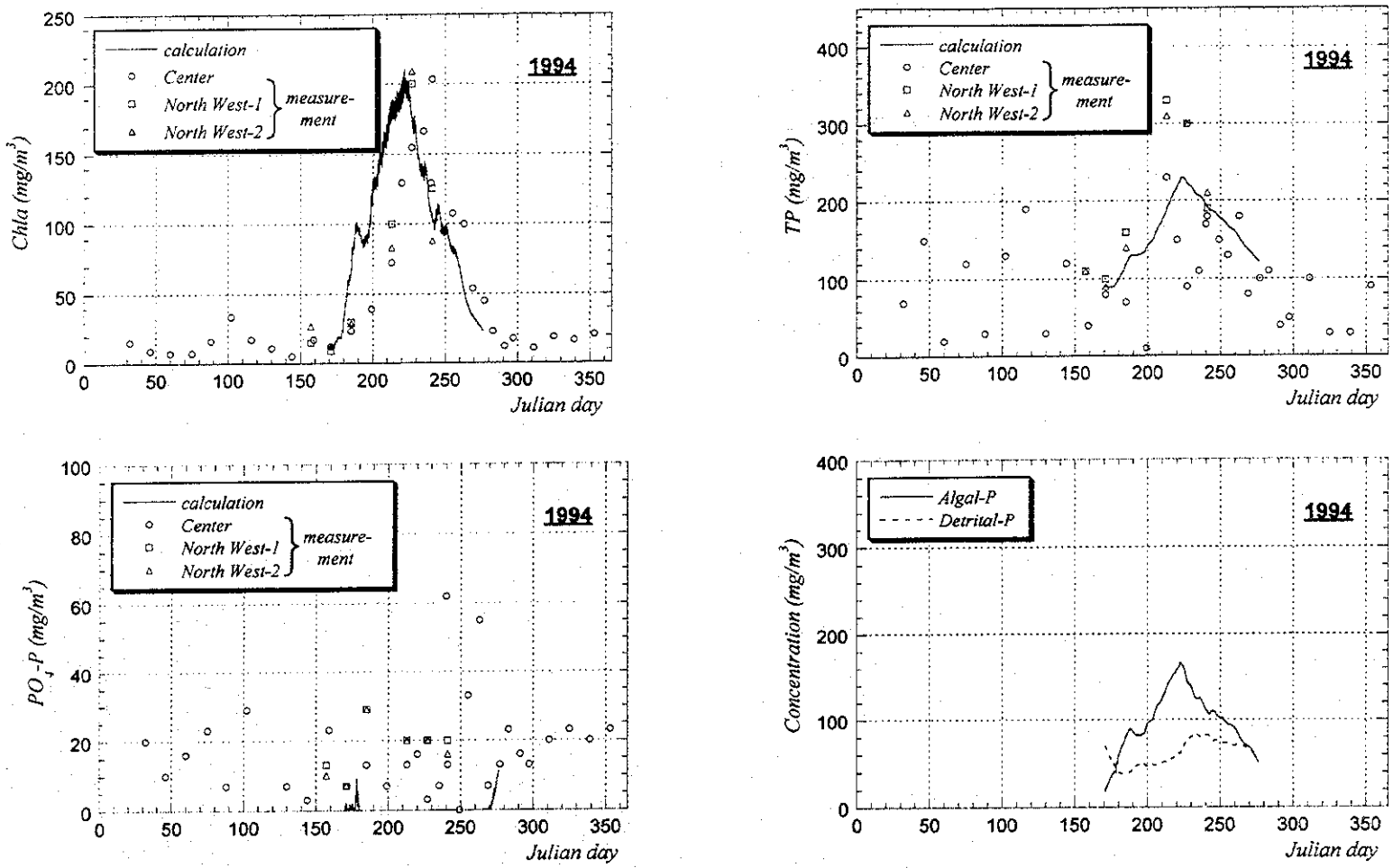

P_up_max = 1.500 half_sat =10.000 R_mineral = 0.040 T_mineral = 1.180
R_mortal = 0.092 T_mortal = 1.040 Growth_max= 1.800 Fop = 0.700
alph = 2.600 Ws-det = 0.100 Ws-bmass = 0.050 L_A/D = 13.30
gamma = 0.100 C_ex = 0.150 P_eq =30.000 P_release = 0.008
psi_min =0.0020 psi_max = 0.018 B/C ratio = 2.11 P/C ratio = 0.02
Saturation PAR = 4.50 CCHL_const =Light_function = non-inhibited
f(1)-0 = 7.000 f(2)-0 =90.000 f(3)-0 =11.100 f(4)-0 = 0.0
SS-0 = 8.0 kyear = 1994 Jday_start= 171 Jday_end = 300
deltat = 0.005

Figure C.60 Sensitivity Analysis of Model Parameters, Case III-1

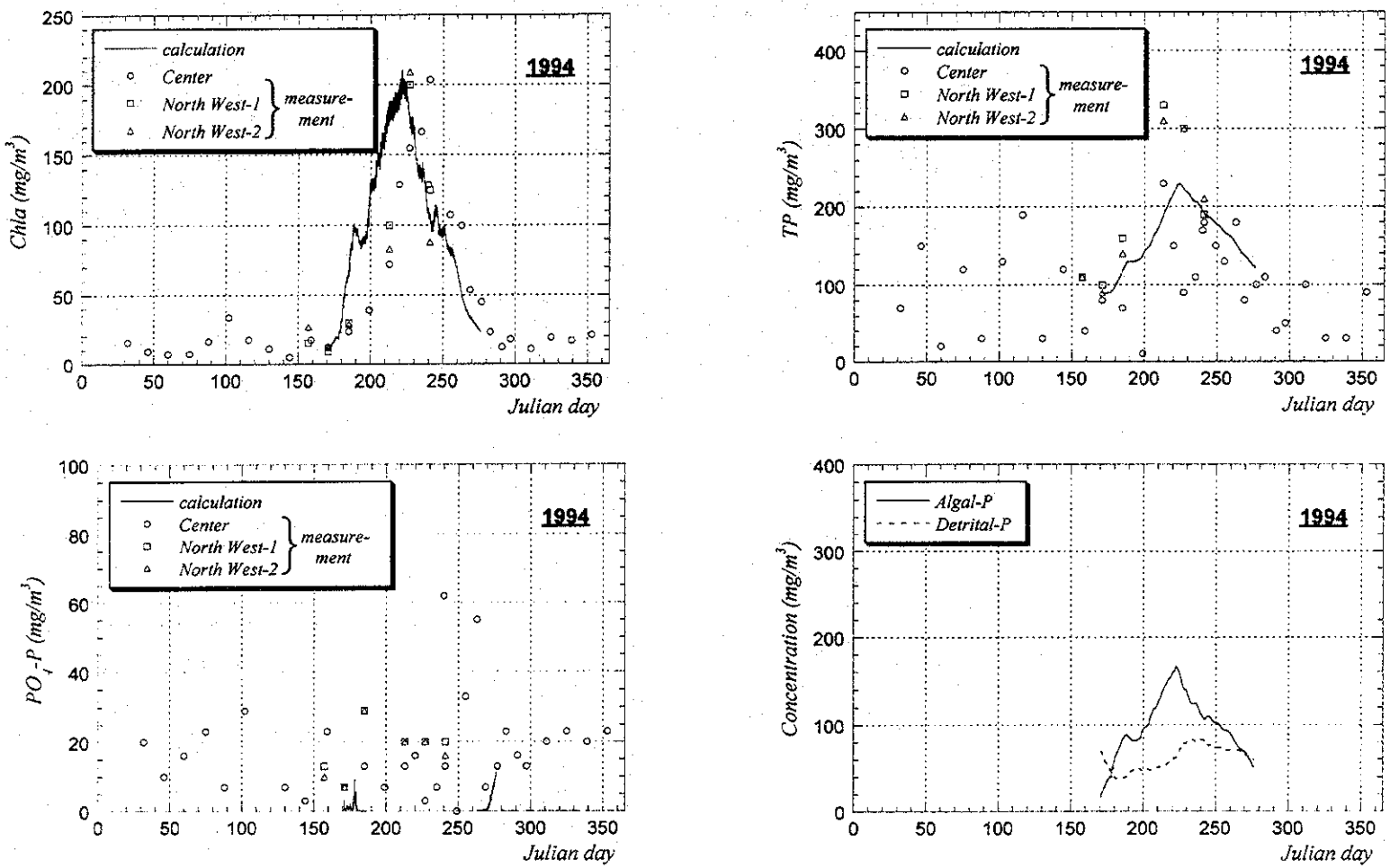

P_up_max = 3.000 half_sat =40.000 R_mineral = 0.040 T_mineral = 1.180
R_mortal = 0.092 T_mortal = 1.040 Growth_max= 1.800 Fop = 0.700
alph = 2.600 Ws-det = 0.100 Ws-bmass = 0.050 L_A/D = 13.30
gamma = 0.100 C_ex = 0.150 P_eq =30.000 P_release = 0.008
psi_min =0.0020 psi_max = 0.018 B/C ratio = 2.11 P/C ratio = 0.02
Saturation PAR = 4.50 CCHL_const =Light_function = non-inhibited
f(1)-0 = 7.000 f(2)-0 =90.000 f(3)-0 =11.100 f(4)-0 = 0.0
SS-0 = 8.0 kyear = 1994 Jday_start= 171 Jday_end = 300
deltat = 0.005

Figure C.61 Sensitivity Analysis of Model Parameters, Case III-2